

PB 283 180

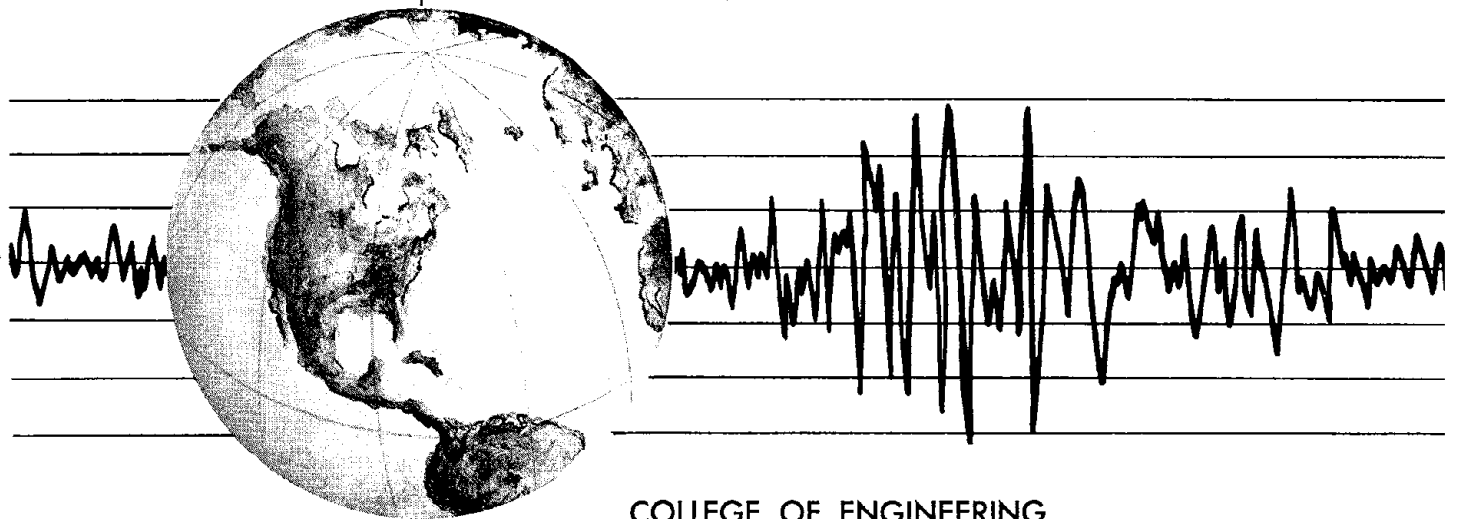
REPORT NO.
UCB/EERC-77/25
NOVEMBER 1977

EARTHQUAKE ENGINEERING RESEARCH CENTER

SEISMIC ANALYSIS OF AN OFFSHORE STRUCTURE SUPPORTED ON PILE FOUNDATIONS

by
DONALD D.-N. LIOU
JOSEPH PENZIEN

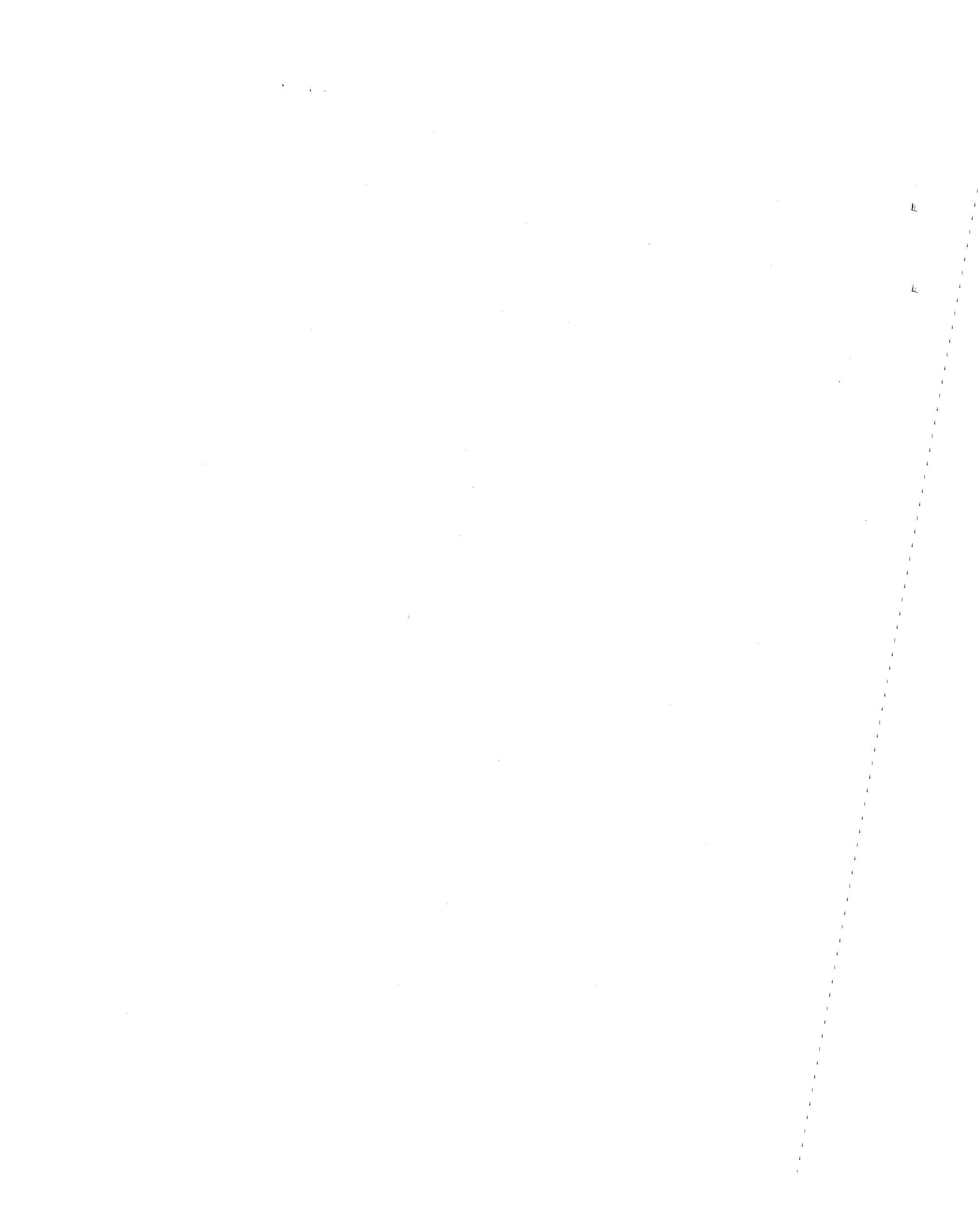
Report to the Standard Oil Company of California



COLLEGE OF ENGINEERING

UNIVERSITY OF CALIFORNIA · Berkeley, California

REPRODUCED BY
**NATIONAL TECHNICAL
INFORMATION SERVICE**
U. S. DEPARTMENT OF COMMERCE
SPRINGFIELD, VA. 22161



BIBLIOGRAPHIC DATA SHEET		1. Report No. UCB/EERC-77/25	2.	3. Record's accession No. 8283180
4. Title and Subtitle Seismic Analysis of an Offshore Structure Supported on Pile Foundations			5. Report Date November 1977	6.
7. Author(s) Donald D.-N Liou and Joseph Penzien			8. Performing Organization Rept. No. 77/25	
9. Performing Organization Name and Address Earthquake Engineering Research Center University of California, Richmond Field Station 47th Street and Hoffman Blvd. Richmond, California 94804			10. Project/Task/Work Unit No.	
			11. Contract/Grant No.	
12. Sponsoring Organization Name and Address Standard Oil Company of California & National Science 555 Market Street San Francisco, California 94105			13. Type of Report & Period Covered	
			14.	
15. Supplementary Notes				
16. Abstracts This report presents an analytical study of the seismic response characteristics of an offshore structure supported on pile foundations. To allow the basic modeling of the structure-foundation system, a simple mathematical model of pile foundation based on the three-dimensional theory of elasticity is developed. The earthquake surface ground motion is prescribed in the time domain, the solution of the system is carried out in the frequency domain, and the desired response quantities are transformed back to the time domain. Foundation-structure interaction effects are examined by comparing response quantities obtained for models with and without foundation flexibility. The interaction effects are found to be quite significant.				
17b. Identifiers/Open-Ended Terms				
17c. COSATI Field/Group				
18. Availability Statement Release Unlimited			19. Security Class (This Report) UNCLASSIFIED	
			20. Security Class (This Page) UNCLASSIFIED	
			21. No.	
			22. Price A06-A01	

SEISMIC ANALYSIS OF AN OFFSHORE STRUCTURE
SUPPORTED ON PILE FOUNDATIONS

by

Donald D.-N. Liou

and

Joseph Penzien

Prepared under the sponsorship of the
Standard Oil Company of California

Report No. UCB/EERC-77/25
Earthquake Engineering Research Center
College of Engineering
University of California
Berkeley, California

November 1977

in



ACKNOWLEDGEMENTS

The research reported herein was submitted in partial fulfillment of the requirements for the degree of Doctor of Philosophy in Engineering by the senior author. He is deeply indebted to Professor Joseph Penzien, chairman of the thesis committee, for his friendship, continuous support and guidance throughout the development of this investigation. He is also indebted to the other members of the committee, Professors Anil K. Chopra and Beresford N. Parlett, for their review of the preliminary draft and for their valuable suggestions. Many thanks are also due to Drs. W. S. Tseng, Y. Sugimura and Mr. M. Takagi for their constructive criticism and valuable suggestions.

Research funds for the major part of this investigation were provided by the Standard Oil Company of California with some financial support also being received from the National Science Foundation. Their support of this research project is sincerely appreciated.

ABSTRACT

This report presents an analytical study of the seismic response characteristics of an offshore structure supported on pile foundations. To allow the basic modeling of the structure-foundation system, a simple mathematical model of pile foundation based on the three-dimensional theory of elasticity is developed. The earthquake surface ground motion is prescribed in the time domain, the solution of the system is carried out in the frequency domain, and the desired response quantities are transformed back to the time domain. Foundation-structure interaction effects are examined by comparing response quantities obtained for models with and without foundation flexibility. The interaction effects are found to be quite significant.

TABLE OF CONTENTS

	<u>Page</u>
ACKNOWLEDGEMENTS	i
ABSTRACT	ii
TABLE OF CONTENTS	iii
1. INTRODUCTION	1
1.1 Review of Past Work	2
1.2 Scope of Investigation	5
2. METHOD OF ANALYSIS	6
2.1 Formulation of Equations of Motion	6
2.2 Linearization of Equations of Motion	12
2.3 Coordinate Transformation of Equations of Motion	14
2.4 Solution of Equations of Motion	19
3. MATHEMATICAL MODEL OF PILE FOUNDATION	22
3.1 Concept of Lateral Soil Modulus	22
3.2 Elastic Lateral Soil Modulus	24
3.2.1 Degenerated Two-Dimensional Approximation	25
3.2.2 Three-Dimensional Static Approximation	30
3.3 Elastic Vertical Soil Modulus	33
3.4 Inelastic Soil Moduli	34
3.5 Dynamic Stiffnesses of a Single Pile	36
3.5.1 Method of Calculation	36
3.5.2 Tip Conditions	38
3.6 A Suggested Procedure in the Study of Pile Behavior	40
3.6.1 A Proposed Procedure	41
3.6.2 Examination of the Procedure	44
3.6.3 Frequency-Dependent Shape Functions	46

3.7	Dynamic Stiffness of a Pile Group	49
3.7.1	Pile Group Without Pile-Cap	49
3.7.2	Group Effect of Laterally Loaded Piles	50
3.7.3	Pile Group With Pile-Cap	51b
4.	EXAMPLE PROBLEM SOLUTION	63
4.1	The Mathematical Model	63
4.1.1	The Structure System	63
4.1.2	Pile Foundation	65
4.2	Results of Analysis	67
4.2.1	Model Shape and Natural Periods of Vibration	67
4.2.2	Lateral Deflections and Accelerations	68
4.2.3	Maximum Leg Axial Forces	69
4.3	Discussion of the Results of the Example Problem	69
5.	CONCLUSIONS	87
	REFERENCES	89
	APPENDIX A	A-1
1.	Structural Stiffness Matrix	A-1
2.	Mass Matrix	A-4



1. INTRODUCTION

Man's ever-increasing need for more and cheaper energy has resulted in various ways of tapping new energy sources, while the techniques used in extracting traditional energy sources have greatly improved. Oil operations have recently been extended into the continental shelf. Fixed offshore structures were constructed first off the coast of Louisiana in 20 feet of water and then in progressively deeper water. With the new oil discoveries in the North Sea and other areas around the world, the importance of offshore structures should keep increasing.

The majority of offshore structures has been and almost certainly will continue to be land-connected. Although foundations for land-connected offshore structures, like those on land, can be divided into many different categories, pile foundations are used for the support of a large number of the permanent offshore structures in areas where the soil deposits exhibit low bearing capacity and medium to high compressibility.

The problems resulting from earthquake forces on offshore structures supported on pile foundations are complex and extensive. Consideration must be given to the fact that these structures are either partially or totally immersed in water and will therefore exhibit different dynamic characteristics than if they were located in air. The structures will also interact during earthquake shaking with the pile foundation and soil below and adjacent to them. A great deal has been published on fluid-structure interaction of offshore structures. Numerical procedures for carrying out dynamic analysis of the complete offshore structure-foundation system are similar to those for determining the dynamic

response of other types of structures, and these procedures have been reported in the literature. However, present knowledge and understanding of the dynamic behavior of a pile foundation is far from complete, although it has been the subject of considerable interest and research in recent years. Since the actions of structure, pile, and soil during earthquakes are interdependent, the behavior of these structures cannot be realistically predicted if the complete structure-foundation system has not been modeled accurately. Therefore, it is important to give full consideration to the problem of defining an appropriate mathematical model for pile foundations.

1.1 Review of Past Work

Early analytical solutions for piles have been obtained along two principal lines (1) using a discrete model with lumped masses, springs and dashpots and (2) using a continuous model and the theory of elasticity. A discrete model was first used by Penzien et al.⁽¹⁾ With this model, the nonlinearity of the surrounding soil deposit can be relatively easily introduced by specifying arbitrary force deformation characteristics for the spring. However, it encounters the difficulty of defining equivalent soil masses and fictitious dashpots to simulate radiation damping. A simplified discrete model was employed by Sugimura⁽²⁾ to study the dynamic behavior of long pile foundations. A group of slender piles was found to be more effective than a few large-diameter piles in resisting load applied at the top of piles when the soil deposits contain layers with extremely different dynamic properties. Yamamoto and Seki⁽³⁾ used the same model to study the dynamic interaction of soil-pile-multistory building systems.

The continuous model treats the pile as a flexural bar buried in

elastic, isotropic, and homogeneous layers. It has the advantage that it can automatically incorporate in the formulation the mass density of soil and pile, as well as the effect of radiation damping. It is, however, restricted to linear soil behavior. An important step in using a continuous model is the determination of the soil reaction to the dynamic motion of an embedded pile. Baranov⁽⁴⁾ derived formulas for evaluating these reactions for cases that can be viewed as plane strain. Novak⁽⁵⁾ studied the formulas and applied them to stiffnesses of piles under dynamic surface loads.

The most versatile approach is the finite element method. It can readily handle nonhomogeneity and nonlinearity. The method has been used extensively to model difficult boundary condition problems in mechanics. With the recent invention of a semi-analytical energy transmitting boundary element by Kausel⁽⁶⁾, the effect of the far field can be reasonably reproduced; so that the field of application of this method has been greatly expanded. However, it does have some limitations. The displacement field of the boundary element is based on the exact displacement functions, whereas the field in the vertical direction is based on low order polynomial functions. Hence the method is more suitable for problems where waves are propagated mainly in the horizontal direction. Besides, determination of the stiffness matrix of the boundary element requires the solution of a quadratic eigen value problem at each discrete frequency. If directly applied to the pile problem, the solution quickly becomes unnecessarily expensive.

Blaney et al.⁽⁷⁾ used a discrete model based on finite elements to study the response of a pile embedded in a horizontally stratified soil deposit, where the properties vary with depth but remain constant

in horizontal planes. They also compared the lateral stiffness of the soil surrounding the pile with the lateral stiffness suggested by Penzien for the static case, and by Novak for steady state harmonic motion with various frequencies. Although the cases studied are not exactly the same, the comparison with Penzien's results can be judged as favorable. Good agreement with Novak's values is also found to exist in the high frequency range. However, in the low frequency range, which is of special interest in earthquake engineering, there are substantial differences. A comparison of the continuous model and the discrete model has also been presented by Flores⁽⁸⁾.

The reliability of the results of analytical methods will depend upon the ability to select, at least approximately, the soil parameters, whatever method is used for the analysis. Hence the importance of experimental studies where soil characteristics are evaluated becomes apparent. Soil parameters required for the analysis of piles in clay have been evaluated by Matlock⁽⁹⁾, Brown and Coyle⁽¹⁰⁾; parameters required for the analysis of piles in sand by Reese et al.⁽¹¹⁾, Wright and Coyle⁽¹²⁾. While there is some theoretical basis for determining these parameters, the real behavior of soil around a pile usually does not yield to a complete analysis. Therefore, a considerable amount of empiricism is involved in the process. Moreover, the soil parameters obtained at a particular experimental site are usually not applicable to other locations. The dynamic behavior of piles was studied by Kubo and Sato⁽¹³⁾ using a large-size shaking table.

Field earthquake observations of a building supported on long piles extending through soft alluvial deposits were conducted by Sugimura⁽¹⁴⁾. He found that the ground and piles behave identically with each other except in the vicinity of the pile cap. A discrete

model similar to that used by Penzien was employed to obtain analytical results. The analytical model was able to simulate fairly well the actual behavior of pile foundations during earthquakes. However, these findings are not conclusive, since the earthquake under observation were comparatively weak earthquakes

In this study, a simple, relatively inexpensive model of pile foundation is developed. The new model is based on the discrete model used by Penzien and the three-dimensional theory of elasticity. Radiation damping is included in the new model. It may prove useful as an alternative to obtaining the dynamic stiffness matrix of pile foundation by three-dimensional finite element discretization method.

1.2 Scope of Investigation

The basic numerical procedure for carrying out the seismic analysis of fixed offshore structures in the frequency-domain is described in Chapter 2. Three-dimensional effects of strong motion earthquake excitations are included in the formulation of the equations of motion. In Chapter 3, the dynamic behavior of pile foundations subjected to surface loadings is investigated. In Chapter 4, the dynamic responses of an offshore structure supported on pile foundations subjected to a recorded strong motion earthquake are obtained. The effects of interaction between the structure and its pile foundations are examined. Finally, the conclusions obtained from this investigation are summarized in Chapter 5.

2. METHOD OF ANALYSIS

Pile-supported offshore structures are constructed in areas where the soil is relatively soft and the sea conditions are usually rough and frequently in regions of high seismicity. Since these conditions develop high dynamic forces in the structure-foundation system, it is important that such forces be predicted realistically for design purposes. Hence, the complete structure-foundation system must be modeled accurately, hydrodynamic forces must be considered properly, and a reliable numerical procedure must be used. The basic numerical procedure for determining the dynamic responses of fixed offshore structures was previously presented by Penzien and Tseng^(15, 16). For completeness, their procedure is summarized here.

2.1 Formulation of Equations of Motion

An offshore structure is a continuous structure with an infinite number of degrees of freedom. For a dynamic analysis, it is convenient and usually adequate to model such a structure as a lumped mass system consisting of discrete masses located at selected nodal points and its foundation as a set of frequency dependent springs and dashpots. Figure 2.1 shows such an idealized model of an offshore structure. Complete dynamic analysis of this model requires consideration of various forces the structure must resist during its lifetime. Among the forces, those due to waves and strong motion earthquakes are of prime importance. For steady state motion of frequency ω , the dynamic equations of motion for this system with n nodal points can be expressed in matrix form as

$$[\bar{m}]\{\ddot{r}^t\} + [c(\omega)]\{\dot{r}\} + [k(\omega)]\{r\} e^{i\omega t} = \{P_w\} e^{i\omega t} \quad (2.1)$$

in which $[\bar{m}]$ is the diagonal matrix of masses lumped at nodal points (including effective water masses contained inside structural members), $[c(\omega)]$ and $[k(\omega)]$ are the total foundation-structure damping and stiffness matrices (including material and radiation damping and structure and foundation stiffness, respectively). The vector $\{\ddot{r}^t\}$ represents the total structure accelerations measured from a fixed reference; vectors $\{\dot{r}\}$ and $\{r\}$ represent the velocities and displacements, respectively, measured relative to its moving base. Vector $\{p_w(t)\}$ consists of hydrodynamic forcing functions. Six degrees of freedom are assigned to each nodal point, namely, translational displacements in the two horizontal directions and in the vertical direction, and the three rotational displacements. Thus, each vector in Eq. (2.1) has N components ($N = 6n$) to represent each of the N degrees of freedom, and each matrix is of order $N \times N$.

The force vector $\{p_w(t)\}$ can be estimated by proper use of the equation developed by Morison et al.⁽¹⁷⁾ The Morison equation was originally developed to estimate the forces exerted by waves on circular cylinders. For a vertical cylinder with its axis normal to the direction of the wave, the horizontal component of force per unit length of the cylinder is given by

$$F_H = F_D + F_I \quad (2.2)$$

with

$$F_D = \rho K_D D |\dot{v}(t)| \dot{v}(t) \quad (2.3)$$

and

$$F_I = \rho K_M \frac{\pi D^2}{4} \ddot{v}(t) \quad (2.4)$$

where D is the diameter of the cylinder, ρ is the density of sea water, K_D and K_M are, respectively, the drag and inertia coefficients, and $\dot{v}(t)$ and $\ddot{v}(t)$ are, respectively, the horizontal components of fluid particle velocity and acceleration at the point under consideration.

The Morison equation states that the hydrodynamic force exerted on a vertical cylinder consists of two components. One component is the drag force which is proportional to the square of the fluid particle velocity. The other component is the inertia force which is proportional to the fluid particle acceleration. The appropriate use of the Morison equation depends primarily on the choice of values of the drag and inertia coefficients. These empirical coefficients are estimated from laboratory and field investigations^(18, 19). Although they may vary considerably for oscillating structures and may be frequency dependent⁽²⁰⁾, they are normally considered to have values in the ranges $1.4 \leq K_M \leq 2.0$ and $0.5 \leq K_D \leq 0.7$.

With the effect of fluid structure interaction included, the hydrodynamic forces exerted on the structure, according to the Morison equation, can be expressed as

$$\{P_w\} = \rho(K_M - 1)[V]\{\ddot{u}_w - \ddot{r}^t\} + \rho[V]\{\ddot{u}_w\} + \rho K_D[A]\{|\dot{u}_w - \dot{r}^t|(\dot{u}_w - \dot{r}^t)\} ; \quad (2.5)$$

where vectors $\{\dot{u}_w\}$ and $\{\ddot{u}_w\}$ represent, respectively, the water particle velocities and accelerations at the instantaneous deflected positions of the nodal points, diagonal matrices $[V]$ and $[A]$ represent, respectively, the effective volumes and effective drag areas of the structural model.

The first term on the right hand side of Eq. (2.5) represents the hydrodynamic inertia forces exerted on the structure due to added mass based on the relative acceleration between the lumped masses and their surrounding fluid. The second term represents the inertia forces induced by the mass of the fluid displaced by the structure. The last term represents the hydrodynamic drag forces exerted on the structure.

When Eq. (2.5) is substituted into Eq. (2.1), the equations of motion become

$$[\bar{m}]\{\ddot{r}^t\} + [c(\omega)]\{\dot{r}\} + [k(\omega)]\{r\} = \rho(K_M - 1)[V]\{\ddot{u}_w - \dot{r}^t\} + \rho[V]\{\ddot{u}_w\} + \rho K_D[A]\{|\dot{u}_w - \dot{r}^t|\}\{\ddot{u}_w - \dot{r}^t\}. \quad (2.6)$$

In Eq. (2.6), the fluid particle velocities and accelerations should be those at the instantaneous deflected positions of the structure. However, for low frequency components of the input forces, the wave particle velocities $\{\dot{u}_w\}$ and accelerations $\{\ddot{u}_w\}$ may be evaluated at the original undeflected coordinate positions of the nodal points with reasonable accuracy⁽²¹⁾.

Since the structural damping and the foundation damping in the complete structure-foundation system are quite different, it is more practical and accurate to consider the structure and the foundation as two substructures of the complete system. Matrices $[c(\omega)]$ and $[k(\omega)]$ can then be decomposed as

$$[c(\omega)] = [\bar{c}] + [\bar{c}(\omega)] \quad (2.7)$$

$$[k(\omega)] = [\bar{k}] + [\bar{k}(\omega)]; \quad (2.8)$$

where $[\bar{c}]$ and $[\bar{k}]$ represent the structural damping and stiffness matrices,

respectively; $[\bar{c}(\omega)]$ and $[\bar{k}(\omega)]$ represent the foundation damping and stiffness matrices, respectively. Matrix $[\bar{k}]$ can be formulated by the standard finite element method. The formulation of the structural damping matrix $[\bar{c}]$ will be discussed in Section 2.3. Both $[\bar{c}(\omega)]$ and $[\bar{k}(\omega)]$ contain non-zero elements only at those degrees of freedom which are located at the interface of the structure and the foundation. If subscript "b" denotes quantities related to the base degrees of freedom and "s" those related to degrees of freedom above the base, then matrices $[\bar{c}(\omega)]$ and $[\bar{k}(\omega)]$ can be partitioned into the following forms

$$[\bar{c}(\omega)] = \begin{bmatrix} \bar{c}_{ss} & \bar{c}_{sb} \\ \bar{c}_{bs} & \bar{c}_{bb} \end{bmatrix} = \begin{bmatrix} 0 & 0 \\ 0 & \bar{c}_{bb} \end{bmatrix} \quad (2.9)$$

$$[\bar{k}(\omega)] = \begin{bmatrix} \bar{k}_{ss} & \bar{k}_{sb} \\ \bar{k}_{bs} & \bar{k}_{bb} \end{bmatrix} = \begin{bmatrix} 0 & 0 \\ 0 & \bar{k}_{bb} \end{bmatrix} \quad (2.10)$$

$[\bar{c}_{bb}(\omega)]$ and $[\bar{k}_{bb}(\omega)]$ together define the relationship between forces and displacements of the foundation subsystem, therefore they can be obtained together by experimental or analytical methods. Let the foundation subsystem be excited by steady state harmonic forces and moments having a frequency ω . The resulting displacements and rotations will also have the same frequency ω , although they will not, in general, be in phase with the applied forces and moments. The relationship between forces and displacements of the foundation subsystem can be expressed as

$$\{p_b\} = [x(\omega)]\{r_b\} \quad (2.11)$$

with

$$[x(\omega)] = [\bar{k}_{bb}(\omega)] + i\omega[\bar{c}_{bb}(\omega)] , \quad (2.12)$$

where $\{r_b\}$ and $\{p_b\}$ are, respectively, the displacement and force vectors at the base degrees of freedom of the structure. $[x(\omega)]$ is the impedance matrix of the foundation subsystem, and is alternatively called the dynamic foundation stiffness matrix or the subgrade stiffness matrix.

The procedure to determine the elements of the dynamic foundation matrices for pile foundations, which constitutes an important part of this investigation, will be discussed in the next chapter.

The vector $\{r^t\}$ representing total structural displacements from a fixed reference can be separated into two parts as

$$\{r^t\} = \{r\} + [b_x]\{u_g(t)\} \quad (2.13)$$

where $\{r\}$ is the vector of displacements with respect to the moving base, $\{u_g(t)\}$ is a vector containing the three translational components of the free-field seismic base displacement, and $[b_x]$ is the influence coefficient matrix. Let the i^{th} component of $\{u_g(t)\}$ represent the translational seismic base displacement in a certain direction, then the corresponding i^{th} vector of matrix $[b_x]$ will contain n components equal to unity representing the n translational components in that direction and $5n$ components equal to zero representing all the other displacement components.

Substituting Eq. (2.13) into Eq. (2.6) and rearranging gives

$$\begin{aligned} [m]\{\ddot{r}\} + [c(\omega)]\{\dot{r}\} + [k(\omega)]\{r\} = & -[m][b_x]\{\ddot{u}_g\} + \rho K_M[V]\{\ddot{u}_w\} \\ & + \rho K_D[A]\{(\dot{u}_w - \dot{r}^t)|(\dot{u}_w - \dot{r}^t)\} \end{aligned} \quad (2.14)$$

where

$$[m] = [\bar{m}] + (K_M - 1)[V] \quad . \quad (2.15)$$

2.2 Linearization of Equations of Motion

Let $\{p(t)\}$ denote the entire force vector on the right hand side of Eq. (2.14), i.e., let

$$\begin{aligned} \{p(t)\} = & -[m][b_x]\{\ddot{u}_g\} + \rho K_M [V]\{\ddot{u}_w\} + \\ & \rho K_D [A]\{(|\dot{u}_w - \dot{r}^t|)(\dot{u}_w - \dot{r}^t)\} \quad . \quad (2.16) \end{aligned}$$

Waves generated by a sudden impulse such as an underwater earthquake, landslide, or volcano are known as tidal waves or tsunamis. Once started, these waves travel great distances at high velocity with little loss of energy. Although on entering shallow water they are able to rise to great height to smash and inundate shore areas, their height in deep water is only a few feet. Tsunamis have periods of more than 15 minutes and wavelengths of several hundred miles⁽¹⁸⁾, whereas the most destructive earthquakes recorded usually have durations less than one minute⁽²²⁾. The probability that a strong motion earthquake occurs concurrently with strong wave excitations generated by wind is very small. It is reasonable therefore to assume a state of quiescent sea ($\dot{u}_w = \ddot{u}_w = 0$) when only the seismic responses of the structure are considered. Hence, Eq. (2.16) can be reduced to

$$\{p(t)\} = -[m][b_x]\{\ddot{u}_g\} - \rho K_D [A]\{|\dot{r}^t|\dot{r}^t\} \quad . \quad (2.17)$$

For earthquake excitation alone, the first term on the right hand side of Eq. (2.17) dominates the response with a relatively small damping effect coming from the nonlinear drag term⁽²¹⁾. In this case, the drag term can be linearized using a technique⁽²³⁾ as reported by Penzien

and Malhotra⁽²¹⁾ that first replaces the nonlinear vector $\{|\dot{r}^t|\dot{r}^t\}$ by a linear vector $[a]\{\dot{r}^t\} + \{b\}$ and then minimizes the error introduced by this approximation in the mean square sense. Term a_i , the i^{th} element of the diagonal matrix $[a]$, is given as

$$a_i = \frac{E[|\dot{r}_i^t|(\dot{r}_i^t)^2] - b_i E[\dot{r}_i^t]}{E[(\dot{r}_i^t)^2]} \quad (2.18)$$

in which \dot{r}_i^t is the i^{th} element of the displacement vector $\{\dot{r}^t\}$, and $E[]$ denotes the time average. Term b_i , which is the i^{th} element of vector $\{b\}$, can be obtained through the relation

$$b_i = -a_i E[\dot{r}_i^t] + E[|\dot{r}_i^t|(\dot{r}_i^t)] \quad (2.19)$$

With the nonlinear term replaced by the equivalent linear term, Eq. (2.17) can now be written as

$$\{p(t)\} = -[m][b_x]\{\ddot{u}_g\} - \rho K_D [A][a]\{\dot{r}^t\} - \rho K_D [A][a]\{b\} \quad (2.20)$$

Now the first term on the right hand side of Eq. (2.20) dominates the response under earthquake conditions. If the earthquake excitation is assumed to be a zero mean Gaussian process, the linearized output of the total velocity vector $\{\dot{r}^t\}$ is also a zero mean Gaussian process, i.e., the probability density function for \dot{r}_i^t is

$$p(\dot{r}_i^t) = \frac{1}{(2\pi)^{\frac{1}{2}} \sigma_{\dot{r}_i^t}} \exp \left[-\frac{1}{2} \left(\frac{\dot{r}_i^t}{\sigma_{\dot{r}_i^t}} \right)^2 \right] \quad (2.21)$$

in which $\sigma_{\dot{r}_i^t}$ is the standard deviation of \dot{r}_i^t . With $p(\dot{r}_i^t)$ known, the expected values of the terms shown in Eqs. (2.18) and (2.19) can be

calculated giving

$$a_i = 1.59\sigma_{r_i} t \quad (2.22)$$

$$b_i = 0 \quad (2.23)$$

Since every element of the vector $\{b\}$ is zero, the term associated with it will vanish from the linearized equations of motion, which now become

$$[m]\{\ddot{r}\} + [c(\omega)]\{\dot{r}\} + [k(\omega)]\{r\} = -[m][b_x]\{\ddot{u}_g\} - \rho K_D [A][a][b_x]\{\ddot{u}_b\} - K_D [A][a]\{\dot{r}\} \quad (2.24)$$

Values of the elements of $\{\dot{r}_i\}$ and $[a]$ can only be calculated from the solution of Eq. (2.24), therefore an iterative procedure is necessary for the solution of the linearized equations of motion. Fortunately, the rate of convergence for the iteration process is fast and only very few cycles are needed. When the total damping in the overall structure-foundaton system is not well known, one can often justify simply increasing the assumed material damping ratios to account for hydrodynamic damping; thus permitting the elimination of the hydrodynamic drag terms completely from the equations of motion. In this case, the equations of motion become

$$[m]\{\ddot{r}\} + [c(\omega)]\{\dot{r}\} + [k(\omega)]\{r\} = -[m][b_x]\{\ddot{u}_g\} \quad (2.25)$$

2.3 Coordinate Transformation of Equations of Motion

In Eq. (2.25), matrices $[c(\)]$ and $[k(\)]$ representing respectively the foundation-structure damping and stiffness coefficients are, in general, frequency dependent. Rather than working directly in the time domain, it is easier to take a frequency expansion of all the time-

dependent quantities of the equations of motion and solve it in the frequency domain. Frequency domain solutions, however, require the solution of a large number of simultaneous algebraic equations over a wide frequency range. This is not only time consuming but also requires a large amount of storage to save the entire set of solutions for future transformation back to the time domain. Therefore, it is desirable to reduce the total number of degrees of freedom in the equations of motion considerably before performing the frequency expansion.

For large systems that possess classical normal modes, it is well known that using the mode superposition method allows great numerical simplification. In the modal coordinates, the equations of motion become uncoupled; and even more important, the earthquake responses of most structures can be adequately expressed by retaining only the first few modes of vibration. When structure-foundation interaction is considered, the complete structure-foundation system does not possess normal modes in the classical sense because of the presence of the frequency dependent matrices $[c(\omega)]$ and $[k(\omega)]$ in the equations of motion. Therefore, the mode superposition method cannot be used directly. A modified coordinate transformation method developed by Gutierrez⁽²⁴⁾ and possessing the same features as the classical mode superposition method is used in this study to reduce the number of degrees of freedom in the equations of motion. The number of degrees of freedom is reduced by introducing a set of generalized coordinates: normal modes of the associated structure supported on a fixed base plus the base degrees of freedom.

The structural stiffness matrix $[\bar{k}]$ can be partitioned into the following form

$$[\bar{k}] = \begin{bmatrix} \bar{k}_{ss} & \bar{k}_{sb} \\ \bar{k}_{bs} & \bar{k}_{bb} \end{bmatrix} \quad (2.26)$$

where matrix $[\bar{k}_{ss}]$ is the stiffness matrix of the fixed base structure, matrix $[\bar{k}_{sb}]$ is the coupling stiffness matrix expressing the forces developed in the degrees of freedom above the base of the fixed base structure caused by pseudostatic displacements of the base degrees of freedom and matrix $[\bar{k}_{bb}]$ is the stiffness matrix of the base degrees of freedom.

The displacement vector $\{r\}$ can be separated into two parts

$$\{r\} = \begin{Bmatrix} r_s \\ r_b \end{Bmatrix} = \begin{Bmatrix} r_s^q \\ r_b \end{Bmatrix} + \begin{Bmatrix} r_s^d \\ 0 \end{Bmatrix} \quad (2.27)$$

where $\{r_s^q\}$ represents the pseudostatic displacements of the degrees of freedom above the base, and $\{r_s^d\}$ represents the dynamic response displacements of the degrees of freedom above the base when the pseudostatic displacement components are excluded.

The pseudostatic displacement vector $\{r_s^q\}$ can be computed from the static equilibrium condition

$$[\bar{k}_{ss}]\{r_s^q\} + [\bar{k}_{sb}]\{r_b\} = \{0\} \quad (2.28)$$

or

$$\{r_s^q\} = [L]\{r_b\} \quad , \quad (2.29)$$

where

$$[L] = -[\bar{k}_{ss}]^{-1}[\bar{k}_{sb}] \quad . \quad (2.30)$$

The displacement vector $\{r_s^d\}$ can be adequately described by a combination of the first few modes of the structure supported on a fixed base, or

$$\{r_s^d\} = [\phi]\{z\} \quad (2.31)$$

where vector $\{z\}$ is the normal coordinate vector and the matrix $[\phi]$ represents the mode shapes of vibration of the associated structure supported on a rigid foundation. The matrix $[\phi]$ usually contains many fewer columns than rows and its j^{th} column vector is the solution of the eigenvalue problem

$$[\bar{k}_{ss}]\{\phi_j\} = \omega_j^2[m_{ss}]\{\phi_j\} \quad , \quad (2.32)$$

where the diagonal matrix $[m_{ss}]$ is the mass matrix of the associated fixed base structure and ω_j is its j^{th} natural frequency of vibration.

Combining Eqs. (2.27), (2.29) and (2.32) gives

$$\{r\} = \begin{bmatrix} \phi & L \\ 0 & I \end{bmatrix} \begin{Bmatrix} z \\ r_b \end{Bmatrix} \quad (2.33)$$

where I is the identity matrix. For clarity, introduce

$$\{Y\} = \begin{Bmatrix} z \\ r_b \end{Bmatrix} \quad (2.34)$$

and

$$[B] = \begin{bmatrix} \phi & L \\ 0 & I \end{bmatrix} \quad (2.35)$$

Equation (2.33) now becomes

$$\{r\} = [B]\{Y\} \quad (2.36)$$

If Eq. (2.25) is pre-multiplied by $[B]^T$, then converted to generalized coordinates using Eq. (2.34), the equations of motion become

$$[M^*]\{\ddot{Y}\} + [C^*(\omega)]\{\dot{Y}\} + [K^*(\omega)]\{Y\} = \{P^*(t)\} \quad (2.37)$$

where

$$[M^*] = [B]^T[m][B] \quad (2.38)$$

$$[C^*(\omega)] = [B]^T[c(\omega)][B] \quad (2.39)$$

$$[K^*(\omega)] = [B]^T[k(\omega)][B] \quad (2.40)$$

$$\{P^*(t)\} = -[B]^T[m][b_x]\{\ddot{u}_g\} \quad (2.41)$$

in which $[M^*]$, $[C^*(\omega)]$ and $[K^*(\omega)]$ represent, respectively, the generalized mass, damping and stiffness matrices, and $\{P^*(t)\}$ represents the generalized force vector.

Now $[\bar{c}]$ which represents the structural damping matrix of the free-free structure, is not yet defined. To determine this matrix, one must rely considerably upon experimental evidence and engineering judgement. A suitable method for evaluating $[\bar{c}]$ is to use the dynamic properties of the fixed base structure along with the pseudostatic influence matrix defined by Eq. (2.30). The structural damping matrix can be partitioned into the following form

$$[\bar{c}] = \begin{bmatrix} \bar{c}_{ss} & \bar{c}_{sb} \\ \bar{c}_{bs} & \bar{c}_{bb} \end{bmatrix} \quad (2.42)$$

where $[\bar{c}_{ss}]$ is the damping matrix for the fixed base structure and can be generated using the relation⁽²⁵⁾

$$[\bar{c}_{ss}] = [m_{ss}] \left[\sum_{j=1}^M \frac{2\xi_j \omega_j}{M_j^*} \{\phi_j\} \{\phi_j\}^T \right] [m_{ss}] \quad , \quad (2.43)$$

where M is the number of normal modes of the fixed base structure to be considered, and ξ_j and M_j^* are the damping ratio and generalized mass, respectively, of the j^{th} normal mode. The matrices $[\bar{c}_{sb}]$ and $[\bar{c}_{bb}]$ can be generated using the relations⁽¹⁵⁾

$$[\bar{c}_{sb}] = -[\bar{c}_{ss}][L] \quad (2.44)$$

$$[\bar{c}_{bb}] = [L]^T [\bar{c}_{ss}] [L] \quad . \quad (2.45)$$

2.4 Solution of Equations of Motion

After the matrices $[M^*]$, $[C^*(\omega)]$, and $[K^*(\omega)]$ and the vector $\{P^*(t)\}$ are determined, Eq. (2.37) can be solved by transforming to the frequency domain. Then

$$[-\omega^2 [M^*] + i\omega [C^*(\omega)] + [K^*(\omega)]] \{\tilde{Y}(\omega)\} = \{\tilde{P}^*(\omega)\} \quad (2.46)$$

where $\{\tilde{Y}(\omega)\}$ and $\{\tilde{P}^*(\omega)\}$ are the direct Fourier transforms of $\{Y(t)\}$ and $\{P^*(t)\}$, respectively, and where ω is the variable circular frequency. Equation (2.46) can be solved simultaneously for the discrete values of ω giving the frequency responses $\{\tilde{Y}(\omega)\}$. The time histories of response $\{Y(t)\}$ can then be obtained by the inverse Fourier transform of $\{\tilde{Y}(\omega)\}$. In this solution process, the direct and inverse Fourier transforms can be obtained very accurately and efficiently using the Fast Fourier Transform (FFT) algorithm developed by Cooley and Tukey^(26, 27).

The nodal point displacements $\{r_s(t)\}$ and $\{r_b(t)\}$ are then obtained using the transformation given in Eq. (2.33). The stresses $\{\tau_p(t)\}$ in element p at any instant of time are related to the displacements $\{r_p(t)\}$ for that element by means of a stress transformation matrix $[S_p]$ as

$$\{\tau_p(t)\} = [S_p]\{r_p(t)\} \quad . \quad (2.47)$$

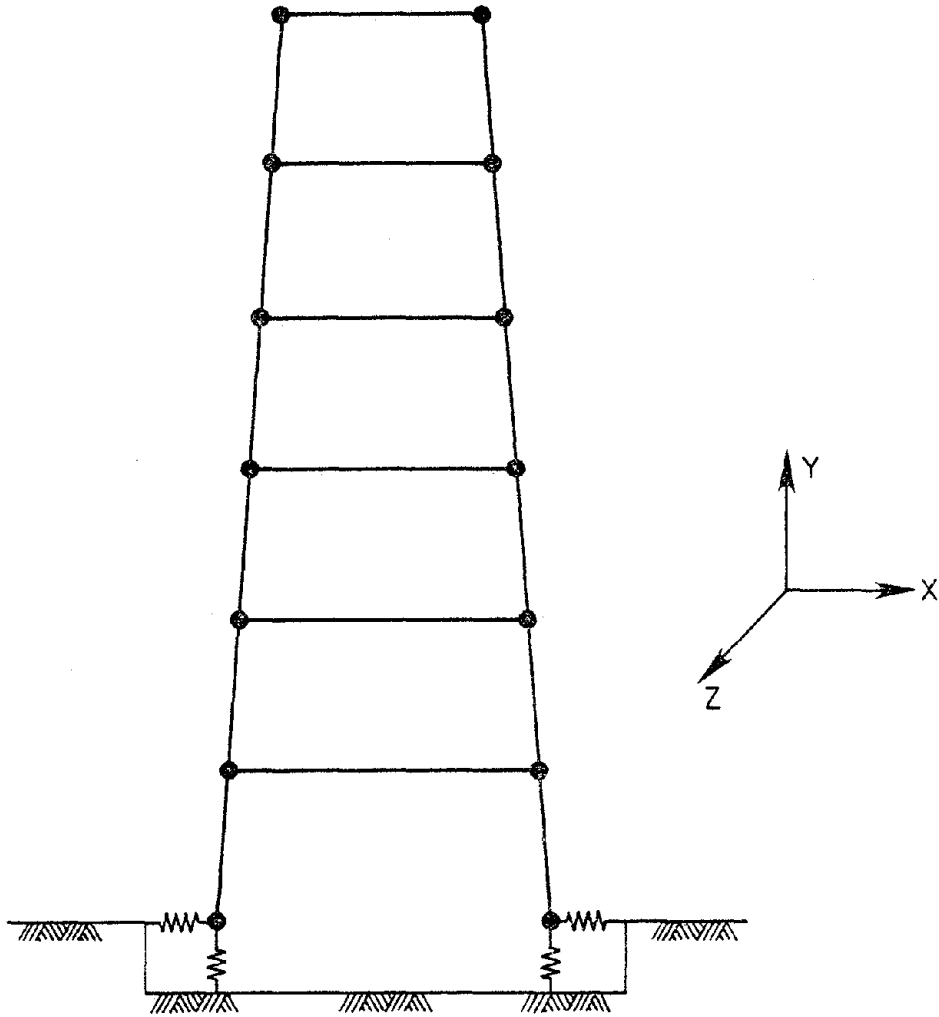


FIG. 2.1 IDEALIZED OFFSHORE STRUCTURE

3. MATHEMATICAL MODELING OF PILE FOUNDATION

3.1 Concept of Lateral Soil Modulus

The classical theories of earth pressures are not reliable for determining lateral resistance of single piles. They assume mobilization of active and passive pressures, which do not occur except at complete failure. Satisfactory methods of determining lateral resistances of single or groups of piles must be applicable to small deflections. In some cases, the governing design criterion is the permissible lateral deflection; in other cases, it is the maximum load that the pile can take without overstress.

Figure 3.1 shows a sketch of a single pile with oscillating loads applied at its top and the spring-dashpot mechanisms that represent the characteristics of the surrounding soil. The deflection of the pile in the lateral direction can be computed by numerical solution of the fourth-order equation of motion

$$E_p I_p \frac{\partial^4 y}{\partial z^4} + m_p \frac{\partial^2 y}{\partial t^2} + E_p I_p C_p \frac{\partial^5 y}{\partial z^4 \partial t} + E_p(z, y, \frac{\partial y}{\partial t})y = 0, \quad (3.1)$$

in which $E_p I_p$ is the flexural rigidity of the pile, m_p is the mass of the pile per unit length, c_p is the damping coefficient of the pile, and E_h is the lateral soil modulus.

In the above equation E_h collectively represents the characteristics of the reaction of the soil to lateral pile displacement, and can be obtained from the so-called p-y curve. This p-y curve can be obtained by observing the behavior of the soil in a thin stratum at a depth z_1 below the surface of the ground, as shown in Figure 3.2a. Figure 3.2b

shows the earth pressure distribution around the pile after the pile is driven into the soil and before harmonic surface loadings are applied, assuming that there is no bending of the pile during driving. Under these conditions, the free body cut through the soil and pile along the planes indicated in Figure 3.2a is in equilibrium. If the center of the pile is deflected a distance y , as shown in Figure 3.2c, a change in soil pressure will be generated in the form in the figure. Integration of the soil pressure and shear around the pile segment would yield an unbalanced force p per unit length of the pile. Here, the shears on the outside wall of the pile parallel to the longitudinal axis of the pile are assumed to be small in relation to the internal shear developed in the pile, and can thus be neglected.

The lateral soil modulus at depth z_1 is the slope of the secant of the corresponding p - y curve, as shown in Figure 3.3. The value of the modulus is not a direct property of the soil, but is a fitting function to correlate pile behavior with soil properties, as reflected by the p - y curve. It can be expected to be a function of depth, diameter of pile, and rate of loading. Among the soil properties that affect the value of the lateral soil modulus, the shear strength is the dominant parameter. While there is not a proportional relationship between p - y curves and shear strength of the soil, weaker p - y curves certainly result from weaker soil.

Many clays are normally consolidated, or nearly so, and will have increasing shear strength with depth. For over-consolidated clay the shear strength is approximately constant with depth, as in the case of overconsolidation of the soil caused by glaciation. However, if the overconsolidation was caused by desiccation, the shear strength may

decrease with depth. Figure 3.4 shows the shear strength distributions with depth for four different soil conditions (28).

The concept of the p-y curve, first developed by McClelland and Focht⁽²⁹⁾ implies that the behavior of the soil at a particular depth is independent of the soil behavior at all other depths. This assumption, of course, is not strictly true. However, it has been found by experiment that, for the patterns of the pile deflections which can occur in practice, the soil reaction at a point is dependent essentially on the pile deflection in the immediate vicinity of that point and not on the pile deflection some distance above or below the point^(9, 11).

3.2 Elastic Lateral Soil Modulus

Although many researchers^(30, 31) have attempted to construct the p-y curves, and hence the lateral soil modulus, for different soils using field or laboratory determined soil parameters, no definite comprehensive method has yet been established. Accuracy depends heavily upon the engineer's experience in assigning values to empirical terms. Moreover, the driving of piles into the soil medium remolds and compresses the soil, thus greatly changing its properties. The presence of piles destroys the continuity of the soil; the piles in effect acting as reinforcing bars in the soil. Furthermore, in practice, a pile often penetrates various strata, each having a different soil modulus.

Even if the soil medium is modeled as an isotropic, elastic half-space, only approximate methods of investigation are available for determining the responses of a pile, since the three-dimensional elasticity problem of a load applied to an elastic medium by an embedded rod has not been solved theoretically.

3.2.1 Degenerated Two-Dimensional Approximation

For a general three-dimensional, homogeneous, isotropic, elastic solid, the displacement vector, $\{u\} = \{u_r u_\theta u_z\}^T$, satisfies the following equation of motion

$$G\nabla^2\{u\} + (\lambda + G)\nabla(\nabla \cdot \{u\}) = \rho_s \frac{\partial^2\{u\}}{\partial t^2}, \quad (3.2)$$

in which ∇ is the divergence, ∇^2 is the Laplace operator, ρ_s is the mass density of the soil, $\nabla \cdot \{u\}$ is the dilatation, and λ and G are the Lamé constants, respectively.

The main difficulty encountered in solving the above displacement equation of motion is that the displacement components u_r , u_θ , u_z are coupled in the second term of the equation. The coupling of displacement components always exists, no matter which geometric coordinate system is employed. To simplify the solution, it is necessary to either make some basic assumptions or introduce a number of potentials and then to transform the equation into a space in which it is more easily solved. The degenerated two-dimensional approximation method employs both ideas.

Using Helmholtz's theorem, the displacement vector function can be written in terms of a scalar point function ϕ and a vector point function $\{\psi\} = \{\psi_1 \psi_2 \psi_3\}^T$ as

$$\{u\} = \nabla\phi + \nabla \times \{\psi\} \quad (3.3)$$

Since $\nabla \cdot (\nabla \times \{u\}) = 0$, by substituting Eq. (3.3) into Eq. (3.2) the equation of motion can be reduced to

$$\nabla \left[\left(\frac{\lambda + 2G}{\rho_s} \right) \nabla^2 \phi - \frac{\partial^2 \phi}{\partial t^2} \right] + \nabla \times \left[\left(\frac{G}{\rho_s} \right) \nabla^2 \{\psi\} - \frac{\partial^2 \{\psi\}}{\partial t^2} \right] = 0 \quad (3.4)$$

Equation (3.4) is satisfied if ϕ and $\{\psi\}$ separately satisfy

$$V_L^2 \nabla^2 \phi = \frac{\partial^2 \phi}{\partial t^2} \quad (3.5)$$

$$V_S^2 \nabla^2 \{\psi\} = \frac{\partial^2 \{\psi\}}{\partial t^2} \quad , \quad (3.6)$$

where V_L = velocity of the dilatational wave

$$= \left(\frac{\lambda + 2G}{\rho_s} \right)^{\frac{1}{2}} \quad (3.7)$$

and V_S = velocity of the rotational wave

$$= \left(\frac{G}{\rho_s} \right)^{\frac{1}{2}} \quad (3.8)$$

The original displacement equation of motion is thus transformed into two uncoupled equations, for which the dependent variables are ϕ and the three components of the vector function $\{\psi\}$.

The following assumptions were first made by Baranov⁽⁴⁾ for the study of the behavior of embedded foundation. The soil medium is assumed to be composed of a set of independent, infinitesimal, horizontal elastic layers that extend to infinity and can only transmit plane-strain waves. The cross-section of the pile is assumed to be circular and to have perfect contact with the soil before and during the application of the oscillating surface loads. With these assumptions, the vertical displacement component is equal to zero everywhere in the soil layer and in the pile segment, and the other two horizontal displacement components can be completely described by the dependent variables ϕ and ψ_1 , with $\psi_2 = \psi_3 = 0$.

The condition of compatibility at the interface of the soil and

pile segment can be written as

$$\begin{pmatrix} u_r(B,\theta,t) \\ u_\theta(B,\theta,t) \end{pmatrix} = \begin{pmatrix} y \cos\theta \\ -y \sin\theta \end{pmatrix} e^{i\omega t} \quad (3.9)$$

where ω represents the angular frequency of the oscillating surface loads, B is the outside radius of the pile, and θ is measured counter-clockwise from the Y axis.

Equations (3.3), (3.5) and (3.6) can be written as

$$\begin{pmatrix} u_r \\ u_\theta \end{pmatrix} = \begin{pmatrix} \frac{\partial\psi}{\partial r} + \frac{1}{r} \frac{\partial\psi_1}{\partial\theta} \\ \frac{1}{r} \frac{\partial\phi}{\partial\theta} - \frac{\partial\psi_1}{\partial r} \end{pmatrix} \quad (3.10)$$

$$(\nabla^2 + h^2)\bar{\phi}(r,\theta) = \frac{1}{r^2} \left(r^2 \frac{\partial}{\partial r} + r \frac{\partial}{\partial r} + h^2 r^2 + \frac{\partial^2}{\partial \theta^2} \right) \bar{\phi} = 0 \quad (3.11)$$

$$(\nabla^2 + k^2)\bar{\psi}_1(r,\theta) = \frac{1}{r^2} \left(r^2 \frac{\partial}{\partial r} + r \frac{\partial}{\partial r} + k^2 r^2 + \frac{\partial^2}{\partial \theta^2} \right) \bar{\psi}_1 = 0 \quad (3.12)'$$

where

$$h = \frac{\omega}{V_L} \quad (3.13)$$

$$k = \frac{\omega}{V_S} \quad (3.14)$$

$$\bar{\phi}(r,\theta) = \phi(r,\theta,t) e^{-i\omega t} \quad (3.15)$$

$$\bar{\psi}_1(r,\theta) = \psi_1(r,\theta,t) e^{-i\omega t} \quad (3.16)$$

The general solutions to Eqs. (3.11) and (3.12) are obtained by

separation of variables in the forms

$$\bar{\phi} = \sum_{n=0}^{\infty} (A_n \cos n\theta + B_n \sin n\theta) [E_n H_n^{(1)}(h_r) + H_n^{(2)}(h_r)] \quad (3.17)$$

$$\bar{\psi}_1 = \sum_{n=0}^{\infty} (C_n \cos n\theta + D_n \sin n\theta) [F_n H_n^{(1)}(k_r) + H_n^{(2)}(k_r)] \quad (3.18)$$

where $H_n^{(1)}$ and $H_n^{(2)}$ represent Hankel functions of the first and second kind of order n , and where A_n , B_n , C_n , D_n , E_n , and F_n are integration constants whose values depend upon the boundary conditions.

The displacement u_r is an even function of θ , and the displacement u_θ is an odd function. At the interface of the soil layer and the pile segment, that is at $r = B$, both displacements satisfy Eq. (3.9), and as r approaches infinity both displacements vanish. After applying all boundary conditions, Eqs. (3.17) and (3.18) reduce to

$$\bar{\phi} = A_1 \cos\theta H_1^{(2)}(h_r) \quad (3.19)$$

$$\bar{\psi}_1 = D_1 \cos\theta H_1^{(2)}(k_r) \quad (3.20)$$

with constants A_1 and D_1 satisfying the following relations

$$A_1 \frac{d}{dB} [H_1^{(2)}(hB)] + D_1 \frac{1}{B} H_1^{(2)}(KB) = y \quad (3.21)$$

$$A_1 \frac{1}{B} H_1^{(2)}(hB) + D_1 \frac{d}{dB} [H_1^{(2)}(KB)] = y \quad (3.22)$$

The stress components σ_r and $\tau_{r\theta}$ are related to the potentials ϕ and ψ_1 through the differential equations

$$\sigma_r = -\lambda h^2 \phi + 2G \left[\frac{\partial^2 \phi}{\partial r^2} + \frac{\partial}{\partial r} \left(\frac{1}{r} \frac{\partial \psi_1}{\partial \theta} \right) \right] \quad (3.23)$$

$$\tau_{r\theta} = -Gk^2 \psi_1 - 2G \left[\frac{\partial^2 \psi_1}{\partial r^2} - \frac{\partial}{\partial r} \left(\frac{1}{r} \frac{\partial \phi}{\partial \theta} \right) \right] \quad (3.24)$$

The net horizontal soil-pile interaction force p in the positive y direction is then equal to the integral

$$P = \int_0^{2\pi} [-\sigma_r(B) \cos \theta + \tau_{r\theta}(B) \sin \theta] B d\theta \quad (3.25)$$

The lateral soil modulus can be obtained by dividing the integrated value of the above equation by $ye^{i\omega t}$. The result is

$$E_h = 2\pi GkB \frac{\frac{1}{s} H_2^{(2)}(kB) H_1^{(2)}(hB) + H_2^{(2)}(hB) H_1^{(2)}(kB)}{H_0^{(2)}(kB) H_2^{(2)}(hB) + H_0^{(2)}(hB) H_2^{(2)}(kB)} \quad (3.26)$$

where s = ratio of shear wave velocity to dilatational wave velocity

$$= \frac{h}{k} = \left[\frac{1 - 2\nu}{2(1-\nu)} \right]^{\frac{1}{2}} \quad (3.27)$$

The lateral soil modulus, as expressed by Eq. (3.26), is a result from two-dimensional elasticity theory. It is indeed a function of pile diameter, rate of loading (through h and k) and shear modulus of the soil and distance from the surface of soil medium (through G). As the plane-strain waves generated by the pile movement propagate radially outward, they encounter an increasing volume of soil, thus the energy density in each wave decreases with distance from the pile. The outward transmission of energy is usually called geometric damping or radiation damping, and is properly taken into account by the imaginary part of the lateral soil modulus.

3.2.2 Three-Dimensional Static Approximation

Sezawa⁽³²⁾ derived general solutions for the wave equation, i.e., Eqs. (3.5) and (3.6). His solutions have been rearranged by Kanai⁽³³⁾ into the following integral forms:

$$u_r = \int_0^\infty dq \sum_m \left\{ -A_m \frac{1}{h^2} \frac{\partial J_m(qr)}{\partial r} e^{-\alpha z} + B_m \frac{m}{q^2} \frac{J_m(qr)}{r} e^{-\beta z} + C_m \frac{\beta}{k^2} \frac{J_m(qr)}{\partial r} e^{-\beta z} \right\} \cos m\theta e^{i\omega t} \quad (3.28a)$$

$$u_\theta = \int_0^\infty dq \sum_m \left\{ -A_m \frac{m}{h^2} \frac{J_m(qr)}{r} e^{-\alpha z} - B_m \frac{1}{q^2} \frac{\partial J_m(qr)}{\partial r} e^{-\beta z} - C_m \frac{m\beta}{k^2} \frac{J_m(qr)}{r} e^{-\beta z} \right\} \sin m\theta e^{i\omega t} \quad (3.28b)$$

$$u_z = \int_0^\infty dq \sum_m \left\{ A_m \frac{\alpha}{h^2} e^{-\alpha z} - C_m \frac{q^2}{k^2} e^{-\beta z} \right\} J_m(qr) \cos m\theta e^{i\omega t} \quad (3.28c)$$

where

$$q^2 = \alpha^2 + h^2 = \beta^2 + k^2, \quad (3.29)$$

h and k are defined by Eqs. (3.13) and (3.14), and $J_m(qr)$ is Bessel's function of order m . In Eq. (3.28), terms with constants A_m are related to dilatational waves and terms with constants B_m or C_m are related to rotational waves. These constants are determined by the appropriate boundary conditions. The associated stresses are given as

$$\sigma_z = G \int_0^\infty dq \sum_m \left\{ A_m \frac{-2q^2 + k^2}{h^2} e^{-\alpha z} + 2C_m \frac{\beta q^2}{h^2} e^{-\beta z} \right\} J_m(qr) \cos m\theta e^{i\omega t} \quad (3.30a)$$

$$\tau_{zr} = G \int_0^{\infty} dq \Sigma_m \left\{ A_m \frac{2\alpha}{h^2} \frac{\partial J_m(qr)}{\partial r} e^{-\alpha z} - B_m \frac{m\beta}{q^2} \frac{J_m(qr)}{r} e^{-\beta z} - C_m \frac{q^2 + \beta^2}{k^2} \frac{\partial J_m(qr)}{\partial r} e^{-\beta z} \right\} \cos m\theta e^{i\omega t} \quad (3.30b)$$

$$\tau_{\theta z} = G \int_0^{\infty} dq \Sigma_m \left\{ -A_m \frac{2m\alpha}{h^2} \frac{J_m(qr)}{r} e^{-\alpha z} + B_m \frac{\beta}{q^2} \frac{\partial J_m(qr)}{\partial r} e^{-\beta z} + C_m \frac{m(q^2 + \beta^2)}{k^2} \frac{J_m(qr)}{r} e^{-\beta z} \right\} \sin m\theta e^{i\omega t} \quad (3.30c)$$

All the integrals in Eqs. (3.28) and (3.30) are improper integrals with Bessel functions or derivatives of Bessel functions as the integrand. Except for a few special cases, their integration requires the use of Fourier's double integral theorem⁽³⁴⁾ which is mathematically difficult. For the static cases, that is when ω approaches zero, the degree of difficulty is much less than for the dynamic cases. The three-dimensional elasticity problem of a static load applied to a point inside an elastic half-space, which is one of the static cases, has been solved theoretically by Mindlin⁽³⁵⁾. The Mindlin equation, which gives the x component of displacement as produced by a single concentrated force P located at any arbitrary point (0,0,c) within an isotropic half-space and acting in the x direction, is

$$u_x(x,y,z) = \frac{P(0,0,c)}{16\pi(1-\nu)G} \left\{ \frac{3-4\nu}{R_1} + \frac{1}{R_2} + \frac{2cz}{R_2^3} + \frac{4(1-\nu)(1-2\nu)}{R_2+z+c} + x^2 \left[\frac{1}{R_1^3} + \frac{3-4\nu}{R_2^3} - \frac{6cz}{R_2^5} - \frac{4(1-\nu)(1-2\nu)}{R_2(R_2+c+z)^2} \right] \right\} \quad (3.31)$$

in which ν is Poisson's ratio, c is the z distance of the load below the

surface xy boundary plane, and

$$R_1^2 = x^2 + y^2 + (z - c)^2$$

$$R_2^2 = x^2 + y^2 + (z + c)^2 .$$

The Mindlin equation permits one to characterize completely an elastic half-space. Penzien ⁽¹⁾ used this equation to obtain a three-dimensional approximate static soil modulus. The horizontal interaction force between soil and pile is assumed to be uniformly distributed along the length of the pile within each height interval $2h$, but the magnitude of the interaction force varies from one interval to the next. The general expression for the weighted average deflection at the outside pile radius B , caused by a uniformly distributed interaction force over the height of one interval, is obtained by substituting the intensity of the interaction force $p(0,0,\bar{c} \pm h)$ between points $(\bar{c} - h)$ and $(\bar{c} + h)$ for the concentrated load $P(0,0,c)$ in Eq. (3.31) and integrating with respect to c over this interval. The static modulus is then taken as the ratio of intensity p and the weighted average deflection at the outside pile radius. For Poisson's ratio ν equal to 0.5, the lateral soil modulus obtained is

$$E_h(B,z) = \frac{8\pi E}{3} \left\{ \sinh^{-1} \frac{\bar{c} + h - z}{B} - \sinh^{-1} \frac{\bar{c} - h + z}{B} \right. \\ \left. + \sinh^{-1} \frac{\bar{c} + h + z}{B} - \sinh^{-1} \frac{\bar{c} - h + z}{B} \right. \\ \left. + \frac{2}{3B^2} \left[\frac{B^2(\bar{c} + h) - 2B^2z + (\bar{c} + h)z^2 + z^3}{\sqrt{B^2 + (\bar{c} + h + z)^2}} \right. \right. \\ \left. \left. - \frac{B^2(\bar{c} - h) - 2B^2z + (\bar{c} - h)z^2 + z^3}{\sqrt{B^2 + (\bar{c} - h + z)^2}} \right] \right\}$$

$$\begin{aligned}
& - \frac{2}{3} \left[\frac{z - (\bar{c} + h)}{\sqrt{B^2 + (\bar{c} + h - z)^2}} - \frac{z - (\bar{c} - h)}{\sqrt{B^2 + (\bar{c} - h - z)^2}} \right] \\
& + \frac{4}{3} \left[\frac{B^2 z + (\bar{c} + h)z^2 + z^3}{\sqrt{[B^2 + (\bar{c} + h - z)^2]^3}} - \frac{B^2 z + (\bar{c} - h)z^2 + z^3}{\sqrt{[B^2 + (\bar{c} - h - z)^2]^3}} \right]^{-1} \quad (3.32)
\end{aligned}$$

Figure 3.5 shows the variation of average static lateral soil modulus with slenderness ratio L/B of pile.

3.3 Elastic Vertical Soil Modulus

The dynamic responses of the pile pertinent to the vertical motion of the pile head can be obtained using the same assumptions for the soil as in the lateral case. The damped equation of motion of the pile in the vertical direction is

$$m_p \frac{\partial^2 w}{\partial t^2} - A_p E_p \frac{\partial^2 w}{\partial z^2} - A_p E_p C_v \frac{\partial^3 w}{\partial z^2 \partial t} + E_v(z,t)w = 0 \quad (3.33)$$

in which w is the vertical displacement of the pile, A_p is the area of the pile's cross-section, c_v is the damping coefficient in the vertical direction. E_v , the counterpart of E_h , defines the vertical soil reaction acting at height z on a pile element dz , and is called the vertical soil modulus.

The vertical soil modulus obtained from the two-dimensional theory of elasticity, based on the assumption that the cross-section of the pile is circular and the pile has perfect contact with the soil before and during the application of the oscillating surface load, is

$$E_v = 2\pi GBk \frac{H_1^{(2)}(KB)}{H_0^{(2)}(KB)} \quad (3.34)$$

Like the lateral soil modulus, E_v can also be estimated from the three-dimensional theory of elasticity by assuming that the vertical interaction force between soil and pile is uniformly distributed along the length of the pile within each height interval $2h$, but that the magnitude of the interaction force varies from one interval to the next. For Poisson's ratio equal to 0.5, the vertical soil modulus for a pile segment between the elevations $(\bar{c} - h)$ and $(\bar{c} + h)$ is then

$$\begin{aligned}
 E_v = \frac{8\pi E}{3} \left\{ 2 \sinh^{-1} \frac{\bar{c} + h - z}{B} - 2 \sinh^{-1} \frac{\bar{c} - h - z}{B} \right. \\
 + 2 \sinh^{-1} \frac{\bar{c} + h + z}{B} - 2 \sinh^{-1} \frac{\bar{c} - h + z}{B} \\
 + \frac{\bar{c} - h - z}{\sqrt{B^2 + (\bar{c} - h - z)^2}} - \frac{\bar{c} + h - z}{\sqrt{B^2 + (\bar{c} + h - z)^2}} \\
 - \frac{\bar{c} + h + z}{\sqrt{B^2 + (\bar{c} + h + z)^2}} - \frac{\bar{c} - h + z}{\sqrt{B^2 + (\bar{c} - h + z)^2}} \\
 - 4z \left[\frac{1}{\sqrt{B^2 + (\bar{c} + h + z)^2}} - \frac{1}{\sqrt{B^2 + (\bar{c} - h + z)^2}} \right] \\
 \left. + 2z \left[\frac{B^2 + z^2 + z(\bar{c} + h)}{\sqrt{[B^2 + (\bar{c} + h + z)^2]^3}} - \frac{B^2 + z^2 + z(\bar{c} - h)}{\sqrt{[B^2 + (\bar{c} - h + z)^2]^3}} \right] \right\}^{-1} \quad (3.35)
 \end{aligned}$$

Figure 3.6 shows the variation of average static vertical soil modulus with slenderness ratio of the pile.

3.4 Inelastic Soil Moduli

Although the soil moduli evaluated by assuming that the soil is composed of a set of ideal elastic plane-strain layers can account for the geometric distribution of elastic-wave energy, they do preclude the

loss of energy caused by the inelastic behavior of the real soil, as reflected in the nonlinear p-y curves. When the soil is set in vibration by the movement of the pile, some of the elastic energy is always converted into heat, and plastic behavior may take place. The various mechanisms by which non-radiating energy is lost are collectively termed internal friction.

The internal friction can be measured by the specific damping capacity, defined by the ratio of the energy dissipated in taking a specimen through a stress cycle to the elastic energy stored in the specimen when the strain is a maximum. In terms of the p-y curve, specific damping capacity represents the ratio of the area enclosed by the hysteresis loop to the total area under the p-y curve when y is a maximum.

A simple method to account for the energy loss due to internal friction is to model the soil medium as an isotropic viscoelastic soil which has the same specific damping capacity as the real soil. The problem is then transformed from one in linear elasticity to one in linear viscoelasticity. The identification of a problem in linear elasticity with one in linear viscoelasticity is guided by the correspondence principle⁽³⁶⁾. The soil modulus for a linear viscoelastic medium can be obtained by simply replacing the real shear modulus G by a complex shear modulus G^* composed of real and imaginary components, each of which is a function of frequency, as

$$G^*(\omega) = G_1(\omega) + iG_2(\omega) \quad (3.36)$$

in which $G_1(\omega)$ is the elastic component and $G_2(\omega)$ is the viscous component.

For a Voigt solid, the stress is the sum of two terms, one

proportional to the strain and the other proportional to the rate of change of strain, and the displacement equation of motion is similar to Eq. (3.2) but with the operator $\lambda + \lambda' \left(\frac{\partial}{\partial t}\right)$ in place of λ , and $G + G' \left(\frac{\partial}{\partial t}\right)$ takes the place of G . Since four constants λ , λ' , G and G' must be used for a Voigt solid, simplifying assumptions have often been made about relations between them in order to treat the problem. Since deformations involve dilatation as well as shear, it is logical to specify that the ratio of G' to G equals the ratio of $K' = \lambda' + \frac{2}{3}G'$ to compressibility $K = \lambda + \frac{2}{3}G$ (37). K' is known as the dilatational viscosity, G' being the shear viscosity. In this case, Eq. (3.36) becomes

$$G^*(\omega) = G \left(1 + i\omega \frac{G'}{G}\right) \quad (3.37)$$

3.5 Dynamic Stiffnesses of a Single Pile

3.5.1 Method of Calculation

After the lateral and vertical soil moduli, which define the interaction forces between soil and pile, are obtained, one needs to solve Eqs. (3.1) and (3.33) in order to evaluate the impedance functions at the head of a single pile. The impedance functions of a pile can be defined as the transfer functions describing the ratios between the dynamic complex response displacements on the head of the pile and its surface harmonic exciting force.

The steady-state solution to Eq. (3.1) can be written as

$$y(z, t) = y(z) e^{i\omega t} \quad (3.38)$$

where complex amplitude is

$$y(z) = y_1(z) + iy_2(z) \quad (3.39)$$

Substituting Eq. (3.38) into Eq. (3.1) yields an ordinary differential equation

$$E_p I_p (1 + ic_p \omega) \frac{d^4 y(z)}{dz^4} + y(z) (E_h - m_p \omega^2) = 0 \quad (3.40)$$

In the same way, the steady-state solution to Eq. (3.33) can be written as

$$w(z, t) = w(z) e^{i\omega t} \quad (3.41)$$

Substituting Eq. (3.41) into Eq. (3.33) yields

$$-A_p E_p (1 + iB_v \omega) \frac{d^2 w(z)}{dz^2} + w(z) (E_v - m_p \omega^2) = 0 \quad (3.42)$$

Solutions of Eqs. (3.40) and (3.42) are straightforward, if the soil moduli are constant with respect to z . Their general solutions are the combination of sine and cosine functions, in the case of Eq. (3.42), plus hyperbolic sine and hyperbolic cosine functions, in the case of Eq. (3.40). The dynamic stiffness of the pile can be determined as the end force producing unit displacement of the pile head. This unit displacement and the other end conditions represent the boundary conditions from which the integration constants can be established.

In this study, Eqs. (3.40) and (3.42) are discretized by finite element method. The masses of the pile are lumped at n selected points along the length of the pile. The interaction effects between soil medium and pile are simulated by boundary springs. The spring constants are calculated using Eqs. (3.32), (3.35) and (3.48). A two-dimensional beam element with three degrees of freedom at each end is used to formulate the stiffnesses of a pile segment between two neighboring control points. The

total stiffness and mass matrices are then assembled and combined together to form the total dynamic stiffness matrix. Finally, a well established static-condensation subroutine is used to obtain the dynamic stiffness matrix at the head of a single pile.

3.5.2 Tip Conditions

End conditions theoretically constitute part of the boundary conditions in the determination of dynamic pile stiffnesses. At the embedded end, the movement of the pile generates reactions from the soil lying below the level of the tip. It is necessary to determine the degree of fixity at the tip in order to evaluate correctly the responses of the pile.

For a pile subjected to lateral movement, a study by Novak⁽⁵⁾ shows that the pile stiffnesses and damping are almost the same for a fixed tip and a pinned tip when the length of the pile is larger than about twenty-five times its radius. The influence of the tip condition appears less than is the case with static loads^(38, 39). This conclusion is in general agreement with results of lateral load tests performed by the Bureau of Reclamation⁽⁴⁰⁾, which concludes that increase in length does not improve lateral resistance if the pile is embedded enough to prevent movement in the lower portion.

For a pile subjected to vertical movement, the reaction of the soil at the tip has been described approximately by Novak⁽⁵⁴⁾ as the reaction of an elastic half-space to the vertical motion of a surface-supported rigid circular disk having the same radius as the pile. Using this kind of approximation, the continuity of displacements across the imaginary horizontal plane which is at the same level as the pile tip is not guaranteed.

For the static case, the degree of fixity at the tip can be

approximated by, again, using the Mindlin equation. The Mindlin equation, which gives the vertical component of displacement produced by a single concentrated force Q located at an arbitrary point $(0,0,c)$ within an isotropic half-space and acting in the vertical direction is

$$u_z(x,y,z) = \frac{Q(0,0,c)}{16\pi G(1-\nu)} \left[\frac{3-4\nu}{R_1} + \frac{8(1-\nu)^2 - (3-4\nu)}{R_2} + \frac{(z-c)^2}{R_1^3} + \frac{(3-4\nu)(z+c)^2 - 2cz}{R_2^3} + \frac{6cz(z+c)^2}{R_2^5} \right] \quad (3.43)$$

where

$$R_1 = [(x+y)^2 + (c-z)^2]^{\frac{1}{2}}$$

$$R_2 = [(x+y)^2 + (c+z)^2]^{\frac{1}{2}} .$$

Equation (3.43) is singular at the loading point, but this difficulty can be avoided by assuming that the vertical reaction of the soil below the level of the pile tip is uniformly distributed over the tip area. After changing Eq. (3.43) from Cartesian coordinates into cylindrical coordinates and setting z and c equal to the length of the pile, the vertical displacement at the center of the pile tip caused by a uniformly distributed reaction force is obtained by substituting the intensity of the reaction force q for the concentrated load Q and integrating with respect to r from 0 to the outside pile radius B . The result is

$$w(0,0,L) = \frac{B^2 q}{8G(1-\nu)} \left\{ (3-4\nu)B + [8(1-\nu)^2 - (3-4\nu)](B^2 + 4L^2)^{\frac{1}{2}} - \frac{2L^2(3-4\nu)}{[B^2+4L^2]^{\frac{3}{2}}} - \frac{8L^4}{(B^2+4L^2)^{\frac{5}{2}}} \right\} \quad (3.44)$$

where L is the length of the pile. The stiffness constant is then taken as the ratio of the total reaction force over the tip area to the approximate deflection at the center of the pile tip as expressed by Eq. (3.44).

3.6 A Suggested Procedure in the Study of Pile Behavior

The soil moduli based on two-dimensional elasticity theory, expressed by Eqs. (3.26) and (3.34), involve calculation of Hankel functions. To make the solutions accessible to practicing engineers, Novak⁽⁵⁾ has transformed these solutions into a dimensionless form and fitted the solutions by polynomials for a few different values of Poisson's ratio. His results for lateral soil modulus are presented as curves of parameter S versus dimensionless frequency a , where S and a are defined as

$$S = \frac{E_p h}{G} \quad (3.45)$$

$$a = \frac{B\omega}{V_s} \quad (3.46)$$

The S versus a curve for a Poisson's ratio of 0.25 is reproduced in Figure 3.7. S consists of both real and imaginary parts. The real part, which accounts for the stiffness and inertia effects of the soil medium surrounding the pile, levels off at high frequency; while the imaginary part, which accounts for the radiation damping effect, is almost a linear function of frequency. The biggest shortcoming in Figure 3.7 is that both the real and imaginary parts of S start from zero at zero frequency. This means that there is no interaction between pile and soil medium for the static case if Baranov's approximation is employed. For offshore structures, for which responses in the low frequency range are, in general, more important than responses in the high frequency range, this shortcoming is intolerable.

Although approximate static soil moduli based on three-dimensional elasticity theory, expressed by Eqs. (3.32) and (3.35) are more suitable for the study of the behavior of piles used in the foundation of offshore structures, they alone do not account for the inertia and radiational damping effects of the soil medium.

3.6.1 A Proposed Procedure

As pointed out in Subsection 3.2.2, the calculation of the soil moduli using three-dimensional elasticity theory involved complicated infinite integrals for the dynamic case, but approximate solutions are available for the static case. It is desirable therefore to extend the solution for the static case to the dynamic case by making certain assumptions which will yield satisfactory solutions for engineering applications while by-passing the difficult mathematics.

In general, the lateral soil modulus can be written as

$$E_h(z, B, G, \nu, \omega) = E_{h1}(z, B, G, \nu, \omega) + iE_{h2}(z, B, G, \nu, \omega) \quad (3.47)$$

in which z is the vertical distance from the surface of the soil, B is the outside radius of the pile, G is the shear modulus of the soil, ν is the Poisson's ratio of the soil, ω is the angular frequency at which the foundation is excited, and E_{h1} and E_{h2} are the real and imaginary parts of the lateral soil modulus, respectively.

It is proposed here to separate the dynamic soil modulus into two factors so that

$$E_h(z, B, G, \nu, \omega) = E_h(z, B, G, \nu, 0)F_h(\omega) \quad (3.48)$$

where $E_h(z, B, G, \nu, 0)$ is the static lateral soil modulus based on elasticity theory and $F_h(\omega)$ is a frequency-dependent shape function. Approximate

value of the static lateral soil modulus $E_h(z, B, G, \nu, 0)$ can be obtained by using the Mindlin equation. For pile foundation of offshore structure, it is reasonable to use a Poisson's ratio ν of 0.5, because of the presence of the sea water above. Thus, the static lateral soil modulus can be calculated by using Eq. (3.32).

The frequency-dependent shape function $F_h(\omega)$ can be constructed using the numerical solution of the dynamic Lamb's problem. Its value equals 1 when ω equals 0. So, in essence, Eq. (3.48) is an asymptotic solution. For the static case, the equation gives the same lateral soil modulus as that obtained by the static three-dimensional approximation method. The procedure for constructing $F_h(\omega)$ will be stated in detail in Subsection 3.6.3

After the static lateral soil modulus and the frequency dependent shape function have been obtained, Eq. (3.48) can then be substituted into Eq. (3.40), which, in turn, can be discretized by numerical method to obtain the dynamic stiffnesses of a single pile. The method of discretization of Eq. (3.40) is already mentioned in Subsection 3.5.1.

Like the lateral soil modulus, the vertical soil modulus can be separated into the product of the static vertical soil modulus and a frequency-dependent function $F_v(\omega)$. For Poisson's ratio equals 0.5, the vertical soil modulus can be calculated by using Eq. (3.35). The value of $F_v(\omega)$ also equal 1, when ω equals 0. Again, $F_v(\omega)$ can be constructed using the numerical solution of the dynamic Lamb's problem. After the vertical soil modulus is obtained, it is substituted into Eq. (3.42), which is then discretized to obtain the dynamic stiffness of a single pile in the vertical direction .

For a given pile in a given soil medium, the lateral soil modulus E_h is a function of two parameters: z and ω . The lateral soil modulus can be visualized as a complex-valued surface in the space with E_h , z and ω as its rectangular coordinates. Eq. (3.48) separates the dynamic lateral soil modulus into the product of two functions of one parameter. It is similar to the method of separation of variables commonly employed in the solution of partial differential equation. All it says is that the complex-valued surface can be constructed from two orthogonal functions of a single variable.

Theoretically, approximate value of the dynamic lateral soil modulus can be obtained by using the solution of the Lamb's problem directly. The problem of a single harmonic force acting at an interior point of a homogeneous half-space is called the Lamb's problem. However, since the closed-form solution of the Lamb's problem is currently not available, one has to use numerical solution. Eq. (3.48) is one way of calculating the dynamic lateral soil modulus by numerical method. It is desirable since the approximate static lateral soil modulus obtained by using the Mindlin equation has a closed form, as given by Eq. (3.32). The Mindlin equation gives the solution of the static case of the Lamb's problem. Therefore, the procedure for calculating the dynamic lateral soil modulus mentioned above can be viewed as an indirect use of the numerical solution of the Lamb's problem. For the Lamb's problem, the only important boundary condition is the stress-free boundary condition, which will be examined both intuitively and numerically in the next two Subsections.

The basic assumption underlying the proposed procedure is that the force-displacement relationship of the interaction effect between the pile and the soil medium will assume the same shape with respect to

to frequency regardless of which position of this effect is in consideration.

3.6.2 Examination of the Procedure

Measurement of the applicability of the proposed procedure is tantamount to measurement of the importance of the stress-free surface boundary condition upon the response of a uniform elastic half-space to the application of a harmonic concentrated force at a certain depth H below the surface.

A procedure, which separates the force-displacement relationship at the point where the external force is applied into the product of a frequency dependent function and a function of other material and geometric properties, is unsuitable for finite systems such as a beam or a string of finite length and having any prescribed boundary conditions. For a finite system, resonance at discrete points along the frequency axis is possible. If a finite system is forced to vibrate near two different resonant frequencies, it will, in general, assume two entirely different vibration shapes. If an external harmonic force happens to be placed near one of the nodes of a vibration mode, the response of the system is very sensitive to the exact location of the force applied around the natural vibration frequency of that mode. It is therefore impossible to separate the force-displacement relationship at the point where the force is applied into the proposed form. But for an infinite system where resonance is not possible, such as an elastic half-space or elastic full-space, the procedure proposed is much better than for the finite system.

From Mindlin's solution of the problem of a static force acting inside an elastic half-space, it can be shown that except when the force

is applied near the free surface, the relationship between the force and the average displacement along a horizontal circle with the loading point as its center is not sensitive to change in the location of the applied force. In other words, only in the immediate vicinity of the loading point does the displacement have a significant magnitude and the stress-free boundary condition of the elastic half-space have little effect.

The problem of a single force acting at an interior point of a homogeneous half-space is usually called Lamb's problem. We consider the dynamic version of Lamb's problem in the time domain instead of in the frequency domain, and designate the shortest time for waves to reach the surface from the loading point inside the elastic half-space as t_1 . With a finite wave speed there always exists a finite boundary surface, at any finite time $t < t_1$, which is yet uninfluenced by the loading initiated at $t = 0$. In other words, the response of the elastic half-space is exactly like an infinite medium with the same material properties during this time interval. For $t > t_1$, only one ray, which impinges the stress-free boundary at right angles, will reflect directly back to the buried wave source. All other rays, no matter if they are incident rotational waves or incident dilatational waves, will reflect and travel away from the surface point directly above the loaded point after impinging on the stress-free surface⁽⁴²⁾. In actual application to the pile problem, the region where Eq. (3.48) is violated is within one to two pile diameters from the surface of soil medium. Because of the presence of the sea water, the soil properties in that region can be expected to differ significantly from that of the rest of the soil medium. So the influence of the stress-free boundary condition is, intuitively, not significant.

3.6.3 Frequency-Dependent Shape Functions

The real measure of the applicability of the proposed procedure is to compare it with results obtained by three-dimensional elasticity theory. Numerical solutions of the dynamic Lamb's problem have been obtained by Kida et al.⁽⁴³⁾ The homogeneous elastic half-space is first divided into two regions: One region is an elastic layer with the stress-free surface of the elastic half-space as its upper boundary and a plane which contains the point where the external harmonic force is applied and is parallel to the half-space surface as its lower boundary; and the other a region which encloses the rest of the elastic half-space. Displacement fields like those expressed by Eq. (3.28) are prescribed for both regions. The unknown constants are then evaluated by matching displacements and stresses across the interface of the two elastic regions.

In cylindrical coordinates (r, θ, z) , the horizontal displacement component which is produced by a single concentrated, horizontal, harmonic force $Pe^{i\omega t}$ acting at any arbitrary point $(0, 0, z_f)$ within an isotropic half-space can be expressed as

$$u(r, \theta, z) = \frac{Pwe^{i\omega t}}{GV_s} [f_{11} + if_{21} + (f_{12} + if_{22}) \cos 2\theta], \quad (3.49)$$

in which f_{11} , f_{12} , f_{21} , f_{22} are frequency-dependent displacement functions. For most of the cases, the displacement function f_{22} is negligible when compared with the values of the other three displacement functions. All the high order terms with respect to θ have been neglected in Eq. (3.49). The displacement functions are more easily expressed in terms of dimensionless parameters c , c_f and a , which are defined as

$$c = \frac{\omega z}{V_s} \quad (3.50)$$

$$c_f = \frac{\omega z_f}{V_s} \quad (3.51)$$

$$a = \frac{\omega r}{V_s} \quad (3.52)$$

Figures 3.8, 3.9 and 3.10 show f_{11} , f_{12} , and f_{21} for cases where $c = c_f$, $\nu = 0.5$ and a equals 0.1, 0.2, 0.4, respectively. It is apparent that all three displacement functions converge horizontally as c exceeds 1.0. This indicates strongly that the stress-free boundary condition indeed does not play an important role in the response of the isotropic half-space when the external force is applied away from that surface. Hence, the proposed procedure appears to be feasible for engineering applications.

When the value of a is small and the value of c is reasonably large, the horizontal displacement component in Eq. (3.49) for cases where $c = c_f$ can be adequately approximated by

$$u(r, \theta, c = c_f) = \frac{P e^{i\omega t}}{32\pi Gr} \left[(6 + 2\cos 2\theta) - i5a \right]. \quad (3.53)$$

To actually apply the procedure, it is necessary to have a reasonably accurate frequency-dependent shape function $F_h(\omega)$. This can be achieved by first graphing the complex displacement $f_{11} + if_{21}$ against a , with $c = c_f$ kept large, 10 say. The resulting complex function $f_{11} + if_{21}$ is then normalized such that its value at $a = 0$ is one. The inverse function of the normalized complex function $f_{11} + if_{21}$ versus a is a good shape function. Figure 3.11 presents the shape

function obtained in this way for Poisson's ratio of 0.5 and for values of a in the range from 0 to 2.0.

This procedure can also be used to evaluate the vertical responses of a single pile. For this, one needs a frequency-dependent function $F_V(\omega)$ which is the counterpart of $F_h(\omega)$ in the vertical direction. $F_V(\omega)$ can be obtained in exactly the same way as $F_h(\omega)$. In cylindrical coordinates, the vertical displacement component produced by a single concentrated vertical harmonic force $Qe^{i\omega t}$ acting at an arbitrary point $(0,0,z_f)$ within an isotropic half-space can be expressed as

$$w(r,\theta,z) = \frac{Qe^{i\omega t}}{GV_s} (F_1 + iF_2) . \quad (3.54)$$

Figure 3.12 presents curves of F_1 and F_2 for three different cases where $c = c_f$ and Poisson's ratio $\nu = 0.5$. In the low frequency range, the vertical displacement can be adequately approximated by

$$w(r,\theta, c = c_f) = \frac{Qe^{i\omega t}}{32\pi Gr} (4 - i5a) . \quad (3.55)$$

Figure 3.11 presents the vertical shape function for the case where Poisson's ratio equals 0.5 and a ranges from 0 to 1.5.

The degree of approximation involved in deriving the soil modulus by the proposed procedure is less than that by the degenerated two-dimensional theory of elasticity. In the degenerated two-dimensional approximation, the important parameter z is eliminated in the early stage of development as mentioned in Section 3.2. The stress-free boundary condition is completely ignored. Therefore, the soil modulus so obtained is independent of parameter z . Whereas the soil modulus obtained by the proposed procedure will vary with parameter z the same

way the static soil modulus varies. The stiffnesses of the pile foundation for an example offshore structure obtained by the two different approximation methods are given in Figures 4.3 to 4.6. Comparisons of the results of the two methods are included in Chapter 4.

3.7 Dynamic Stiffnesses of a Pile Group

3.7.1 Pile Group Without Pile-Cap

Both theory and tests have shown that the total bearing value of a group of friction piles, particularly in clay, may be less than the product of the bearing value of an individual pile multiplied by the number of piles in the group^(44,45,46,47). The reduction in value per pile depends on the size and shape of the pile group and on the size, shape, spacing, and length of the piles. No reduction due to grouping occurs when the piles are end-bearing piles; however, for groups which partake of both actions, only that portion taken in friction is reduced.

For offshore structures, several "efficient formulae" are in use for assigning reductions to the carrying capacity of piles in a group. Some of these were established before the actions as explained by soil mechanics were understood and have been incorporated in building codes. This fact, together with the desire to keep footings as small as possible and the wish not to increase footing sizes for one type of pile over those required for another, have resulted in the general use of the specified minimum spacings as the maximums.

For offshore structures, the factors considered in designing pile foundations are generally different from those considered when designing pile foundations for onshore structures. In general, there is no need to limit either the size of the footing or the size of the piles. Piles used in the foundations of offshore structures are generally quite long

and uniformly spaced. It is not uncommon to find these piles exceeding 150 feet in length and spaced 5 diameters apart.

To calculate the total dynamic stiffness matrix of the pile group where there is no reduction of carrying capacity due to grouping, it is advantageous to choose the centroid of the pile group in the horizontal plane as the reference point. Then the dynamic stiffness coefficients are defined as forces that must act at the centroid to produce a sole unit displacement at the reference point. From this definition, the dynamic stiffness coefficients of the pile group are

$$\begin{aligned}
 K_{hh} &= \sum_i k_{hh}^e \\
 K_{vv} &= \sum_i k_{vv}^e \\
 K_{rr} &= \sum_i k_{rr}^e + \sum_i k_{vv}^e x_i^2 \\
 K_{hr} &= \sum_i k_{hr}^e
 \end{aligned} \tag{3.56}$$

in which k_{hh}^e , k_{vv}^e , k_{rr}^e are the dynamic stiffness coefficients defined at the head of an element pile for the horizontal, vertical and rocking motions, respectively; k_{hr}^e is the coupling term between horizontal and rocking motions; x_i is the horizontal distance parallel to the plane of action from the center of the cross-section of i^{th} element pile to the centroid of the pile group; k_{hh} , k_{vv} , k_{rr} are the dynamic stiffness coefficients of the pile group for the horizontal, vertical and rocking motions. The summations are to be taken over all piles in the group.

3.7.2 Group Effect of Laterally Loaded Piles

When piles within a group are spaced less than five diameters apart, like those in most onshore pile foundations, interaction effects

between individual piles become prominent and can no longer be neglected. Because of these interaction effects between piles within a group, the actual dynamic stiffness coefficients at the reference point of the pile group will be less than those calculated by Eq. (3.56). Each dynamic stiffness coefficient of a pile group as expressed by Eq. (3.56) has to be multiplied by a reduction factor in order to obtain the actual dynamic stiffness coefficient. The reduction factors are, in general, not unique.

For laterally loaded pile groups, the reduction factor, which is normally called the group efficiency, can be obtained by using Eq. (3.53). Equation (3.53) gives, approximately, the horizontal component of displacement which is parallel and is produced by a single, concentrated, horizontal, harmonic force applied at a certain depth below the surface of a uniform, elastic half-space. When the frequency of the applied concentrated force is small, i.e., when the applied force is close to the static force, the imaginary part of Eq. (3.53) can be neglected, yielding

$$u_x(r, \theta, c = c_f) = \frac{P(0,0,c_f)}{32\pi Gr} (6 + 2\cos 2\theta) . \quad (3.57)$$

The above equation can also be obtained independently from the Mindlin equation (Eq. (3.31)), thereby giving a cross check between the numerical solution and the closed-form static solution. Equation (3.57) can be rearranged as

$$u_x(r, \theta, c = c_f) = \frac{P(0,0,c_f)}{32\pi Gr} (8\cos^2\theta + 4\sin^2\theta) . \quad (3.58)$$

The function $(8\cos^2\theta + 4\sin^2\theta)$ expresses the trace of an ellipse whose major axis is twice as long as its minor axis. Therefore, the displacement field as expressed by Eq. (3.58) depends upon the direction as well as the distance from the loading position.

Consider now the determination of the group efficiency for a laterally loaded pile group consisting of M individual piles. By applying a single, concentrated horizontal force at a certain depth of one of the intended pile axes within the pile group and using Eq. (3.58), one can obtain the horizontal displacements of all the other unloaded pile axes at the same level as the applied force. The displacements are denoted by u_{rs} , where r refers to the pile axis being loaded, $S = 1, 2, \dots, M$, and $r \neq s$. The horizontal displacement at the loaded pile axis, u_{rr} , can be approximated by taking the weighted average of the displacement around the outside radius of the pile. By moving the concentrated horizontal load to each of the M intended pile axes within the pile group, one can obtain $M \times M$ displacement functions. The group efficiency for the laterally loaded pile group can now be approximated by

$$\zeta = \frac{\sum_{r=1}^M u_{rr}}{\sum_{r=1}^M \sum_{s=1}^M u_{rs}} \quad (3.59)$$

3.7.3 Pile Group With Pile-Cap

To calculate the total dynamic stiffness matrix of a pile group with a pile-cap, the stiffness and damping contributions from the pile-cap should be considered. After they have been determined, the remaining procedure does not differ from that required for the case of a pile group without a pile cap. One simple method is to take the dynamic stiffnesses of the pile-cap as that for a rigid, massless plate resting on an elastic half-space. One major assumption in calculating the impedance functions of a rigid, massless plate resting on an elastic half-space has been that the rigid foundation is welded to the supporting

ground, that there is no slip between the foundation and the soil medium. Whether the dynamic stiffnesses of a pile group with a pile-cap will equal the stiffnesses of the pile group plus the stiffnesses of the pile-cap on a homogeneous half space is also questionable. It is not attempted here to elaborate on the justification of these assumptions. The dynamic stiffnesses of the pile-cap are completely neglected in this investigation.

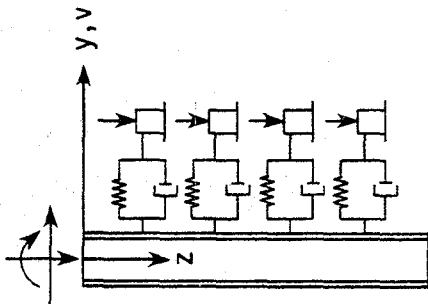


FIG. 3.1 MODEL OF PILE AND SOIL

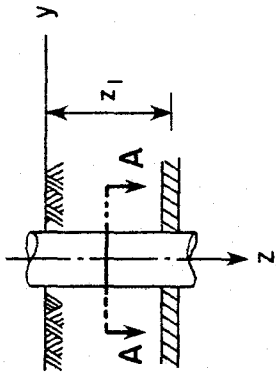


FIG. 3.2a

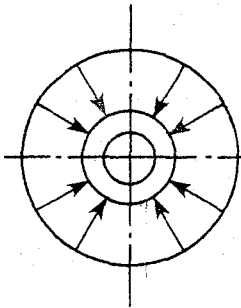


FIG. 3.2b EARTH PRESSURE DISTRIBUTION PRIOR TO LATERAL MOVEMENT

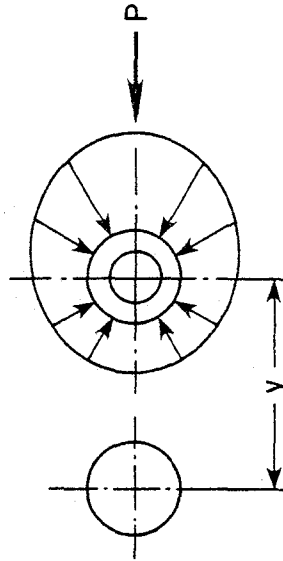


FIG. 3.2c EARTH PRESSURE DISTRIBUTION AFTER LATERAL MOVEMENT

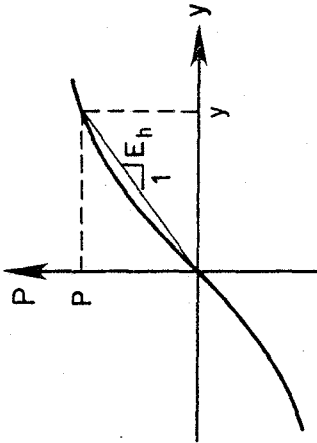


FIG. 3.3 DEFINITION OF LATERAL SOIL MODULUS

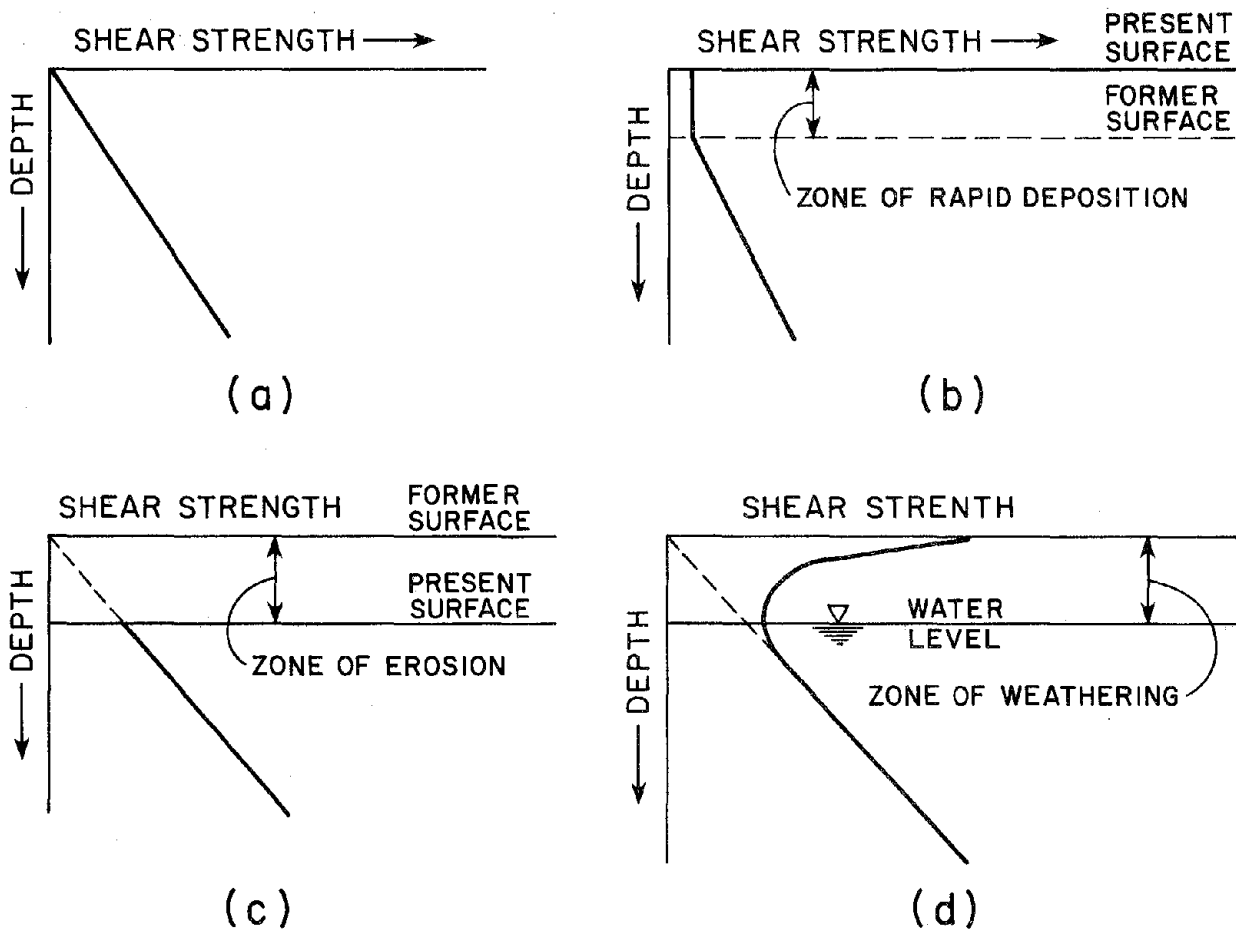


FIG. 3.4 GENERALIZED SHEAR STRENGTH PROFILES: (a) NORMALLY CONSOLIDATED CLAY; (b) NORMAL PROFILE MODIFIED BY RAPID DEPOSITION OF NEW SEDIMENT; (c) NORMAL PROFILE MODIFIED BY EROSION; (d) NORMAL PROFILE MODIFIED BY DESICCATION AND SHRINKAGE ABOVE THE WATER TABLE. (AFTER McCLELLAND)

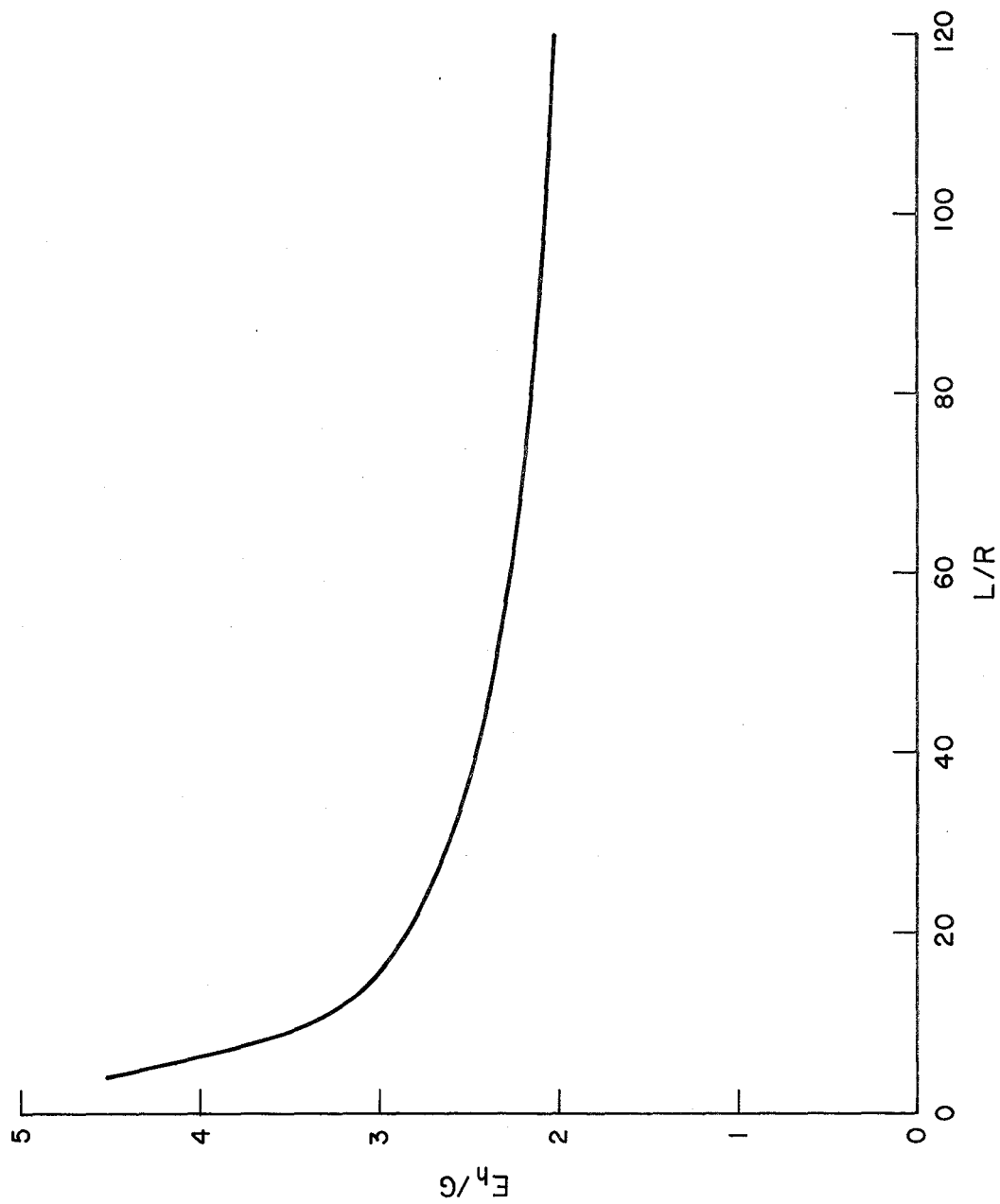


FIG. 3.5 AVERAGE LATERAL SOIL MODULUS VERSUS SLENDERNESS RATIO L/R OF PILE AT ZERO FREQUENCY

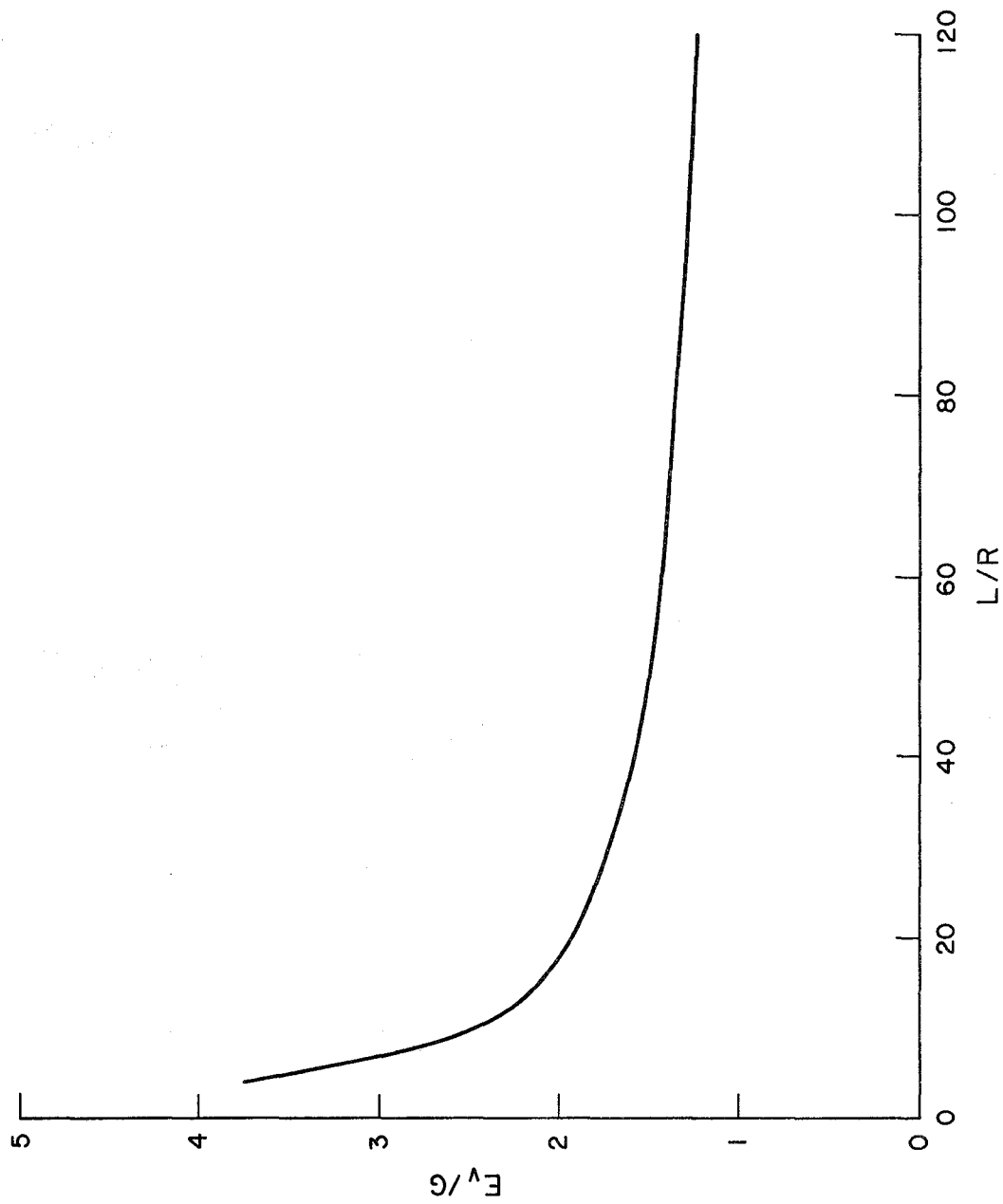


FIG. 3.6 AVERAGE VERTICAL SOIL MODULUS VERSUS SLENDERNESS RATIO L/R OF PILE AT ZERO FREQUENCY

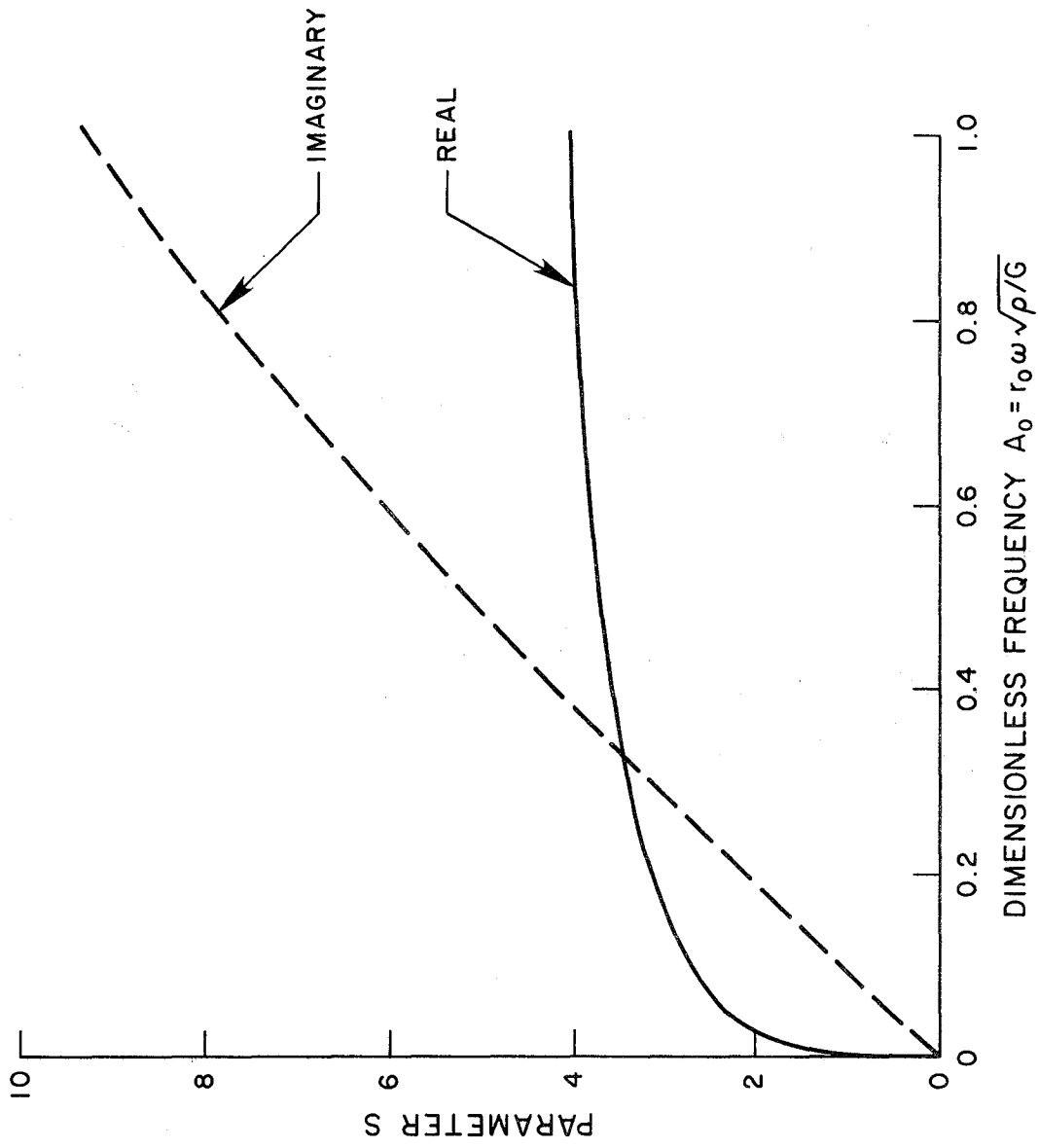
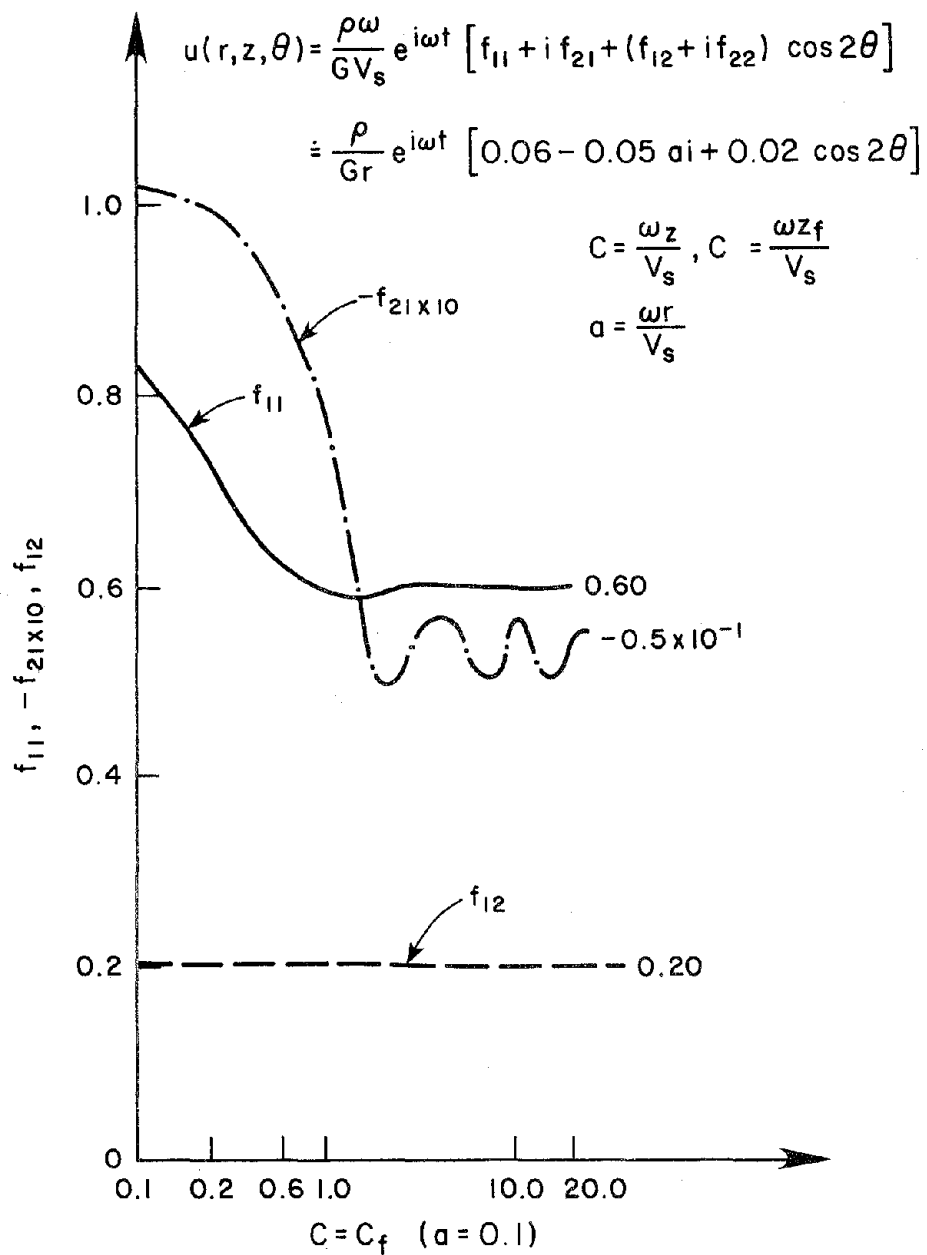


FIG. 3.7 PARAMETER S FOR $\nu = 0.25$. (AFTER NOVAK)


 FIG. 3.8 HORIZONTAL DISPLACEMENT FUNCTIONS FOR $a = 0.1$

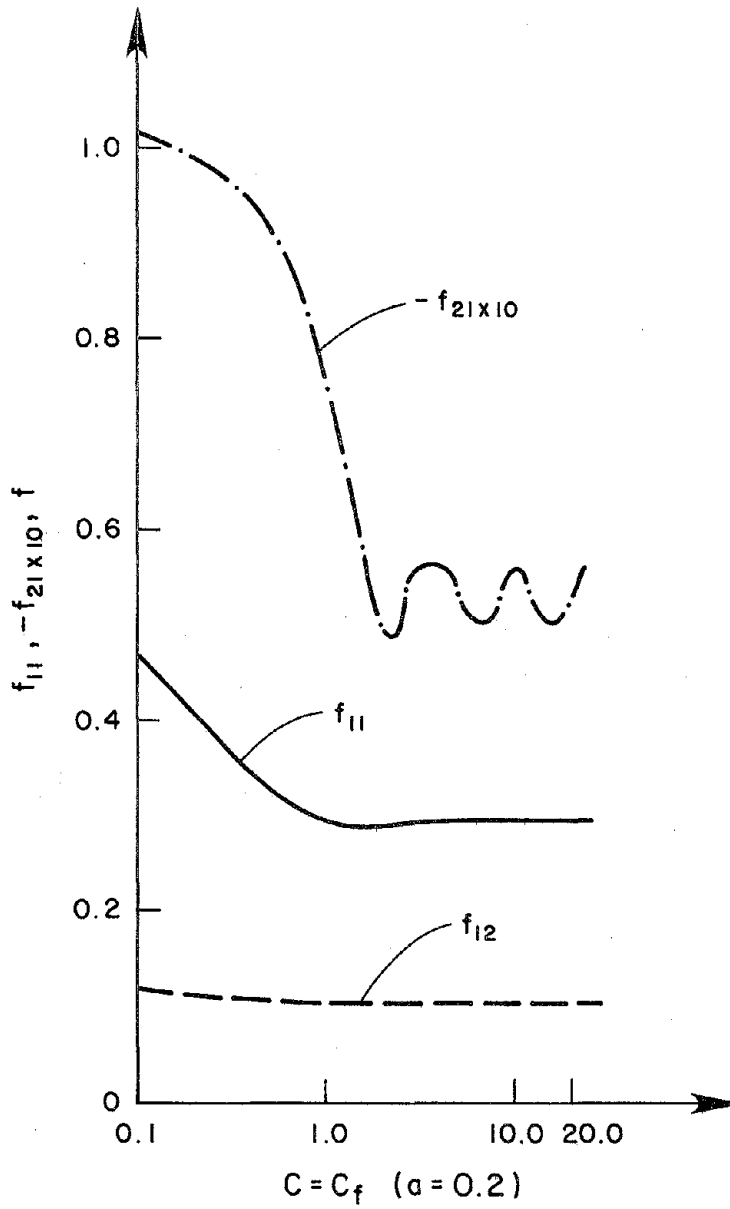


FIG. 3.9 HORIZONTAL DISPLACEMENT FUNCTIONS FOR $\alpha = 0.2$

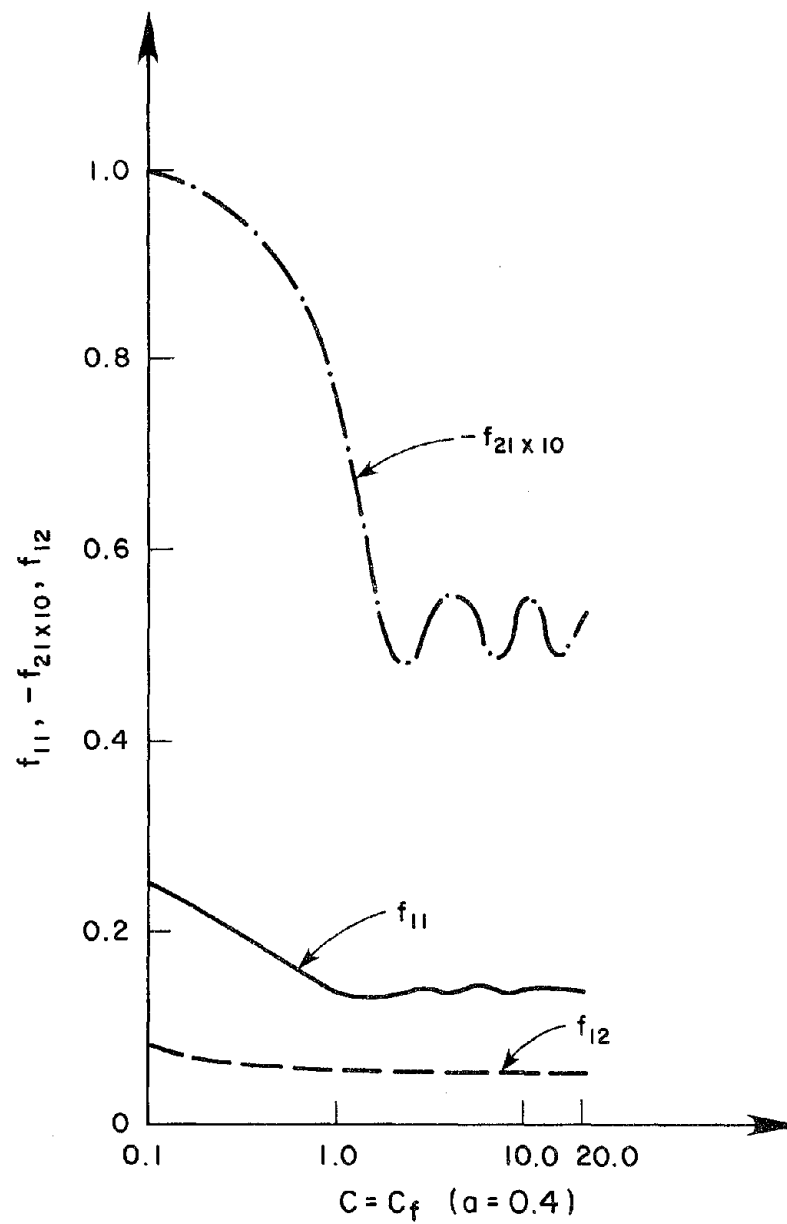


FIG. 3.10 HORIZONTAL DISPLACEMENT FUNCTIONS FOR $a = 0.4$

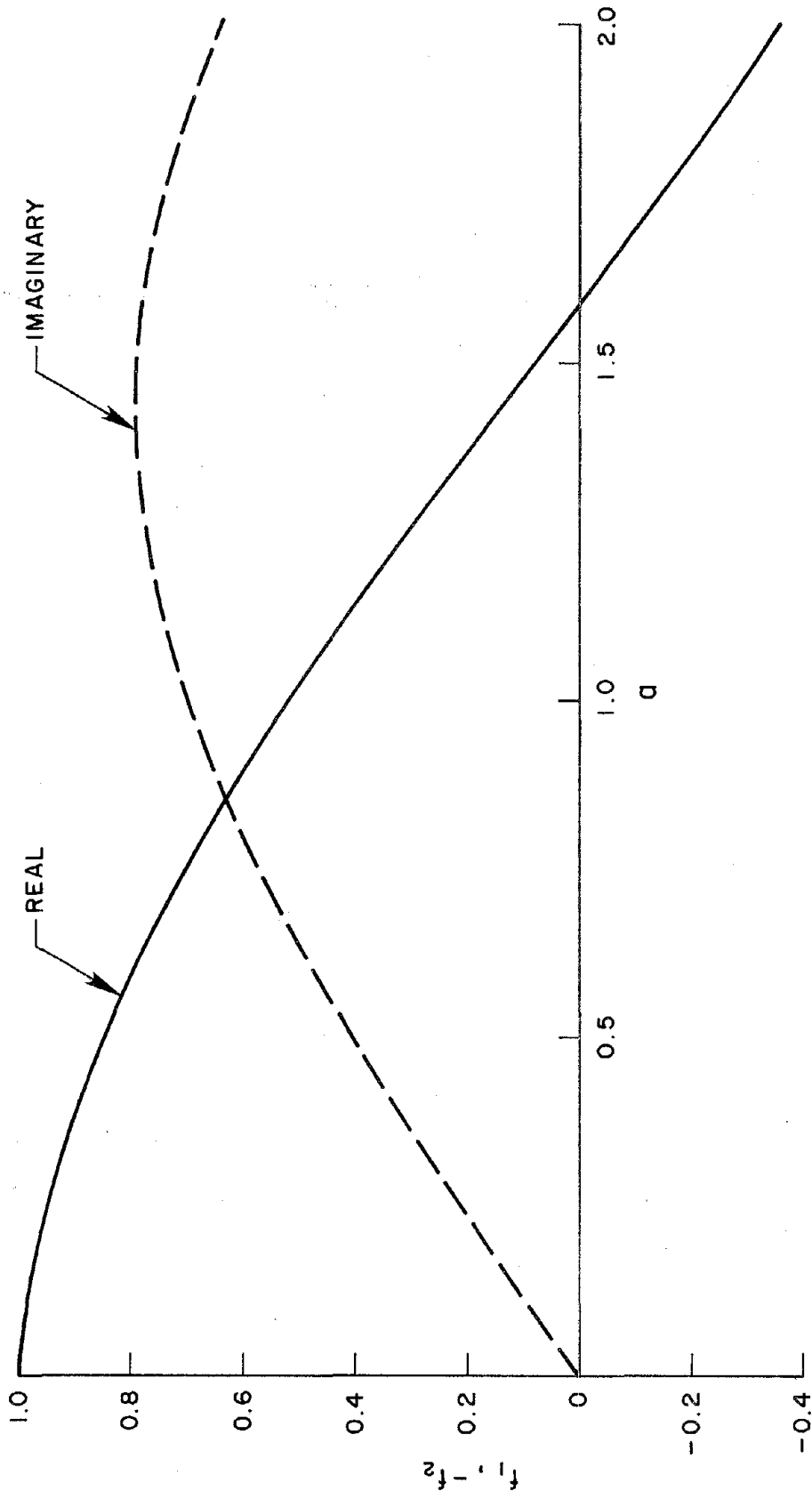


FIG. 3.11 HORIZONTAL SHAPE FUNCTION $F_n(\omega)$ FOR $\nu = 0.5$

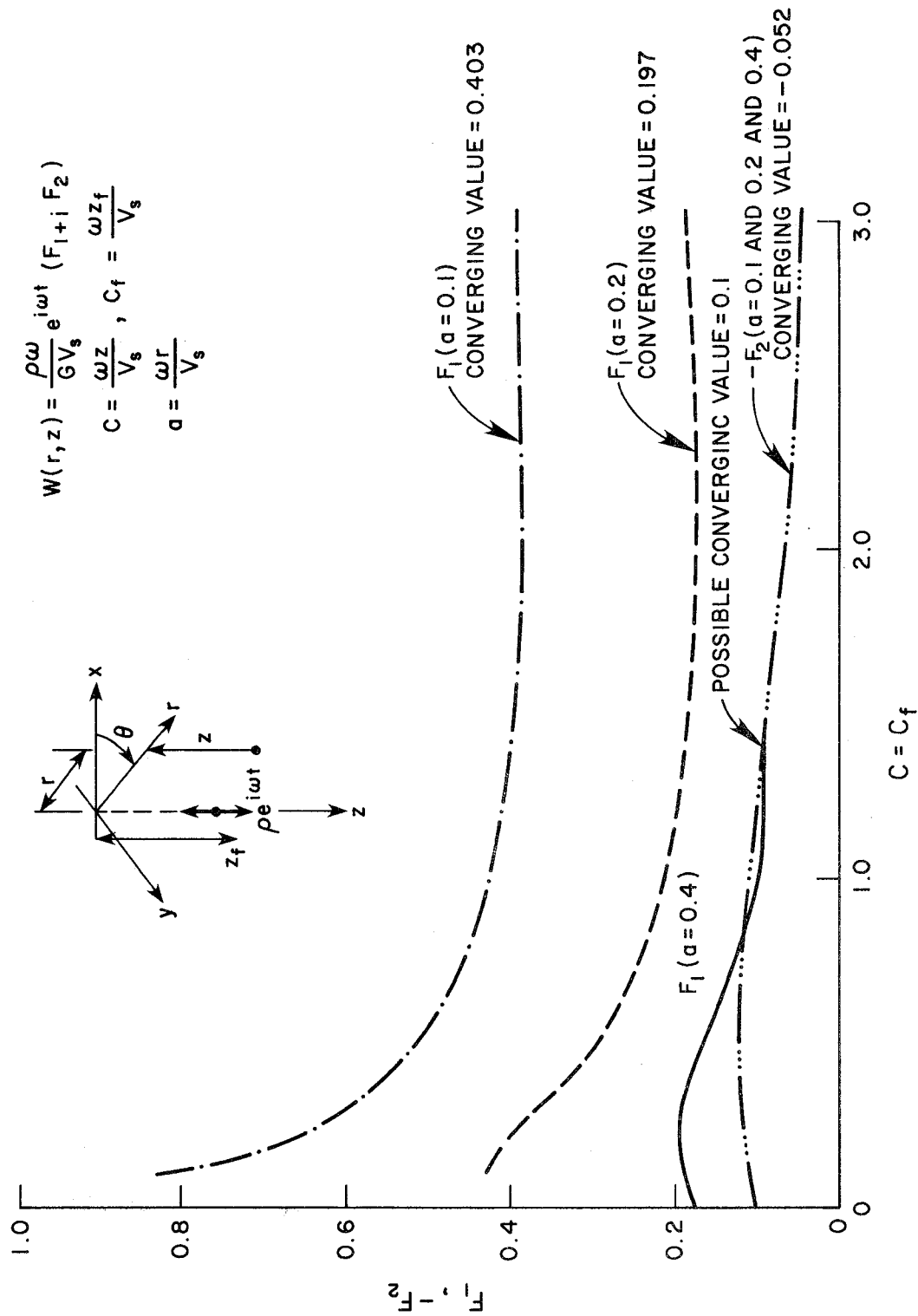


FIG. 3.12 VERTICAL DISPLACEMENT FUNCTIONS

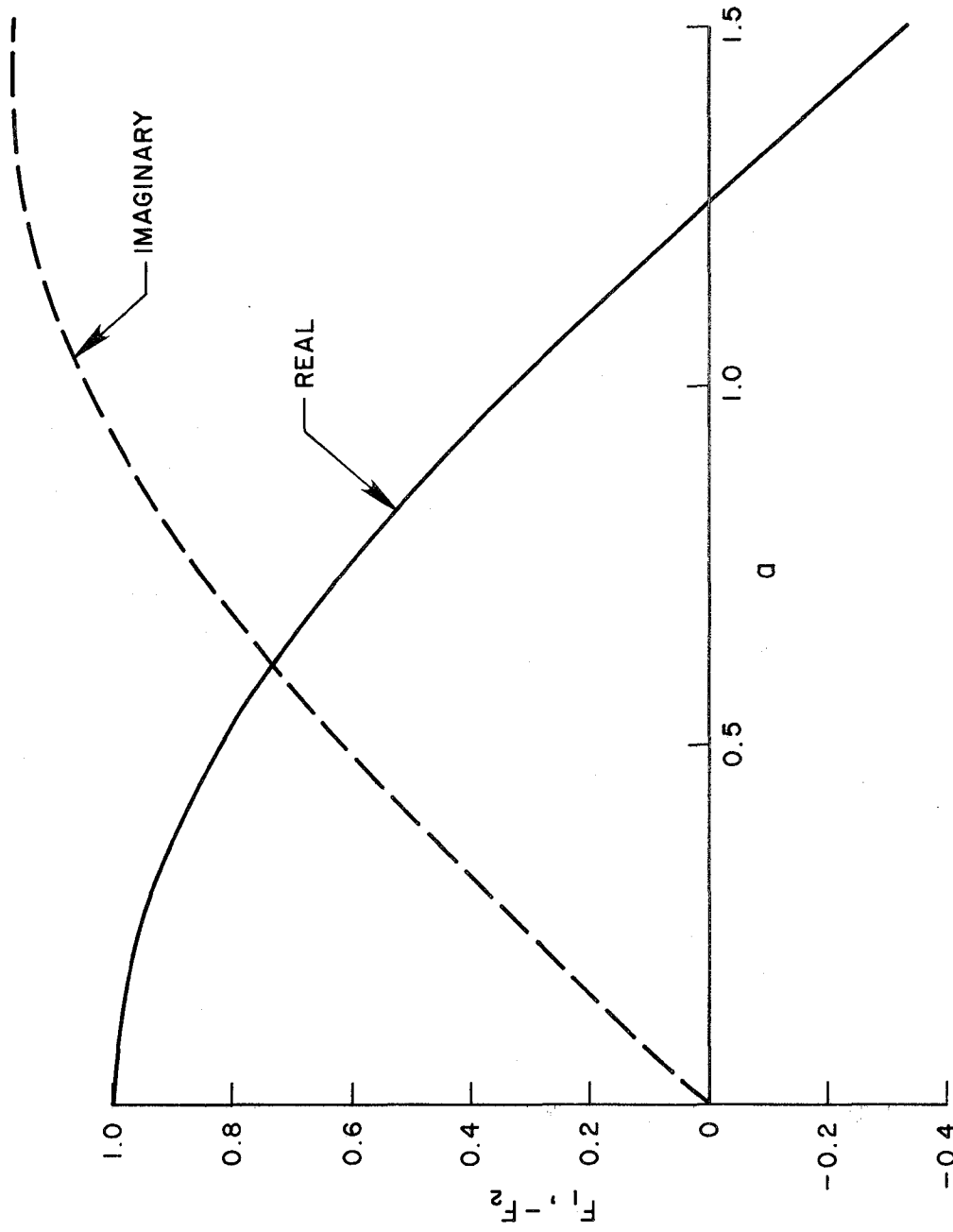


FIG. 3.13 VERTICAL SHAPE FUNCTION $F_v(\omega)$ FOR $\nu = 0.5$

4. EXAMPLE PROBLEM SOLUTION

To study the interaction effects between an offshore structure and its pile foundation during strong motion earthquakes, a problem is analyzed in this chapter as an example. The modeling method described in Chapter 3 is used to calculate the dynamic stiffness matrices of the pile foundations. These foundation stiffnesses are obtained for two different soil conditions. The dynamic responses of the complete structure-foundation system subjected to a recorded strong motion earthquake are obtained. The effects of interaction are examined by comparing these responses with responses obtained for the same structure supported on rigid foundations.

4.1 The Mathematical Model

4.1.1 Structural System

The example offshore structure, shown in Figure 4.1, is a steel structure consisting of four main vertical legs with cross-bracing members connected to these legs at 7 different levels. The height from sea floor to the upmost bracing level is 551.5 feet. The width from centerline of the main legs at the upmost bracing level is 185 feet. The width at the lowest bracing level is 250 feet. The still water depth is 460 feet. All members in the main structural system are tubular; member sizes are given in Table 4.1. The modulus of elasticity of the steel is 4.32×10^9 psf.

The N-S component of the ground acceleration recorded at the 1940 El Centro, California, Earthquake is used as the prescribed excitation. The orientation of this earthquake excitation is assumed along the X-axis.

and coincides with an axis of structural plan symmetry. Thus, the problem can be treated as two-dimensional in the X-Y plane.

A mathematical model is selected to simulate the most relevant features of the response of the structure when subjected to strong motion earthquakes. The formulation of equations of motion of the structure is discussed in Section 2.1. The idealized structure, shown in Figure 4.2, has 16 nodal points. Each nodal point, in the two dimensional case, has three degrees of freedom--two translational and rotational. Altogether, there are 48 degrees of freedom in the structure model. Six of them, associated with two lowest nodal points, are contact degrees of freedom. The vertical members are allowed to have both axial deformation and flexural deformation. The level bracing assemblies are idealized as comparatively rigid diagrams. Although further simplification of the structure model that will reduce the total number of degrees of freedom is possible, it is not made in order to test the general features of the computer program. The total structural stiffness matrix is given in Appendix A. All the mass of the main vertical legs and cross-bracing members are lumped at the nodal points. The nodal masses are augmented by the so-called added mass of the surrounding water as indicated by Eq. (2.15) and the mass of the deck structure. The inertia coefficient used in the calculation of the vertical masses is taken as 2.0. The unit weight of the water is assumed equal to 62.4 pcf. The weight of the deck structure is 55,000 kips. The total diagonal mass matrix is also given in Appendix A.

Since the outside diameter of the main vertical legs of the structure, 30 feet, is large in comparison with the wave height normally expected for earthquake excitations, the structure can be classified as a large volume structure⁽⁶⁰⁾. It is, therefore, reasonable to neglect

the hydrodynamic damping effects. The structural damping matrix is calculated assuming Rayleigh damping. Because the complete structure-foundation system does not possess normal modes in the classical sense, as discussed in Section 2.3, the damping matrix is calculated using the properties of the associated undamped fixed base structure. The Rayleigh damping mass and stiffness coefficients are assigned so that the damping ratios of the first two modes are equal to 0.05. The damping matrix can also be calculated using Eqs. (2.43), (2.44) and (2.45).

4.1.2 Pile Foundation

The foundations of the example offshore structure are made of steel pipe piles. Each foundation contains 8 piles. The piles are clustered around the perimeter of each main vertical leg of the structure. After having been driven, they are grouted into the pile sleeves. The piles are so designed that their friction holding capacity within the sub-strata is sufficient to support the weight of the deck and their cross-sectional resistance counteracts the horizontal forces to which the upper parts of the structure are subjected.

The outside diameter of the piles used is 72 inches and the wall thickness is 2.5 inches. The depth of penetration of the piles is 200 feet.

Using the linear theory of a homogeneous, isotropic, elastic half-space, the stiffness of the pile foundations is calculated for two different soil conditions. A Poisson's ratio of 0.5 is assumed for both soils. The characteristic shear wave velocities of the foundation soils are 760 ft./sec. and 1140 ft./sec., corresponding respectively to soil shear moduli of 2×10^6 psf and 4.5×10^6 psf. From now on, the pile foundation embedded in soil with characteristic shear wave velocity equal to 760 ft./sec. is referred to as Foundation A and the one embedded in soil with

characteristic shear wave velocity equal to 1140 ft./sec. is referred to as Foundation B.

The vertical stiffness at zero frequency of a single pile in Foundation A is found to be 2.34×10^5 kips/ft. Multiplying this stiffness by the number of piles in the pile foundation and the estimated pile-group efficiency, a static vertical stiffness equal to 1.28×10^6 kips/ft. is obtained for Foundation A. The dynamic vertical stiffness of Foundation A versus frequency in the range of 0 to 10 cps is shown in Figure 4.3 together with the dynamic vertical stiffness of Foundation A based on two-dimensional elasticity theory.

The static stiffness of a single pile in Foundation A is estimated to be 7.6×10^4 kips/ft. and the static rotational stiffness is found to be 9.10×10^6 kip-ft./rad. The frequency-dependent lateral stiffnesses, rotational stiffness and the coupling stiffness of Foundation A based on both two- and three-dimensional elasticity theory are given in Figures 4.4, 4.5 and 4.6. Their values at zero frequency are 5.56×10^5 kips/ft., 2.57×10^8 kip-ft./rad. and 3.14×10^6 kips/rad., respectively.

By comparing the curves in Figure 4.3, one can clearly see that there is considerable difference between the results based on the two different theories. The stiffness based on the three-dimensional theory of elasticity has an almost constant real part and a linear imaginary part in the frequency range of practical interest. The imaginary part is small in comparison with the real part. The imaginary part of the stiffness based on two-dimensional elasticity theory is also linear in shape but its value is much higher than that based on three-dimensional theory. Around 3 cps, the two real parts are equal; below that, the real part based on two-dimensional theory is smaller; above that, larger. The curves in Figures 4.4 through 4.6 also show a similar trend.

The vertical stiffness at zero frequency of Foundation B is estimated to be 1.02×10^6 kips/ft. and the static rotational stiffness is found to be 3.62×10^8 kip-ft./rad.

The real part of any stiffness function of a single pile should start from its static value at zero frequency. In the low frequency range, it should be a decreasing function of frequency due to the inertia effect of the soil medium. From Figures 4.3 to 4.8, one can clearly see that the stiffnesses based on the degenerated two-dimensional theory of elasticity fail to observe that two rules. The reason is, as already mentioned in Section 3.6, there is no interaction forces between pile and soil medium at zero frequency in the two-dimensional approximation. At 1 cps, which is close to the resonance frequency of the first mode of the example structure, the real part of the vertical stiffness obtained by two-dimensional approximation is only about 70 percent of its static value. So, it is better to use the stiffnesses obtained by the three-dimensional theory of elasticity.

4.2 Results of Analysis

The numerical procedure described in Chapter 2 is used to carry out the dynamic elastic analysis of the model offshore structure supported on both Foundation A and Foundation B. The seismic responses of the model structure supported on rigid foundations are also obtained. The results of all dynamic analysis are based on the combined effects of the first 3 modes of vibration of the fixed-base structure and the motions of the 6 contact degrees of freedom.

4.2.1 Mode Shapes and Natural Periods of Vibration

Mode shapes and natural periods of vibration of all modes of vibration for the associated fixed-base structure are obtained. The

first three mode shapes are shown in Figure 4.7 and the first ten natural periods of vibration are given in Table 4.2.

4.2.2 Lateral Deflections and Accelerations

Figure 4.8 shows the lateral deflections at the upmost cross-bracing level caused by the prescribed earthquake excitation of the structure on Foundation A. Figure 4.9 shows the lateral deflection response at the same level of the structure on Foundation B. Figure 4.10 shows the lateral deflection response of the structure on a rigid foundation.

Under dynamic conditions, the lateral level displacements change continuously and their maximum values usually occur at different times. To summarize the maximum dynamic displacement response of the structure, the maximum dynamic displacements for all the cross-bracing levels are jointed together to obtain an envelope of maximum lateral displacements. The envelopes for each of the three different foundations are presented in Figure 4.11.

Comparisons of the curves in Figures 4.8 through 4.11 indicate that the dynamic responses are significantly different for models with and without foundation flexibility. The structure-soil-pile interaction effects are quite prominent. The maximum lateral displacement at the upmost cross-bracing level of the rigid-base structure model is 0.86 feet which is about 3.2 times that of the model supported on Foundation A. The maximum lateral deflections of the structure model supported on Foundation B are, in general, about 20 percent higher than the maximum deflections of the model supported on Foundation A.

To examine further the interaction effects between the structure and its foundation, the maximum lateral acceleration envelopes are also plotted and presented in Figure 4.12. The lateral acceleration time

histories at the lowest cross-bracing level, which is only 10 feet above the sea floor, are given for the three foundations in Figures 4.13, 4.14 and 4.15. The maximum lateral acceleration envelope of the rigid-base model is quite similar to the mode shape of vibration of its first normal mode, whereas the envelopes of the two models with foundation flexibility are quite different. The large contributions of the second and the third modes to the lateral accelerations of the models with foundation flexibility are quite apparent when subjected to the prescribed earthquake excitation.

4.2.3 Maximum Leg Axial Forces

Because of the large distance between the two main vertical legs, which is 250 feet wide at the lowest cross-bracing level, the maximum axial forces developed in the legs at a certain elevation form a couple which is considerably larger than the leg bending moments developed at the same elevation. The couples formed by the maximum axial forces in the main legs are almost equal to the maximum dynamic overturning moments. The envelopes of the maximum axial forces in the main legs of the three different structure-foundation models are shown in Figure 4.16. These envelopes show that the maximum dynamic overturning moments of the rigid-base model are considerably larger than those of models with foundation flexibility. The maximum dynamic overturning moments developed in the structure model supported on Foundation B are about 40 percent higher than those developed in the model supported on Foundation A below cross-bracing level 5.

4.3 Discussion of the Results of the Example Problem

A. The real parts of the stiffnesses of the pile foundation calculated by the two-dimensional theory of elasticity are smaller than those

calculated by the method described in Chapter 3, around the first natural frequency of vibration of the rigid-base structure, while the imaginary parts are considerably larger. The discrepancies between the stiffnesses based on the two different methods will be larger if the diameter of the piles used in the foundation is reduced or the characteristic shear wave velocity is increased.

B. The stiffnesses of the pile foundation calculated by the three-dimensional theory of elasticity will have a constant real and a linear imaginary part in the frequency range of practical interest. The imaginary parts are small in comparison with their associated real parts. This indicates that for pile foundations consisting of pipe piles of large diameter, like those used in the example structure, the radiation damping in the foundation system is small. For pile foundations made of piles of small diameter, however, the radiation damping may be larger.

C. Comparisons of the dynamic responses of the models with and without foundation flexibility indicate that the effects of structure-foundation interaction are quite prominent for the example structure. Interaction effects are important because the ratio of structure stiffness to foundation stiffness is large for the particular offshore structure. The contributions of the second and third modes of vibration are more apparent when the foundation flexibility is included in the model. The reason for causing the difference in the responses of the three different structure-foundation models would be more clear if enough members of the complex frequency response functions are output and plotted. Unfortunately, due to the negligence of the author, this has not been done. From the lateral displacement responses at the first cross-bracing level, as shown in Figures 4.8 to 4.10, the first periods of vibration of the three models can be estimated. The estimated first

periods of vibration do not differ much. So, one possible explanation is that the inclusion of the radiation damping in the foundation model will increase the damping ratio of the total structure-foundation system.

D. A reduction in the foundation stiffness increases the structure-foundation interaction effects. Correct estimation of the foundation stiffness is quite important if the dynamic responses of the structure are to be correctly predicted. This, in turn, depends upon a correct estimation of the properties of the soil strata in which the piles are embedded.

Table 4.1 Details of Tower Members

Member	Diameter	Thickness
<u>Main Vertical</u>		
Level 1 - 2	30'0" O.D.	8"
2 - 3	30'0" O.D.	8"
3 - 4	30'0" O.D.	9"
4 - 5	30'0" O.D.	10"
5 - 6	30'0" O.D.	11"
6 - 7	30'0" O.D.	12"
<u>Horizontals</u>		
Up to level 5	72" O.D.	2"
Below level 5	72" O.D.	3"
<u>Diagonals</u>		
Up to level 5	72" O.D.	2"
Below level 5	72" O.D.	3"
<u>Foundation</u>		
Piles	72" O.D.	2½"

Table 4.2 Natural Periods of Vibration
of the Fixed-Base Structure

Mode	Period of Vibration (sec)
1	0.988
2	0.272
3	0.138
4	0.124
5	0.102
6	0.087
7	0.076
8	0.046
9	0.043
10	0.029

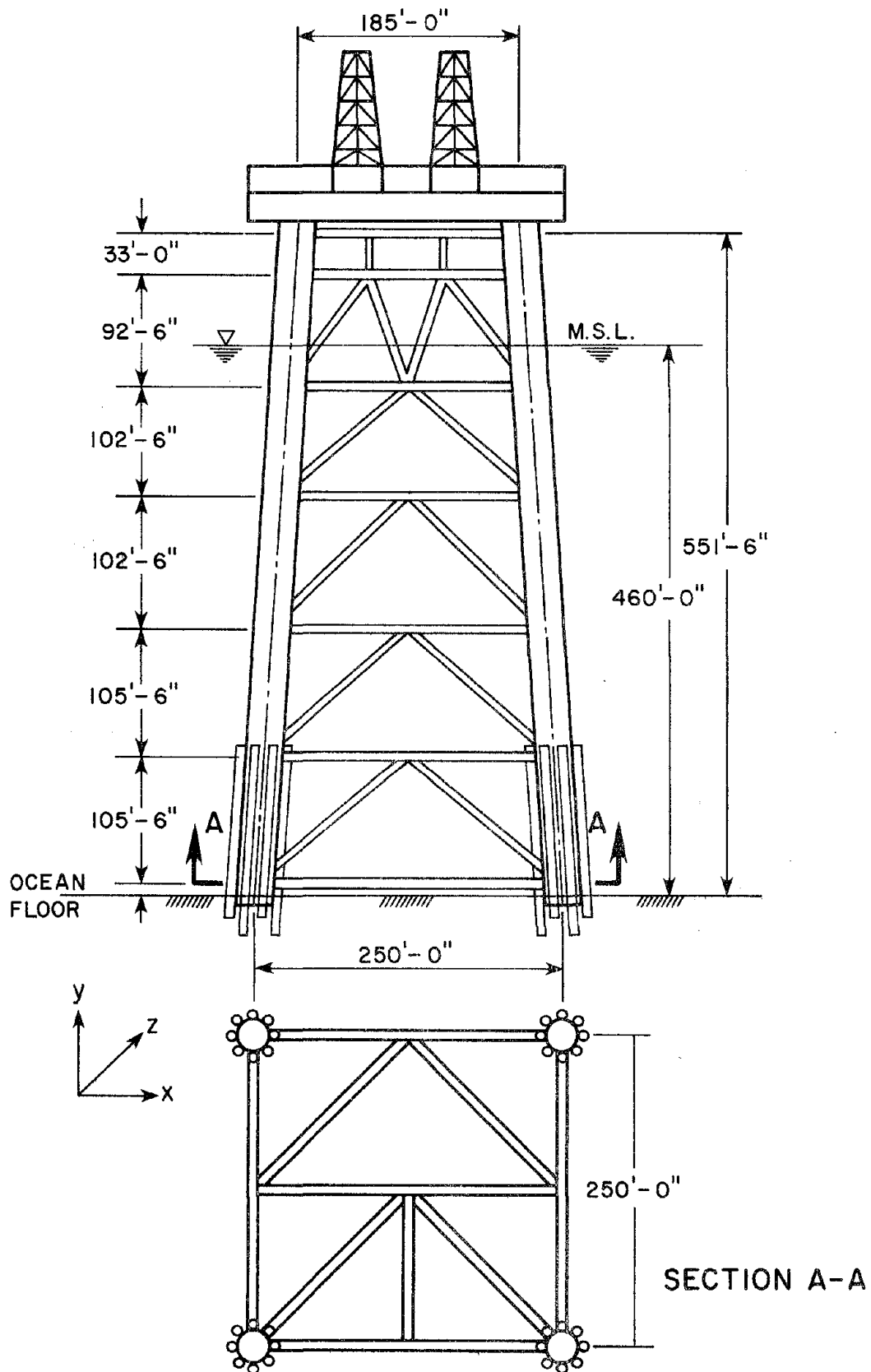


FIG. 4.1 EXAMPLE OFFSHORE STRUCTURE

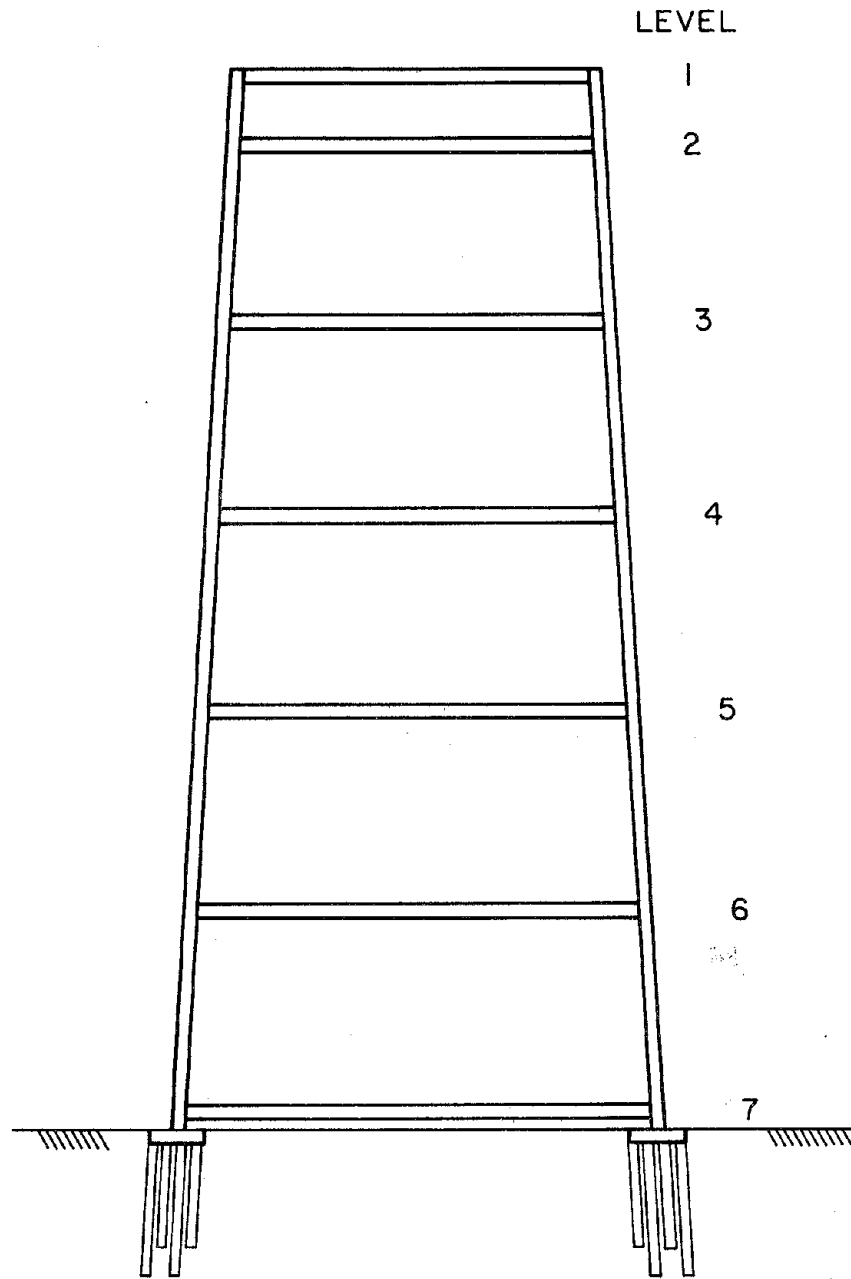


FIG. 4.2 THE IDEALIZED STRUCTURE FOR THE EXAMPLE PROBLEM

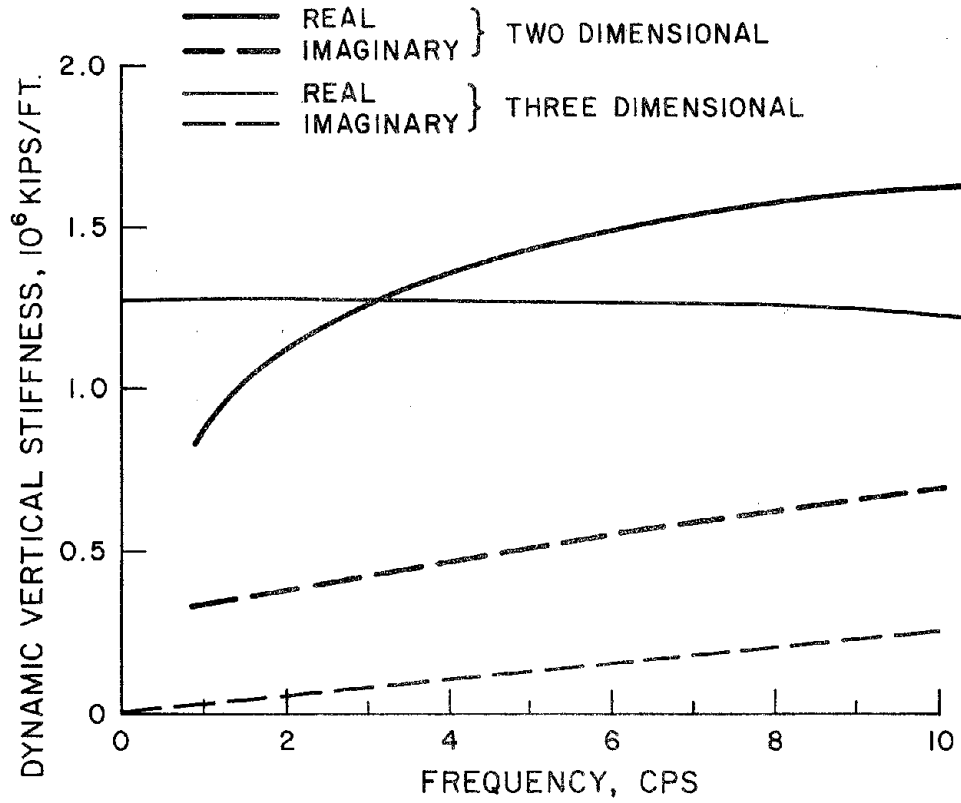


FIG. 4.3 VERTICAL STIFFNESS OF FOUNDATION A

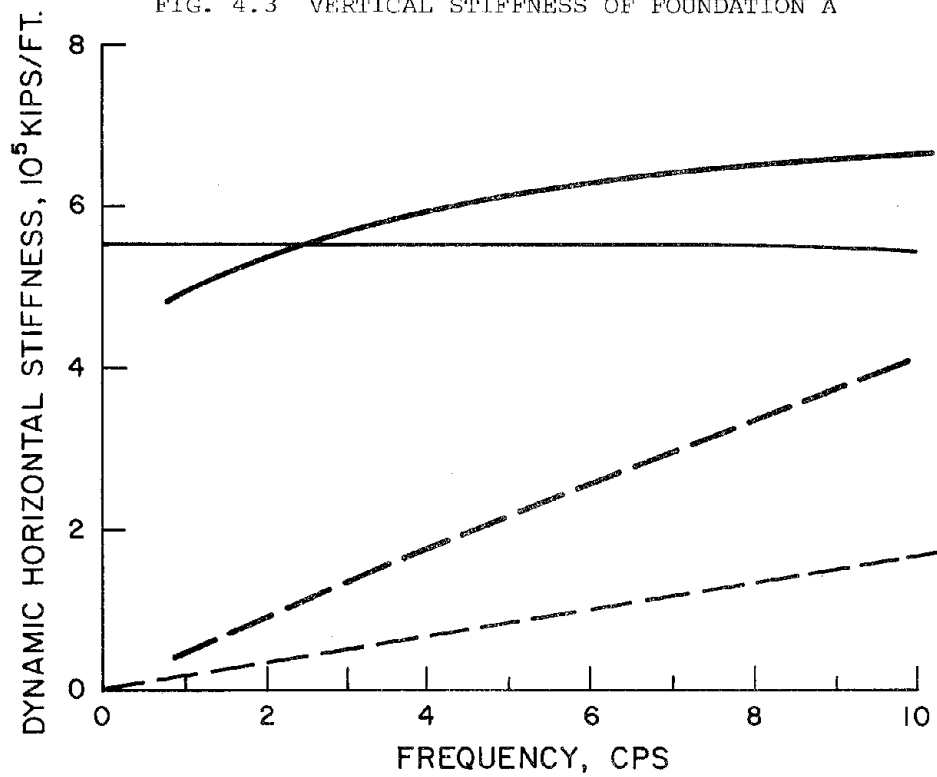


FIG. 4.4 HORIZONTAL STIFFNESS OF FOUNDATION A

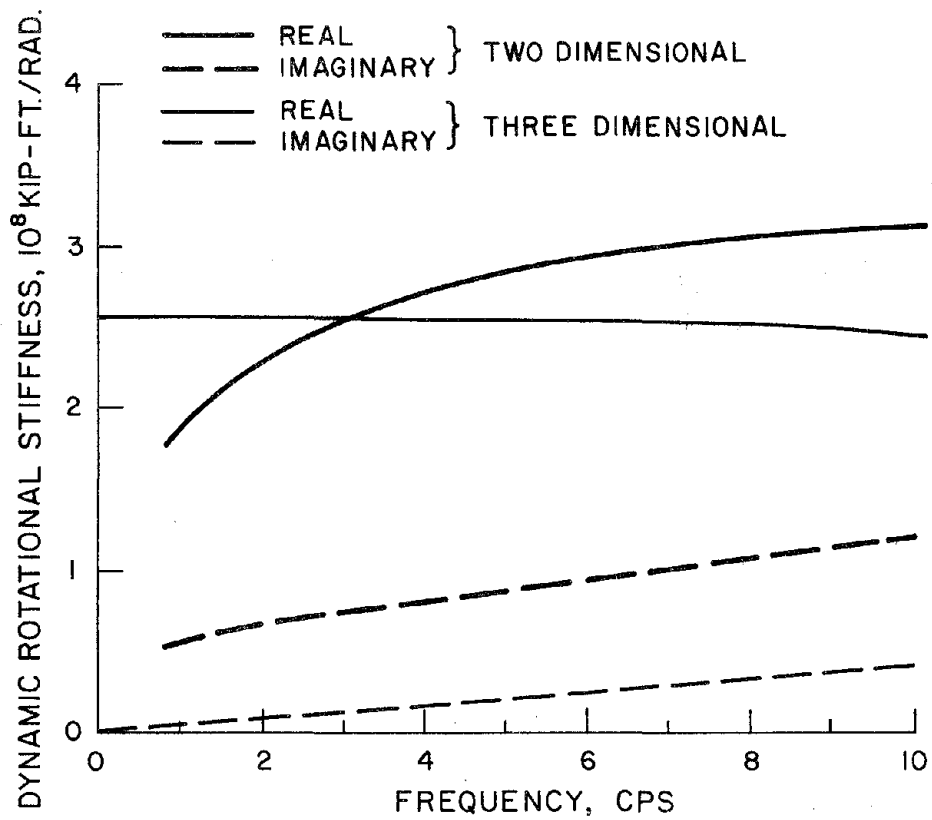


FIG. 4.5 ROTATIONAL STIFFNESS OF FOUNDATION A

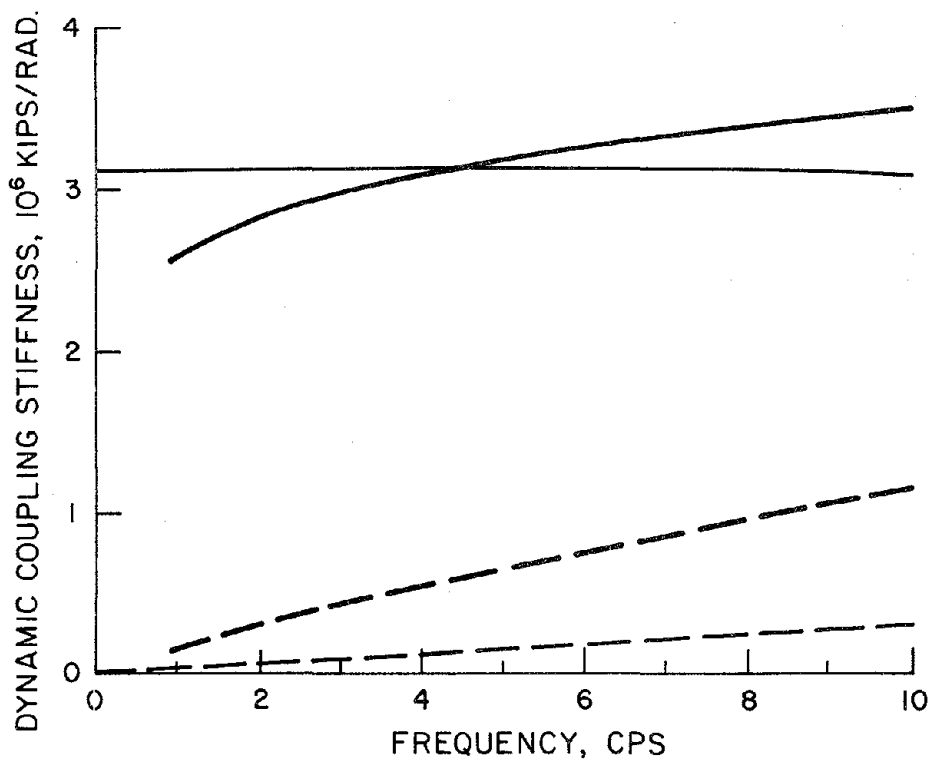


FIG. 4.6 COUPLING STIFFNESS OF FOUNDATION A

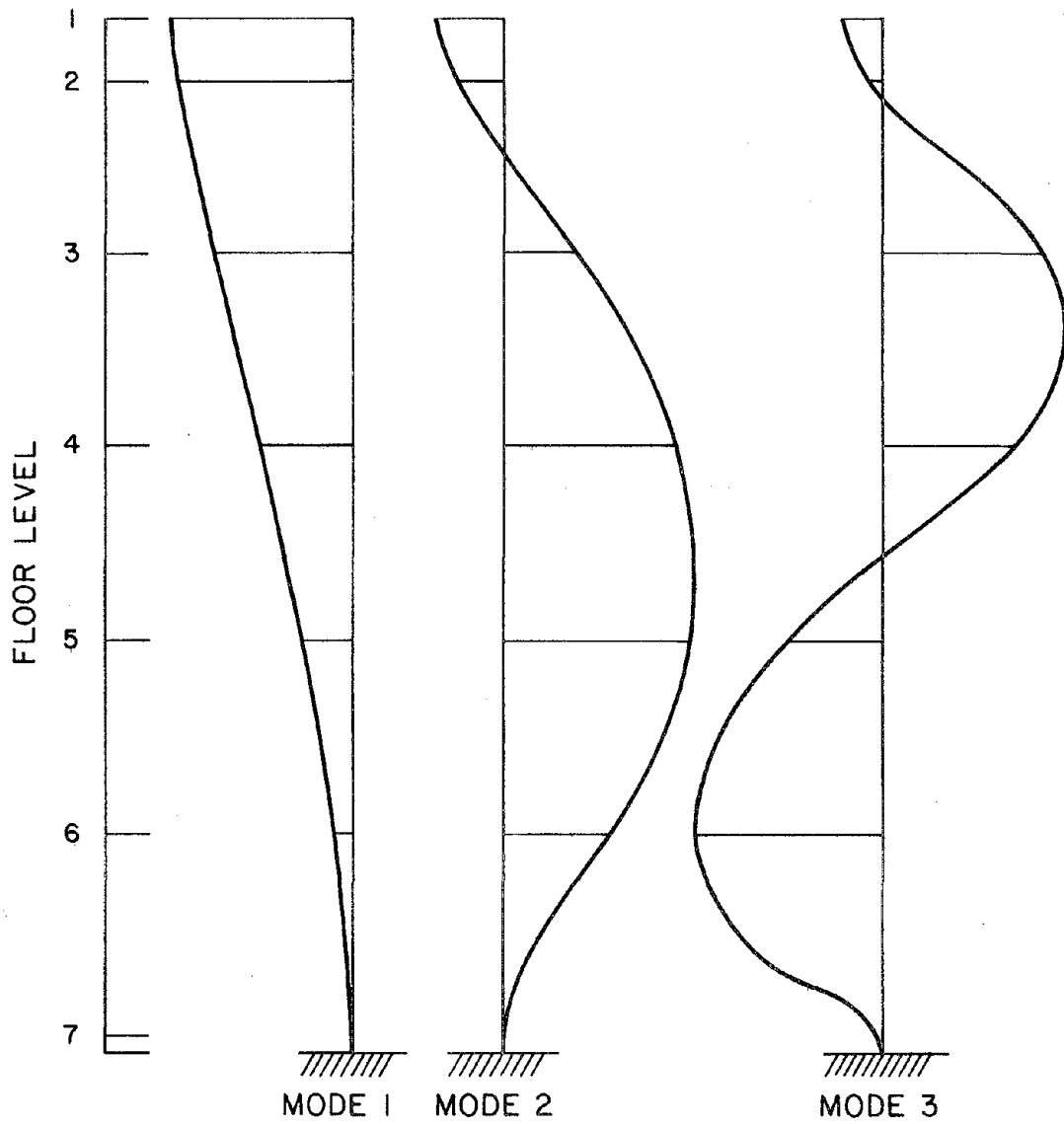


FIG. 4.7 MODE SHAPES OF FIXED-BASE STRUCTURES

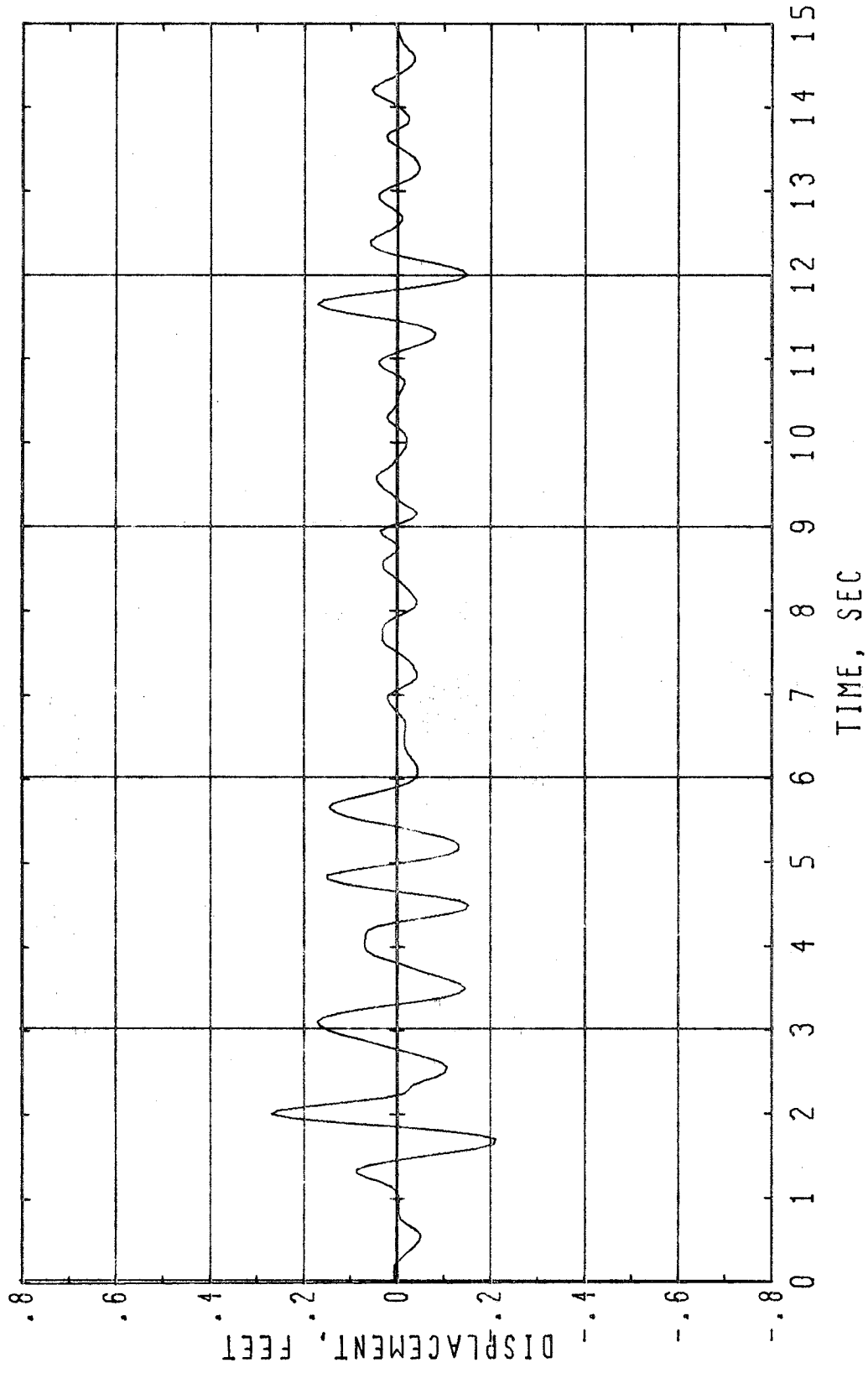


FIG. 4.8 LATERAL DISPLACEMENT TIME HISTORY AT LEVEL 1, FOUNDATION A MODEL

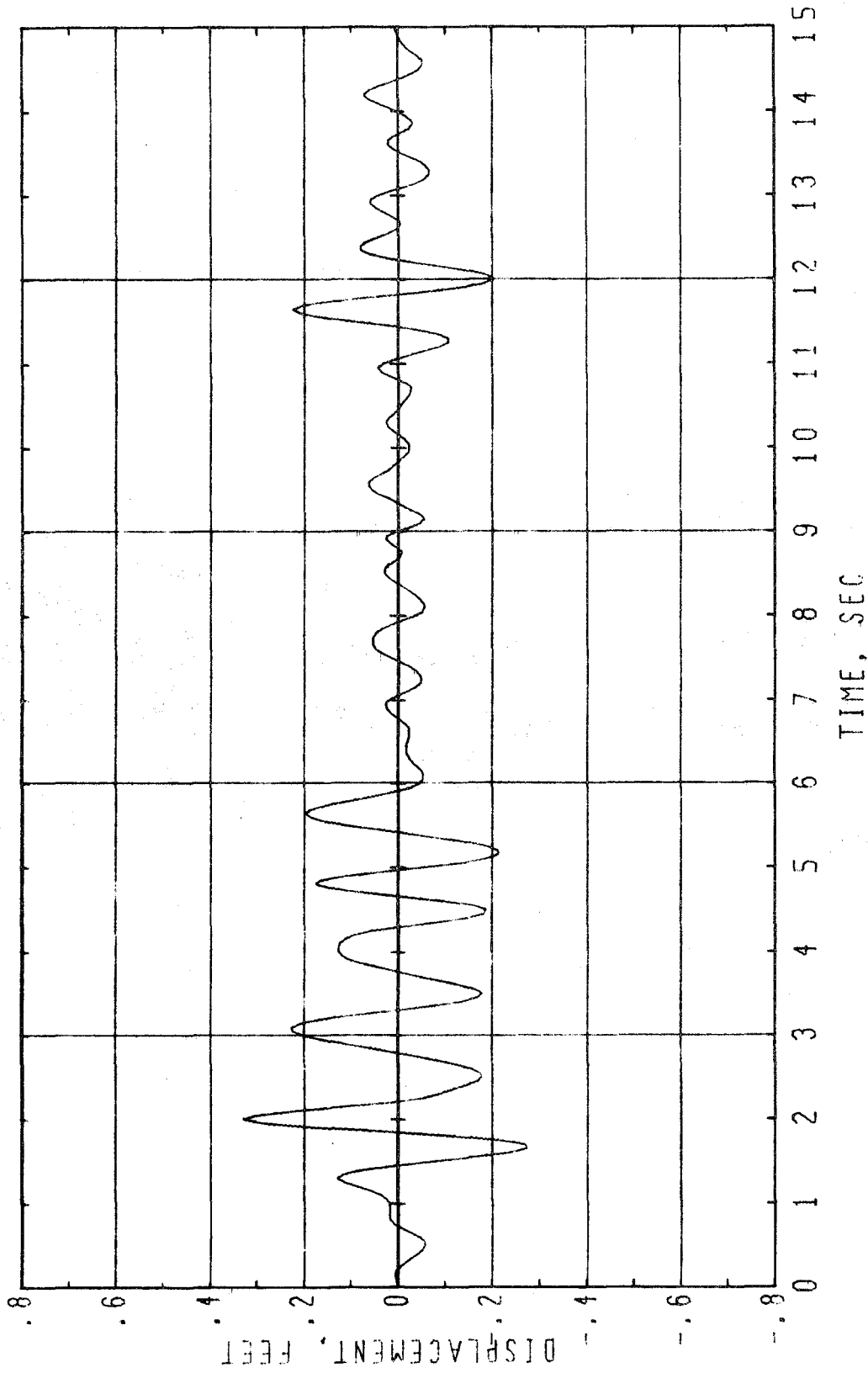


FIG. 4.9 LATERAL DISPLACEMENT TIME HISTORY AT LEVEL 1, FOUNDATION B MODEL

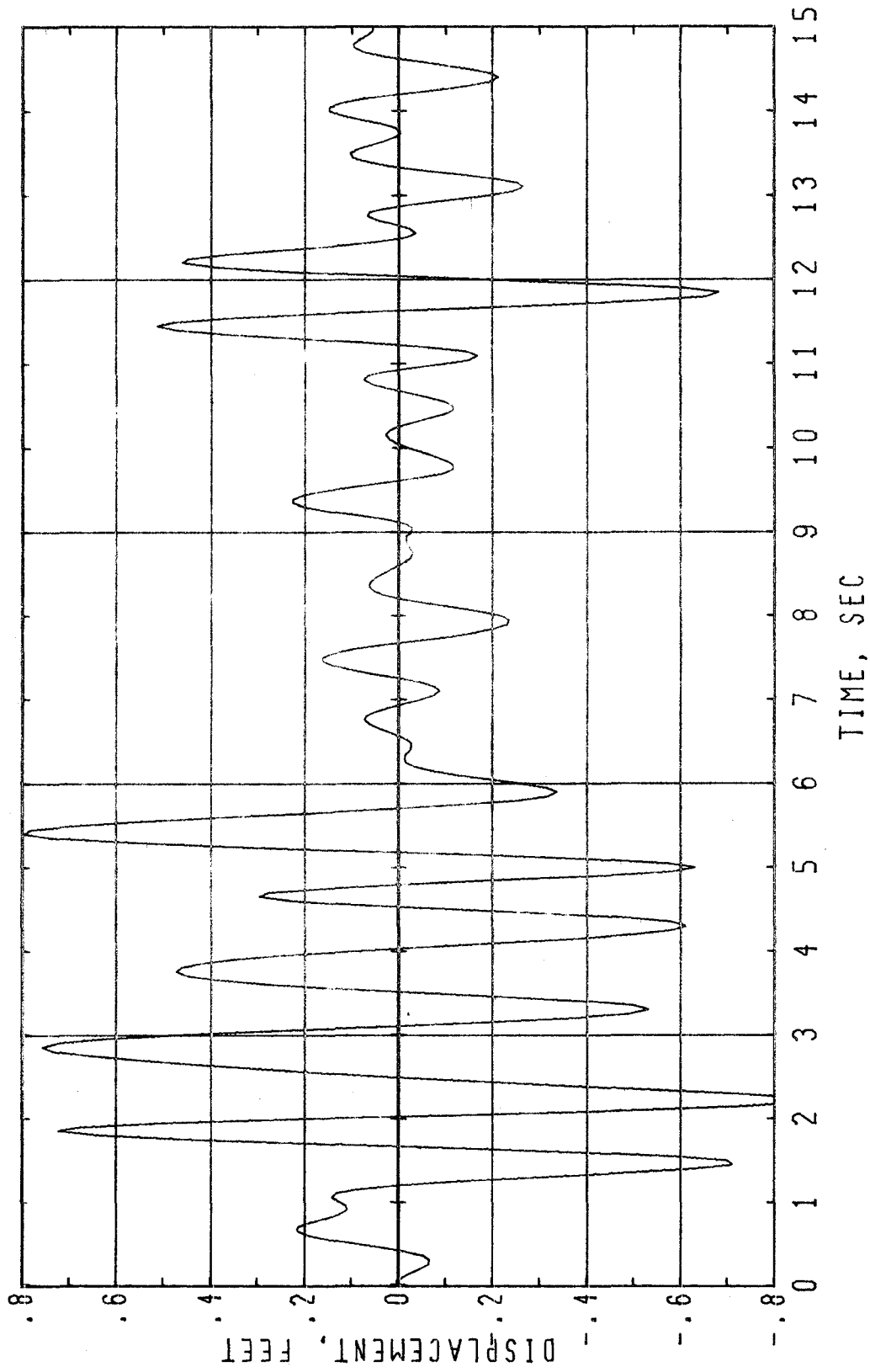


FIG. 4.10 LATERAL DISPLACEMENT TIME HISTORY AT LEVEL 1, RIGID FOUNDATION MODEL

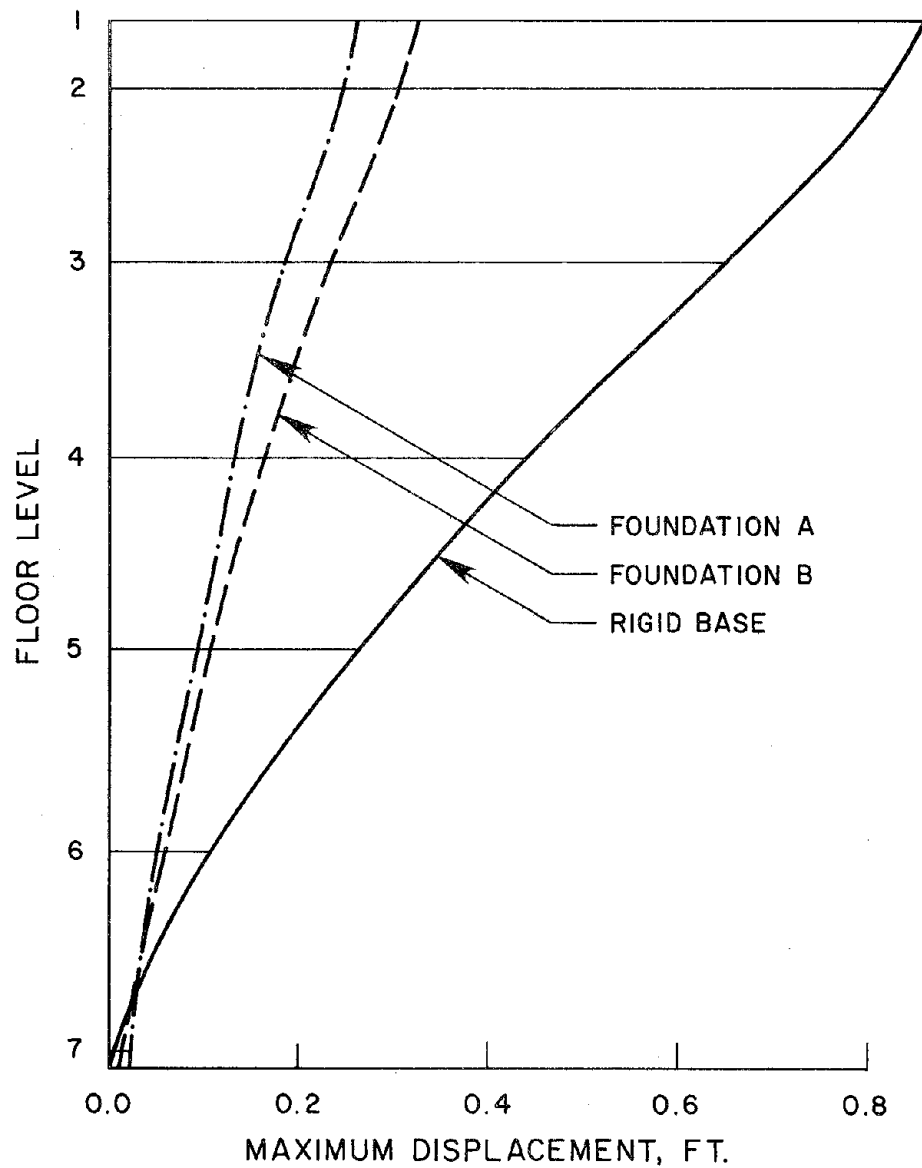


FIG. 4.11 ENVELOPES OF MAXIMUM HORIZONTAL DISPLACEMENT
RELATIVE TO THE FREE-FIELD MOTION

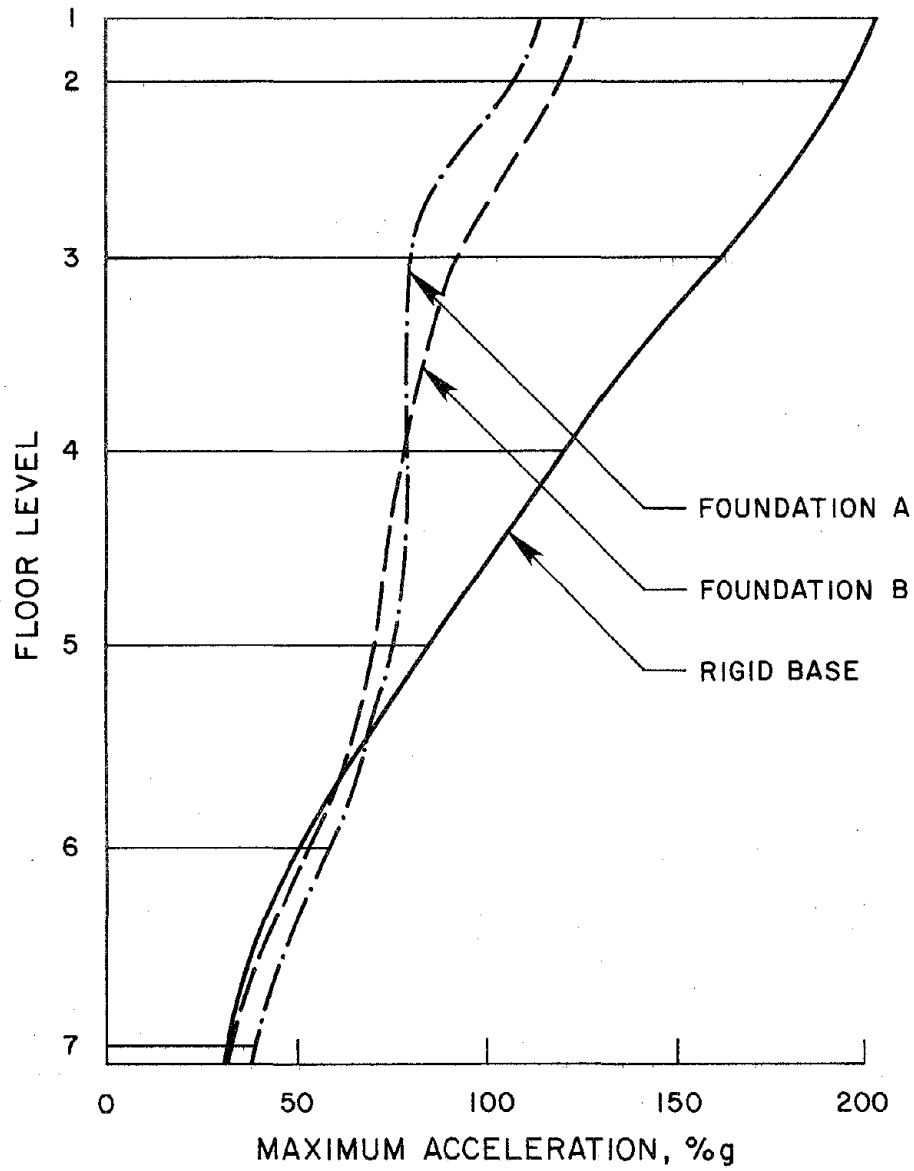


FIG. 4.12 ENVELOPES OF MAXIMUM HORIZONTAL ACCELERATION

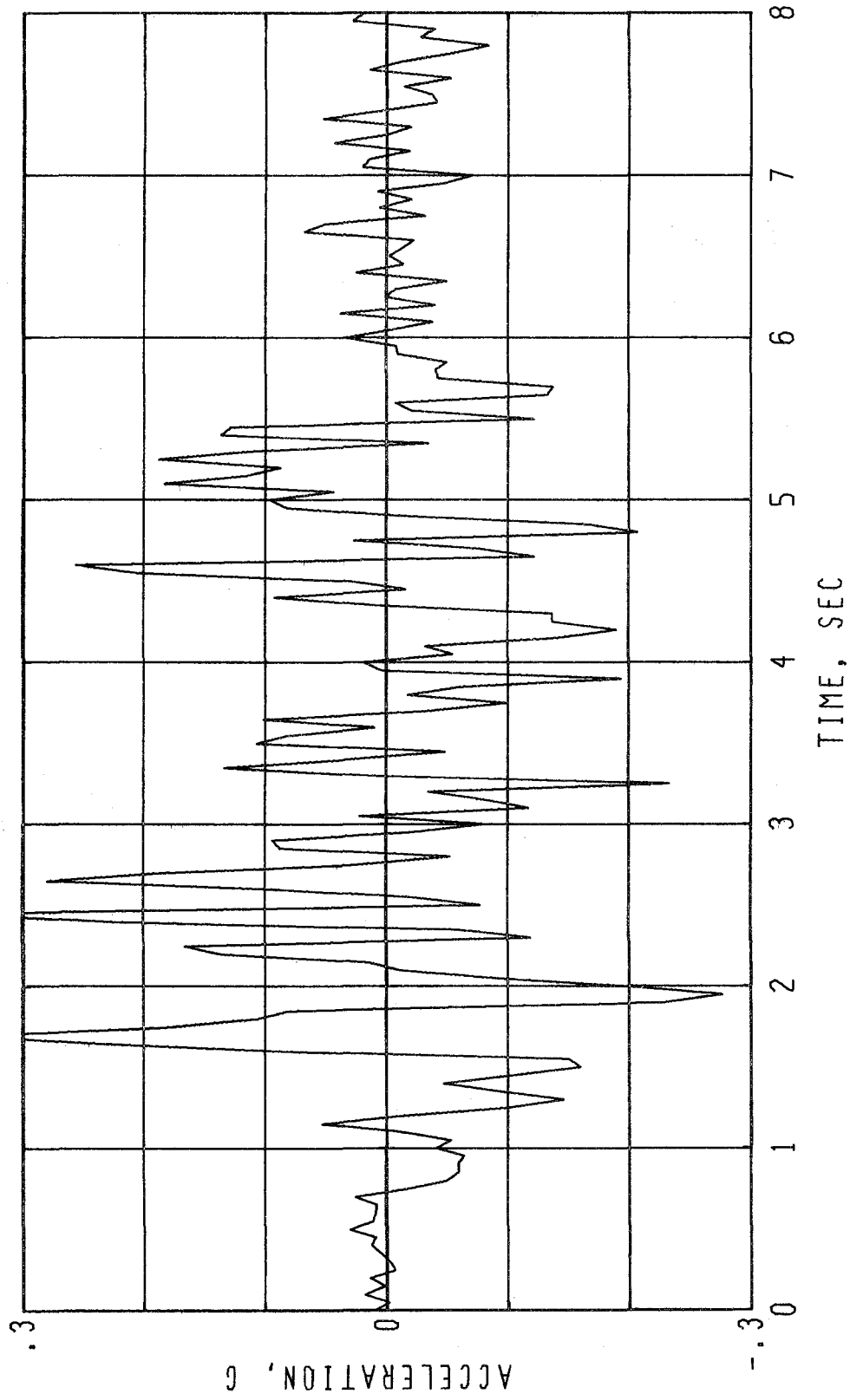


FIG. 4.13 LATERAL ACCELERATION TIME HISTORY AT LEVEL 7, FOUNDATION A MODEL

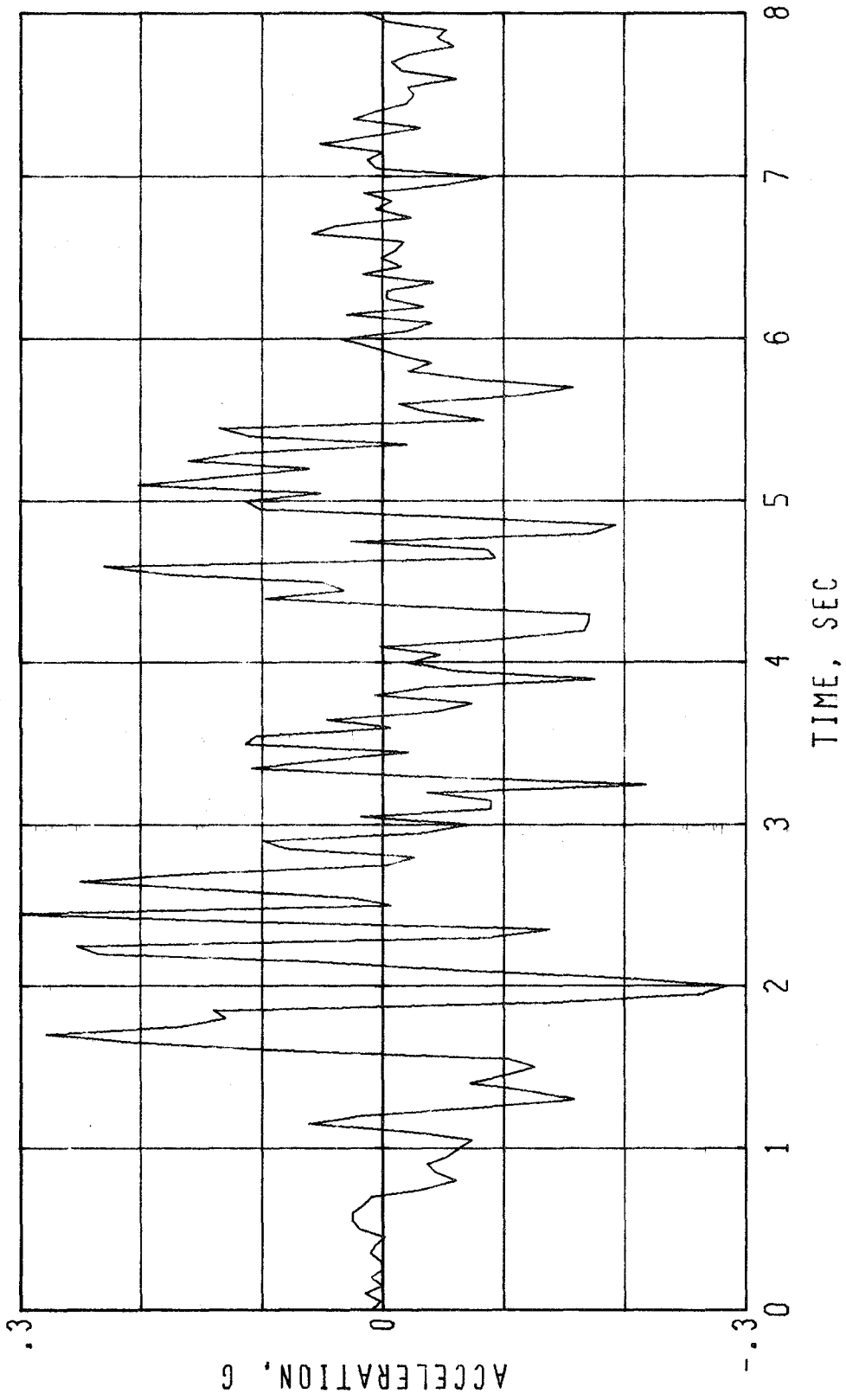


FIG. 4.14 LATERAL ACCELERATION TIME HISTORY AT LEVEL 7, FOUNDATION B MODEL

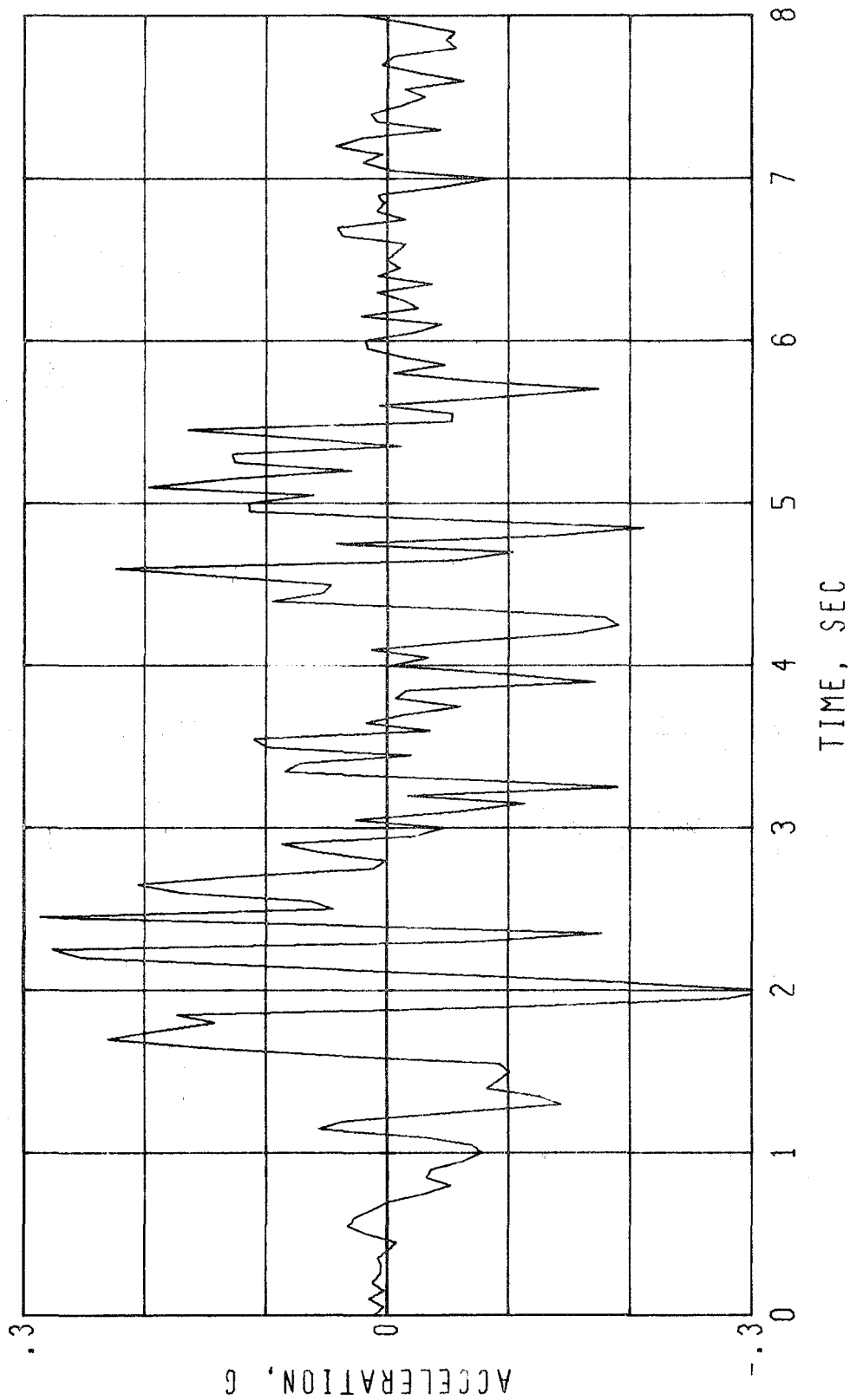


FIG. 4.15 LATERAL ACCELERATION TIME HISTORY AT LEVEL 7, RIGID FOUNDATION MODEL

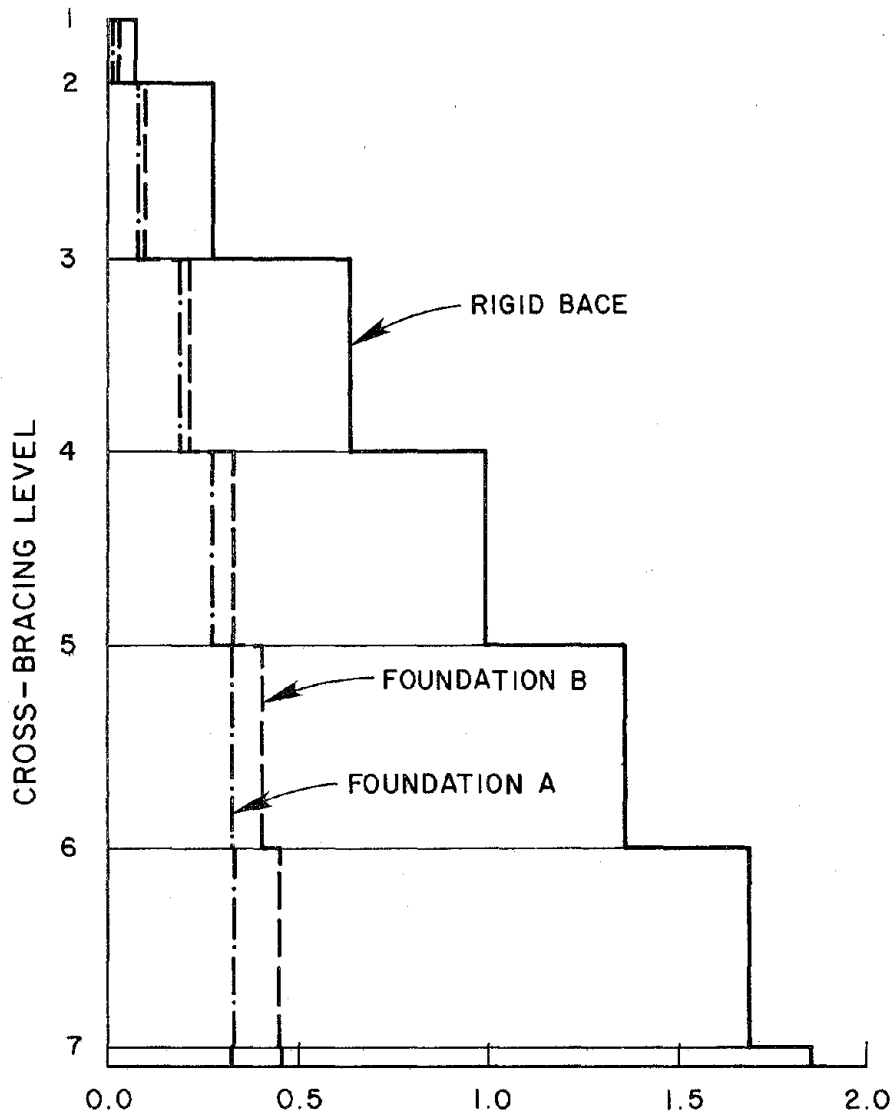


FIG. 4.16 ENVELOPES OF MAXIMUM AXIAL FORCE IN THE MAIN VERTICAL LEG, 10^5 kips.

5. CONCLUSIONS

This study has led to the following principal conclusions:

(1) The procedure suggested in Chapter 3 for computing the dynamic stiffnesses of pile foundations by-passes the expensive and difficult solution of integral equations involved in a more rigorous approach, yet gives results within engineering accuracy. It can be used to study the dynamic response of piles embedded in a soil medium where the energy attenuation due to wave radiation is an important factor.

(2) In this study, the soil medium is modeled as an isotropic, elastic half-space; therefore, the mechanism of dissipative attenuation in the ground is not taken into consideration. To account for this, the soil medium can be assumed to be an isotropic viscoelastic half-space which has the same specific damping capacity as the real soil. By simply replacing the shear modulus (a real value) of the soil by a complex shear modulus, the stiffnesses of piles embedded in an isotropic viscoelastic half-space can be obtained using the same suggested procedure.

(3) In the low frequency range which is of practical interest in earthquake engineering, the pile foundation stiffnesses calculated have a constant real part and a linear imaginary part. The imaginary parts are small in comparison with their associated real parts. This indicates that for pile foundations consisting of pipe piles of large diameter, like those used in the example structure in Chapter 4, the radiation damping in the foundation system is small and for most purposes negligible. The earthquake responses of an offshore structure can be evaluated in

the time domain if only the frequency independent real parts of the stiffnesses of its pile foundations are used. Such practical treatment will result in considerable saving of computer time and should be used in the preliminary analysis of any structural system supported on pile foundations.

(4) Study of the dynamic response characteristics of the example pile supported offshore structure indicates that the effects of structure-foundation interaction are quite prominent. The contributions of the second mode and the third mode of vibration also become more apparent if the foundation flexibility is included in the mathematical model. The interaction effects between pile foundation and structure are prominent for the particular offshore structure because its ratio of structure to foundation stiffnesses is large. The interaction effects will increase if the foundation stiffness is reduced. Therefore, correct estimation of the foundation stiffness is very important if the dynamic responses of the structure are to be correctly predicted.

(5) Since the reasonableness of the results of the analytical solutions of pile foundations depends significantly upon the ability to select the soil parameters, present efforts spent in determining the soil parameters should be continued. More field observations of the dynamic responses of piles and pile supported buildings during strong motion earthquakes should also be conducted. Furthermore, an analytical model of pile foundations should be refined continuously to keep up with new findings through field investigations.

REFERENCES

1. Penzien, J., "Soil-Pile Foundation Interaction," Chapter 14, Earthquake Engineering (Edited by R. L. Wiegel), Prentice Hall, 1970, pp. 349-381.
2. Sugimura, Y., "Dynamic Behavior of a Long Pile Foundation Extended through Soft Soil Layers during an Earthquake," (in Japanese), Ph.D. Dissertation, Waseda University, 1972.
3. Yamamoto, S. and Seki, T., "Earthquake Responses of Multi-Story Building Supported on Piles," Proceedings, The Third Japanese Earthquake Engineering Symposium.
4. Baranov, V. A., "On the Calculation of Excited Vibration of an Embedded Foundation," (in Russian), Voprosy Dynamiki Prochnosti, No. 14, Polytech. Institute Riga, pp. 195-209, 1967.
5. Novak, M., "Dynamic Stiffness and Damping of Piles," Canadian Geotechnical Journal, Vol. 11, No. 4, 1974, pp. 574-598.
6. Kausel, E., "Forced Vibrations of Circular Foundations on Layered Media," Research Report R74-11, Civil Engineering Department, M.I.T., January 1974.
7. Blaney, G. W., Kausel, E. and Roesset, J. M., "Dynamic Stiffness of Piles," Numerical Method in Geomechanics, ASCE, New York, 1976.
8. Flores, R., "Response of Pile Foundation to Earthquake Loading," Ph.D. Thesis, National University of Mexico, 1974.
9. Matlock, H., "Correlations for Design of Laterally Loaded Piles in Soft Clay," Paper No. OTC 1204, Proceedings, Second Annual Offshore Technology Conference, Houston, Texas, 1970.
10. Brown and Coyle, H. M., "Soil Parameters Required for the Analysis of Lateral Responses of Piles in Clay," Sea Grant Publication No. TAMU-SG-71-219, Texas A & M University, 1971.
11. Reese, L. C., Cox, W. R. and Koop, F. D., "Analysis of Laterally Loaded Piles in Sand," Paper No. OTC 2080, Proceedings, Sixth Annual Offshore Technology Conference, Houston, Texas, 1974, Vol. 2, pp. 473-483.
12. Wright and Coyle, H. M., "Soil Parameters Required for the Analysis of Lateral Response of Pile in Sand," Sea Grant Publication No. TAMU-SG-71-219, Texas A & M University, 1971.
13. Kubo, K. and Sato, N., "Vibration Test of a Structure Supported by Pile Foundation," Bulletin of ERS, No. 1, University of Tokyo, 1969.

14. Sugimura, Y., "Earthquake Observation and Dynamic Analysis of a Building Supported on Long Piles," Proceedings, Sixth World Conference on Earthquake Engineering, New Delhi, 1977.
15. Penzien, J., "Structure Dynamics of Fixed Offshore Structure," Behavior of Offshore Structures, The Norwegian Institute of Technology, 1976.
16. Penzien, J. and Tseng, W. S., "Three-Dimensional Dynamic Analysis of Fixed Offshore Platforms," Proceedings, International Symposium on Numerical Methods, Offshore Engineering, Swansea, Wales, January 11 - 15, 1977.
17. Morison, J. R., O'Brien, M. P., Johnson, J. W., and Schaff, S. A., "The Force Exerted by Surface Waves on Piles," Petroleum Transactions, Vol. 189, TP 3846, 1950, pp. 149-154.
18. Wiegel, Robert L., "Oceanographical Engineering," Prentice Hall, Inc., 1964.
19. Wilson, B. W. and Reid, R. O., "A Discussion of Wave Force Coefficients for Offshore Pipelines," Proceedings, ASCE, 1963, pp. 61-65.
20. Laird, A. D. K., "Water Forces on Flexible Oscillating Cylinder," Journal of Waterways and Harbors Division, ASCE, 88(3), pp. 125-137, 1962.
21. Malhotra, A. K., and Penzien, J., "Nondeterministic Analysis of Offshore Structures," Journal of the Engineering Mechanics Division, ASCE, EM6, pp. 985-1003, December 1970.
22. Bolt, B. A., Horn, W. L., Macdonald, G. A., and Scoff, R. F., "Geological Hazards," Springer-Verlag, 1975.
23. Krylov, N. and Bogoliubov, N., "Introduction to Nonlinear Mechanics: Approximate and Asymptotic Methods," Translation by S. Lefshetz in Annals of Mathematics Studies, Vol. 11, Princeton University Press, 1947.
24. Gutierrez, J. A., "A Substructure Method for Earthquake Analysis of Structure-Soil Interaction," EERC 76-9, University of California, Berkeley, April 1976.
25. Clough, R. W. and Penzien, J., "Dynamics of Structures," McGraw-Hill, 1975.
26. Bergland, G. D., "A Guided Tour of the Fast Fourier Transform," IEEE Spectrum, Vol. 6, pp 41-52, July 1969.
27. Brigham, E. O., "The Fast Fourier Transform," Prentice-Hall, 1974.
28. McClelland, B., "Foundations," Section 8 in Handbook of Ocean and Underwater Engineering (Edited by Mayers, J. J., Holm, C. H. and McAllister, R. F.), McGraw-Hill, 1969, pp. 8-98 to 8-125.

29. McClland, Bramlette and Roacht, J. A., Jr., "Soil Modulus of Laterally Loaded Piles," Transactions, ASCE, Vol. 123, pp. 1049-1063, New York, 1958.
30. Parker, Frazier, and Reese, L. C., "Lateral Pile-Soil Interaction Curves for Sand," Proceedings, The International Symposium on the Engineering Properties of Sea-Floor Soils and Their Geophysical Identification, University of Washington, Seattle, July 25, 1971.
31. Reese, L. C. and Cox, W. R., "Field Testing and Analysis of Laterally Loaded Piles in Stiff Clay," Paper No. OTC 2312, Proceedings, Seventh Annual Offshore Technology Conference, Houston, Texas, 1975.
32. Sezawa, K., "Further Studies on Rayleigh-Waves Having Some Aximuthal Distribution," Bulletin of Earthquake Research Institute, Tokyo University, Vol. 6, March 1929.
33. Kanai, K., "Wave Propagation in Elastic Half Space Due to Pointed Surface Loadings," (in Japanese) Chapter 4, Earthquake Engineering, Shokokusha, 1968, pp. 91-105.
34. Watson, "Theory of Bessel Functions," Cambridge University Press, 1922.
35. Mindlin, R., "Displacements and Stress Due to Nuclei of Strain in the Elastic Half-Space," Report of the Department of Civil Engineering and Engineering Mechanics, Columbia University, New York, July 1961.
36. Fung, Y. C., "Foundation of Solid Mechanics," Prentice-Hall, 1965.
37. Kolsky, H., "Stress Waves in Solids," Oxford University Press, 1953.
38. Poulos, H. G., "Behavior of Laterally Loaded Piles: I-Single Piles," Journal of the Soil Mechanics and Foundation Division, ASCE, Vol. 97, SM5, May, 1971, pp. 711-731.
39. Poulos, H. G., "Behavior of Laterally Loaded Piles: II - Pile Groups," Journal of the Soil Mechanics and Foundation Division, ASCE, Vol. 97, SM5, May 1971, pp. 733-751.
40. Chellis, R. D., "Pile Foundations," McGraw-Hill, 1961.
41. Arnold, R. N., Bycroft, G. N. and Warburton, G. B., "Forced Vibrations of a Body on an Infinite Elastic Solid," Journal of Applied Mechanics, Vol. 22, September 1955, pp. 391-400.
42. Pekeris, C. C. and Lifson, H., "Motion of the Surface of a Uniform Elastic Half-Surface produced by a Buried Pulse," Journal of Acoustical Society of America, Vol. 29, 1957, pp. 1233-1238.
43. Kida, Y., Takagi, M., Fugitani, Y. and Saito, K., "Coupling Analysis Between Embedded Wall and Soil Medium by Wave Propagation Theory," (in Japanese) Collection of Lecture Notes of Architecture Institute of Japan, Paper No. 2055 and 2056, October 1976, pp. 545-548.

44. Wagner, A. A., "Lateral Load Tests on Piles for Design Information," ASTM Spec. Tech. Publ. 154, 1953, pp. 59-74.
45. Tajimi, H., "Seismic Effects of Piles, State of the Art Report," Specialty Session No. 10 of IX ICSMFE, Tokyo, 1977.
46. Esashi, Y., Yoshida, Y. and Ikemi, Y., "Pile Spacing Effects on Lateral Behavior of Piles," (in Japanese) Proceedings, Annual Meeting of JSSMFE, 8th, pp. 451-454.
47. Sugimura, Y., "The Effects of Pile Group on the Reduction of their Horizontal Soil Reaction," Research work for the period April 1971-March 1972, Building Research Institute of Japan, pp. 267-271.
48. Richart, F. E., Jr., Hall, J. R., Jr., and Woods, R. D., "Vibrations of Soils and Foundations," Prentice-Hall, 1970
49. Papoulis, A., "Probability, Random Variables, and Stochastic Processes," McGraw-Hill, 1965.
50. Crandall, S. H. and Mark, W. D., "Random Vibration," Academic Press, 1963.
51. Kuhlemeyer, R. L., "Static and Dynamic Laterally Loaded Piles," Research Report No. CE 76-9, University of Calgary, Canada, 1976.
52. Veletsos, A. S. and Verbic, B., "Vibration of Viscoelastic Foundations," International Journal of Earthquake Engineering and Structural Dynamics, Vol. 2, No. 1, 1973, pp. 87-102.
53. Luco, J. E., "Impedance Functions for a Rigid Foundation on a Layered Medium," Nuclear Engineering and Design, 31, 1974, pp. 204-217.
54. Nogami, T. and Novak, M., "Soil-Pile Interaction in Vertical Vibration," International Journal of Earthquake Engineering and Structural Dynamics, Vol. 4, No. 3, 1976, pp. 277-293.
55. Zeevaert, L., "Pile Design and Installation in Earthquake Areas," in Piletips, by Associated Pile & Fitting Corp., 1977.
56. Wu, S. C. and Tung, C. C., "Random Response of Offshore Structures to Wave and Current Forces," University of North Carolina, Sea Grant Publication UNC-SG-75-22, 1975.
57. Wong, K. S. and Duncan, J. M., "Hyperbolic Stress-Strain Parameters for Nonlinear Finite Element Analysis of Stresses and Movements in Soil Masses," Report No. TE-74-3, University of California, Berkeley, 1974.
58. "Seismic Analysis of the Charaima Building, Caraballeda, Venezuela," by Subcommittee of the SEAONC Research Committee, EERC 70-4, University of California, Berkeley, August 1970.

59. Seed, H. B. and Idriss, I. M., "Soil Moduli and Damping Factors for Dynamic Response Analyses," EERC 70-10, University of California, Berkeley, December 1970.
60. Garrison, C. J., "Wave Forces on Large Volume Structures -- A Comparison Between Theory and Model Tests," Paper No. OTC 2137, Proceedings, Sixth Annual Offshore Technology Conference, Houston, Texas, 1974.

APPENDIX A

STRUCTURAL STIFFNESS AND MASS MATRICES OF EXAMPLE PROBLEM

1. Structural Stiffness Matrix

The structural stiffness matrix $[\bar{k}]$ may be written in partitioned form according to the definition of Eq. (2.26). Since the stiffness matrix is symmetric, only $[\bar{k}_{ss}]$, $[\bar{k}_{sb}]$ and $[\bar{k}_{bb}]$ need to be generated and stored. The submatrix $[\bar{k}_{ss}]$ can always be arranged as a symmetric band matrix. In many cases, the maximum semi-bandwidth is much smaller than its order. In this case, a special band algorithm which performs Gaussian elimination can be used to advantage. Let matrix $[d]$ be the banded form of submatrix $[\bar{k}_{ss}]$.

For the example problem, $[\bar{k}_{bb}]$ is

BASE STIFFNESS MATRIX

.491E+13	.292E+12	-.246E+14	0.	0.	0.
.292E+12	.568E+11	-.148E+13	0.	0.	0.
-.246E+14	-.148E+13	.165E+15	0.	0.	0.
0.	0.	0.	.491E+13	-.292E+12	-.246E+14
0.	0.	0.	-.292E+12	.568E+11	.148E+13
0.	0.	0.	-.246E+14	.148E+13	.165E+15

and $[d]$ equals

2. Mass Matrix

Since the example offshore structure is modeled as a lumped mass system, all the off-diagonal elements in the total mass matrix [m] are zero. The diagonal elements of the total mass matrix can be conveniently stored as one-dimensional array, giving

DIAGONAL MASS MATRIX

.874E+06	.202E+05	0.	.874E+06	.202E+05	0.	.642E+05	.642E+05	0.
.642E+05	.642E+05	0.	.221E+06	.104E+06	0.	.221E+06	.104E+06	0.
.262E+06	.121E+06	0.	.262E+06	.121E+06	0.	.277E+06	.135E+06	0.
.277E+06	.135E+06	0.	.296E+06	.152E+06	0.	.296E+06	.162E+06	0.
.177E+06	.906E+05	0.	.177E+06	.906E+06	0.	.709E+04	.709E+04	0.
.709E+04	.709E+04	0.						

The unit of the mass matrix is lb-sec²/ft.

EARTHQUAKE ENGINEERING RESEARCH CENTER REPORTS

NOTE: Numbers in parenthesis are Accession Numbers assigned by the National Technical Information Service; these are followed by a price code. Copies of the reports may be ordered from the National Technical Information Service, 5285 Port Royal Road, Springfield, Virginia, 22161. Accession Numbers should be quoted on orders for reports (PB --- ---) and remittance must accompany each order. Reports without this information were not available at time of printing. Upon request, EERC will mail inquirers this information when it becomes available.

- EERC 67-1 "Feasibility Study Large-Scale Earthquake Simulator Facility," by J. Penzien, J.G. Bouwkamp, R.W. Clough and D. Rea - 1967 (PB 187 905)A07
- EERC 68-1 Unassigned
- EERC 68-2 "Inelastic Behavior of Beam-to-Column Subassemblages Under Repeated Loading," by V.V. Bertero - 1968 (PB 184 888)A05
- EERC 68-3 "A Graphical Method for Solving the Wave Reflection-Refraction Problem," by H.D. McNiven and Y. Mengi - 1968 (PB 187 943)A03
- EERC 68-4 "Dynamic Properties of McKinley School Buildings," by D. Rea, J.G. Bouwkamp and R.W. Clough - 1968 (PB 187 902)A07
- EERC 68-5 "Characteristics of Rock Motions During Earthquakes," by H.B. Seed, I.M. Idriss and F.W. Kiefer - 1968 (PB 188 338)A03
- EERC 69-1 "Earthquake Engineering Research at Berkeley," - 1969 (PB 187 906)A11
- EERC 69-2 "Nonlinear Seismic Response of Earth Structures," by M. Dibaj and J. Penzien - 1969 (PB 187 904)A08
- EERC 69-3 "Probabilistic Study of the Behavior of Structures During Earthquakes," by R. Ruiz and J. Penzien - 1969 (PB 187 886)A06
- EERC 69-4 "Numerical Solution of Boundary Value Problems in Structural Mechanics by Reduction to an Initial Value Formulation," by N. Distefano and J. Schujman - 1969 (PB 187 942)A02
- EERC 69-5 "Dynamic Programming and the Solution of the Biharmonic Equation," by N. Distefano - 1969 (PB 187 941)A03
- EERC 69-6 "Stochastic Analysis of Offshore Tower Structures," by A.K. Malhotra and J. Penzien - 1969 (PB 187 903)A06
- EERC 69-7 "Rock Motion Accelerograms for High Magnitude Earthquakes," by H.B. Seed and I.M. Idriss - 1969 (PB 187 940)A02
- EERC 69-8 "Structural Dynamics Testing Facilities at the University of California, Berkeley," by R.M. Stephen, J.G. Bouwkamp, R.W. Clough and J. Penzien - 1969 (PB 189 111)A04
- EERC 69-9 "Seismic Response of Soil Deposits Underlain by Sloping Rock Boundaries," by H. Dezfulian and H.B. Seed - 1969 (PB 189 114)A03
- EERC 69-10 "Dynamic Stress Analysis of Axisymmetric Structures Under Arbitrary Loading," by S. Ghosh and E.L. Wilson - 1969 (PB 189 026)A10
- EERC 69-11 "Seismic Behavior of Multistory Frames Designed by Different Philosophies," by J.C. Anderson and V. V. Bertero - 1969 (PB 190 662)A10
- EERC 69-12 "Stiffness Degradation of Reinforcing Concrete Members Subjected to Cyclic Flexural Moments," by V.V. Bertero, B. Bresler and H. Ming Liao - 1969 (PB 202 942)A07
- EERC 69-13 "Response of Non-Uniform Soil Deposits to Travelling Seismic Waves," by H. Dezfulian and H.B. Seed - 1969 (PB 191 023)A03
- EERC 69-14 "Damping Capacity of a Model Steel Structure," by D. Rea, R.W. Clough and J.G. Bouwkamp - 1969 (PB 190 663)A06
- EERC 69-15 "Influence of Local Soil Conditions on Building Damage Potential during Earthquakes," by H.B. Seed and I.M. Idriss - 1969 (PB 191 036)A03
- EERC 69-16 "The Behavior of Sands Under Seismic Loading Conditions," by M.L. Silver and H.B. Seed - 1969 (AD 714 982)A07
- EERC 70-1 "Earthquake Response of Gravity Dams," by A.K. Chopra - 1970 (AD 709 640)A03
- EERC 70-2 "Relationships between Soil Conditions and Building Damage in the Caracas Earthquake of July 29, 1967," by H.B. Seed, I.M. Idriss and H. Dezfulian - 1970 (PB 195 762)A05
- EERC 70-3 "Cyclic Loading of Full Size Steel Connections," by E.P. Popov and R.M. Stephen - 1970 (PB 213 545)A04
- EERC 70-4 "Seismic Analysis of the Charaima Building, Caraballeda, Venezuela," by Subcommittee of the SEAONC Research Committee: V.V. Bertero, P.F. Fratessa, S.A. Mahin, J.H. Sexton, A.C. Scordelis, E.L. Wilson, L.A. Wyllie, H.B. Seed and J. Penzien, Chairman - 1970 (PB 201 455)A06

- EERC 70-5 "A Computer Program for Earthquake Analysis of Dams," by A.K. Chopra and P. Chakrabarti - 1970 (AD 723 994)A05
- EERC 70-6 "The Propagation of Love Waves Across Non-Horizontally Layered Structures," by J. Lysmer and L.A. Drake 1970 (PB 197 896)A03
- EERC 70-7 "Influence of Base Rock Characteristics on Ground Response," by J. Lysmer, H.B. Seed and P.B. Schnabel 1970 (PB 197 897)A03
- EERC 70-8 "Applicability of Laboratory Test Procedures for Measuring Soil Liquefaction Characteristics under Cyclic Loading," by H.B. Seed and W.H. Peacock - 1970 (PB 198 016)A03
- EERC 70-9 "A Simplified Procedure for Evaluating Soil Liquefaction Potential," by H.B. Seed and I.M. Idriss - 1970 (PB 198 009)A03
- EERC 70-10 "Soil Moduli and Damping Factors for Dynamic Response Analysis," by H.B. Seed and I.M. Idriss - 1970 (PB 197 869)A03
- EERC 71-1 "Koyna Earthquake of December 11, 1967 and the Performance of Koyna Dam," by A.K. Chopra and P. Chakrabarti 1971 (AD 731 496)A06
- EERC 71-2 "Preliminary In-Situ Measurements of Anelastic Absorption in Soils Using a Prototype Earthquake Simulator," by R.D. Borcherdt and P.W. Rodgers - 1971 (PB 201 454)A03
- EERC 71-3 "Static and Dynamic Analysis of Inelastic Frame Structures," by F.L. Porter and G.H. Powell - 1971 (PB 210 135)A06
- EERC 71-4 "Research Needs in Limit Design of Reinforced Concrete Structures," by V.V. Bertero - 1971 (PB 202 943)A04
- EERC 71-5 "Dynamic Behavior of a High-Rise Diagonally Braced Steel Building," by D. Rea, A.A. Shah and J.G. Bouwhamp 1971 (PB 203 584)A06
- EERC 71-6 "Dynamic Stress Analysis of Porous Elastic Solids Saturated with Compressible Fluids," by J. Ghaboussi and E. L. Wilson - 1971 (PB 211 396)A06
- EERC 71-7 "Inelastic Behavior of Steel Beam-to-Column Subassemblages," by H. Krawinkler, V.V. Bertero and E.P. Popov 1971 (PB 211 335)A14
- EERC 71-8 "Modification of Seismograph Records for Effects of Local Soil Conditions," by P. Schnabel, H.B. Seed and J. Lysmer - 1971 (PB 214 450)A03
- EERC 72-1 "Static and Earthquake Analysis of Three Dimensional Frame and Shear Wall Buildings," by E.L. Wilson and H.H. Dovey - 1972 (PB 212 904)A05
- EERC 72-2 "Accelerations in Rock for Earthquakes in the Western United States," by P.B. Schnabel and H.B. Seed - 1972 (PB 213 100)A03
- EERC 72-3 "Elastic-Plastic Earthquake Response of Soil-Building Systems," by T. Minami - 1972 (PB 214 868)A08
- EERC 72-4 "Stochastic Inelastic Response of Offshore Towers to Strong Motion Earthquakes," by M.K. Kaul - 1972 (PB 215 713)A05
- EERC 72-5 "Cyclic Behavior of Three Reinforced Concrete Flexural Members with High Shear," by E.P. Popov, V.V. Bertero and H. Krawinkler - 1972 (PB 214 555)A05
- EERC 72-6 "Earthquake Response of Gravity Dams Including Reservoir Interaction Effects," by P. Chakrabarti and A.K. Chopra - 1972 (AD 762 330)A08
- EERC 72-7 "Dynamic Properties of Pine Flat Dam," by D. Rea, C.Y. Liaw and A.K. Chopra - 1972 (AD 763 928)A05
- EERC 72-8 "Three Dimensional Analysis of Building Systems," by E.L. Wilson and H.H. Dovey - 1972 (PB 222 438)A06
- EERC 72-9 "Rate of Loading Effects on Uncracked and Repaired Reinforced Concrete Members," by S. Mahin, V.V. Bertero, D. Rea and M. Atalay - 1972 (PB 224 520)A08
- EERC 72-10 "Computer Program for Static and Dynamic Analysis of Linear Structural Systems," by E.L. Wilson, K.-J. Bathe, J.E. Peterson and H.H. Dovey - 1972 (PB 220 437)A04
- EERC 72-11 "Literature Survey - Seismic Effects on Highway Bridges," by T. Iwasaki, J. Penzien and R.W. Clough - 1972 (PB 215 613)A19
- EERC 72-12 "SHAKE-A Computer Program for Earthquake Response Analysis of Horizontally Layered Sites," by P.B. Schnabel and J. Lysmer - 1972 (PB 220 207)A06
- EERC 73-1 "Optimal Seismic Design of Multistory Frames," by V.V. Bertero and H. Kamil - 1973
- EERC 73-2 "Analysis of the Slides in the San Fernando Dams During the Earthquake of February 9, 1971," by H.B. Seed, K.L. Lee, I.M. Idriss and F. Makdisi - 1973 (PB 223 402)A14

- EERC 73-3 "Computer Aided Ultimate Load Design of Unbraced Multistory Steel Frames," by M.B. El-Hafez and G.H. Powell 1973 (PB 248 315)A09
- EERC 73-4 "Experimental Investigation into the Seismic Behavior of Critical Regions of Reinforced Concrete Components as Influenced by Moment and Shear," by M. Celebi and J. Penzien - 1973 (PB 215 884)A09
- EERC 73-5 "Hysteretic Behavior of Epoxy-Repaired Reinforced Concrete Beams," by M. Celebi and J. Penzien - 1973 (PB 239 568)A03
- EERC 73-6 "General Purpose Computer Program for Inelastic Dynamic Response of Plane Structures," by A. Kanaan and G.H. Powell - 1973 (PB 221 260)A08
- EERC 73-7 "A Computer Program for Earthquake Analysis of Gravity Dams Including Reservoir Interaction," by P. Chakrabarti and A.K. Chopra - 1973 (AD 766 271)A04
- EERC 73-8 "Behavior of Reinforced Concrete Deep Beam-Column Subassemblages Under Cyclic Loads," by O. Küstü and J.G. Bouwkamp - 1973 (PB 246 117)A12
- EERC 73-9 "Earthquake Analysis of Structure-Foundation Systems," by A.K. Vaish and A.K. Chopra - 1973 (AD 766 272)A07
- EERC 73-10 "Deconvolution of Seismic Response for Linear Systems," by R.B. Reimer - 1973 (PB 227 179)A08
- EERC 73-11 "SAP IV: A Structural Analysis Program for Static and Dynamic Response of Linear Systems," by K.-J. Bathe, E.L. Wilson and F.E. Peterson - 1973 (PB 221 967)A09
- EERC 73-12 "Analytical Investigations of the Seismic Response of Long, Multiple Span Highway Bridges," by W.S. Tseng and J. Penzien - 1973 (PB 227 816)A10
- EERC 73-13 "Earthquake Analysis of Multi-Story Buildings Including Foundation Interaction," by A.K. Chopra and J.A. Gutierrez - 1973 (PB 222 970)A03
- EERC 73-14 "ADAP: A Computer Program for Static and Dynamic Analysis of Arch Dams," by R.W. Clough, J.M. Raphael and S. Mojtahedi - 1973 (PB 223 763)A09
- EERC 73-15 "Cyclic Plastic Analysis of Structural Steel Joints," by R.B. Pinkney and R.W. Clough - 1973 (PB 226 843)A08
- EERC 73-16 "QUAD-4: A Computer Program for Evaluating the Seismic Response of Soil Structures by Variable Damping Finite Element Procedures," by I.M. Idriss, J. Lysmer, R. Hwang and H.B. Seed - 1973 (PB 229 424)A05
- EERC 73-17 "Dynamic Behavior of a Multi-Story Pyramid Shaped Building," by R.M. Stephen, J.P. Hollings and J.G. Bouwkamp - 1973 (PB 240 718)A06
- EERC 73-18 "Effect of Different Types of Reinforcing on Seismic Behavior of Short Concrete Columns," by V.V. Bertero, J. Hollings, O. Küstü, R.M. Stephen and J.G. Bouwkamp - 1973
- EERC 73-19 "Olive View Medical Center Materials Studies, Phase I," by B. Bresler and V.V. Bertero - 1973 (PB 235 986)A06
- EERC 73-20 "Linear and Nonlinear Seismic Analysis Computer Programs for Long Multiple-Span Highway Bridges," by W.S. Tseng and J. Penzien - 1973
- EERC 73-21 "Constitutive Models for Cyclic Plastic Deformation of Engineering Materials," by J.M. Kelly and P.P. Gillis 1973 (PB 226 024)A03
- EERC 73-22 "DRAIN - 2D User's Guide," by G.H. Powell - 1973 (PB 227 016)A05
- EERC 73-23 "Earthquake Engineering at Berkeley - 1973," (PB 226 033)A11
- EERC 73-24 Unassigned
- EERC 73-25 "Earthquake Response of Axisymmetric Tower Structures Surrounded by Water," by C.Y. Liaw and A.K. Chopra 1973 (AD 773 052)A09
- EERC 73-26 "Investigation of the Failures of the Olive View Stairtowers During the San Fernando Earthquake and Their Implications on Seismic Design," by V.V. Bertero and R.G. Collins - 1973 (PB 235 106)A13
- EERC 73-27 "Further Studies on Seismic Behavior of Steel Beam-Column Subassemblages," by V.V. Bertero, H. Krawinkler and E.P. Popov - 1973 (PB 234 172)A06
- EERC 74-1 "Seismic Risk Analysis," by C.S. Oliveira - 1974 (PB 235 920)A06
- EERC 74-2 "Settlement and Liquefaction of Sands Under Multi-Directional Shaking," by R. Pyke, C.K. Chan and H.B. Seed 1974
- EERC 74-3 "Optimum Design of Earthquake Resistant Shear Buildings," by D. Ray, K.S. Pister and A.K. Chopra - 1974 (PB 231 172)A06
- EERC 74-4 "LUSH - A Computer Program for Complex Response Analysis of Soil-Structure Systems," by J. Lysmer, T. Udaka, H.B. Seed and R. Hwang - 1974 (PB 236 796)A05

- EERC 74-5 "Sensitivity Analysis for Hysteretic Dynamic Systems: Applications to Earthquake Engineering," by D. Ray 1974 (PB 233 213)A06
- EERC 74-6 "Soil Structure Interaction Analyses for Evaluating Seismic Response," by H.B. Seed, J. Lysmer and R. Hwang 1974 (PB 236 519)A04
- EERC 74-7 Unassigned
- EERC 74-8 "Shaking Table Tests of a Steel Frame - A Progress Report," by R.W. Clough and D. Tang - 1974 (PB 240 869)A03
- EERC 74-9 "Hysteretic Behavior of Reinforced Concrete Flexural Members with Special Web Reinforcement," by V.V. Bertero, E.P. Popov and T.Y. Wang - 1974 (PB 236 797)A07
- EERC 74-10 "Applications of Reliability-Based, Global Cost Optimization to Design of Earthquake Resistant Structures," by E. Vitiello and K.S. Pister - 1974 (PB 237 231)A06
- EERC 74-11 "Liquefaction of Gravelly Soils Under Cyclic Loading Conditions," by R.T. Wong, H.B. Seed and C.K. Chan 1974 (PB 242 042)A03
- EERC 74-12 "Site-Dependent Spectra for Earthquake-Resistant Design," by H.B. Seed, C. Ugas and J. Lysmer - 1974 (PB 240 953)A03
- EERC 74-13 "Earthquake Simulator Study of a Reinforced Concrete Frame," by P. Hidalgo and R.W. Clough - 1974 (PB 241 944)A13
- EERC 74-14 "Nonlinear Earthquake Response of Concrete Gravity Dams," by N. Pal - 1974 (AD/A 006 583)A06
- EERC 74-15 "Modeling and Identification in Nonlinear Structural Dynamics - I. One Degree of Freedom Models," by N. Distefano and A. Rath - 1974 (PB 241 548)A06
- EERC 75-1 "Determination of Seismic Design Criteria for the Dumbarton Bridge Replacement Structure, Vol. I: Description, Theory and Analytical Modeling of Bridge and Parameters," by F. Baron and S.-H. Pang - 1975 (PB 259 407)A15
- EERC 75-2 "Determination of Seismic Design Criteria for the Dumbarton Bridge Replacement Structure, Vol. II: Numerical Studies and Establishment of Seismic Design Criteria," by F. Baron and S.-H. Pang - 1975 (PB 259 408)A11 (For set of EERC 75-1 and 75-2 (PB 259 406))
- EERC 75-3 "Seismic Risk Analysis for a Site and a Metropolitan Area," by C.S. Oliveira - 1975 (PB 248 134)A09
- EERC 75-4 "Analytical Investigations of Seismic Response of Short, Single or Multiple-Span Highway Bridges," by M.-C. Chen and J. Penzien - 1975 (PB 241 454)A09
- EERC 75-5 "An Evaluation of Some Methods for Predicting Seismic Behavior of Reinforced Concrete Buildings," by S.A. Mahin and V.V. Bertero - 1975 (PB 246 306)A16
- EERC 75-6 "Earthquake Simulator Study of a Steel Frame Structure, Vol. I: Experimental Results," by R.W. Clough and D.T. Tang - 1975 (PB 243 981)A13
- EERC 75-7 "Dynamic Properties of San Bernardino Intake Tower," by D. Rea, C.-Y. Liaw and A.K. Chopra - 1975 (AD/A008 406) A05
- EERC 75-8 "Seismic Studies of the Articulation for the Dumbarton Bridge Replacement Structure, Vol. I: Description, Theory and Analytical Modeling of Bridge Components," by F. Baron and R.E. Hamati - 1975 (PB 251 539)A07
- EERC 75-9 "Seismic Studies of the Articulation for the Dumbarton Bridge Replacement Structure, Vol. 2: Numerical Studies of Steel and Concrete Girder Alternates," by F. Baron and R.E. Hamati - 1975 (PB 251 540)A10
- EERC 75-10 "Static and Dynamic Analysis of Nonlinear Structures," by D.P. Mondkar and G.H. Powell - 1975 (PB 242 434)A08
- EERC 75-11 "Hysteretic Behavior of Steel Columns," by E.P. Popov, V.V. Bertero and S. Chandramouli - 1975 (PB 252 365)A11
- EERC 75-12 "Earthquake Engineering Research Center Library Printed Catalog," - 1975 (PB 243 711)A26
- EERC 75-13 "Three Dimensional Analysis of Building Systems (Extended Version)," by E.L. Wilson, J.P. Hollings and H.H. Dovey - 1975 (PB 243 989)A07
- EERC 75-14 "Determination of Soil Liquefaction Characteristics by Large-Scale Laboratory Tests," by P. De Alba, C.K. Chan and H.B. Seed - 1975 (NUREG 0027)A08
- EERC 75-15 "A Literature Survey - Compressive, Tensile, Bond and Shear Strength of Masonry," by R.L. Mayes and R.W. Clough - 1975 (PB 246 292)A10
- EERC 75-16 "Hysteretic Behavior of Ductile Moment Resisting Reinforced Concrete Frame Components," by V.V. Bertero and E.P. Popov - 1975 (PB 246 388)A05
- EERC 75-17 "Relationships Between Maximum Acceleration, Maximum Velocity, Distance from Source, Local Site Conditions for Moderately Strong Earthquakes," by H.B. Seed, R. Murarka, J. Lysmer and I.M. Idriss - 1975 (PB 248 172)A03
- EERC 75-18 "The Effects of Method of Sample Preparation on the Cyclic Stress-Strain Behavior of Sands," by J. Mullis, C.K. Chan and H.B. Seed - 1975 (Summarized in EERC 75-28)

- EERC 75-19 "The Seismic Behavior of Critical Regions of Reinforced Concrete Components as Influenced by Moment, Shear and Axial Force," by M.B. Atalay and J. Penzien - 1975 (PB 258 842)A11
- EERC 75-20 "Dynamic Properties of an Eleven Story Masonry Building," by R.M. Stephen, J.P. Hollings, J.G. Bouwkamp and D. Jurukovski - 1975 (PB 246 945)A04
- EERC 75-21 "State-of-the-Art in Seismic Strength of Masonry - An Evaluation and Review," by R.L. Mayes and R.W. Clough - 1975 (PB 249 040)A07
- EERC 75-22 "Frequency Dependent Stiffness Matrices for Viscoelastic Half-Plane Foundations," by A.K. Chopra, P. Chakrabarti and G. Dasgupta - 1975 (PB 248 121)A07
- EERC 75-23 "Hysteretic Behavior of Reinforced Concrete Framed Walls," by T.Y. Wong, V.V. Bertero and E.P. Popov - 1975
- EERC 75-24 "Testing Facility for Subassemblages of Frame-Wall Structural Systems," by V.V. Bertero, E.P. Popov and T. Endo - 1975
- EERC 75-25 "Influence of Seismic History on the Liquefaction Characteristics of Sands," by H.B. Seed, K. Mori and C.K. Chan - 1975 (Summarized in EERC 75-28)
- EERC 75-26 "The Generation and Dissipation of Pore Water Pressures during Soil Liquefaction," by H.B. Seed, P.P. Martin and J. Lysmer - 1975 (PB 252 648)A03
- EERC 75-27 "Identification of Research Needs for Improving Aseismic Design of Building Structures," by V.V. Bertero - 1975 (PB 248 136)A05
- EERC 75-28 "Evaluation of Soil Liquefaction Potential during Earthquakes," by H.B. Seed, I. Arango and C.K. Chan - 1975 (NUREG 0026)A13
- EERC 75-29 "Representation of Irregular Stress Time Histories by Equivalent Uniform Stress Series in Liquefaction Analyses," by H.B. Seed, I.M. Idriss, F. Makdisi and N. Banerjee - 1975 (PB 252 635)A03
- EERC 75-30 "FLUSH - A Computer Program for Approximate 3-D Analysis of Soil-Structure Interaction Problems," by J. Lysmer, T. Udaka, C.-F. Tsai and H.B. Seed - 1975 (PB 259 332)A07
- EERC 75-31 "ALUSH - A Computer Program for Seismic Response Analysis of Axisymmetric Soil-Structure Systems," by E. Berger, J. Lysmer and H.B. Seed - 1975
- EERC 75-32 "TRIP and TRAVEL - Computer Programs for Soil-Structure Interaction Analysis with Horizontally Travelling Waves," by T. Udaka, J. Lysmer and H.B. Seed - 1975
- EERC 75-33 "Predicting the Performance of Structures in Regions of High Seismicity," by J. Penzien - 1975 (PB 248 130)A03
- EERC 75-34 "Efficient Finite Element Analysis of Seismic Structure - Soil - Direction," by J. Lysmer, H.B. Seed, T. Udaka, R.N. Hwang and C.-F. Tsai - 1975 (PB 253 570)A03
- EERC 75-35 "The Dynamic Behavior of a First Story Girder of a Three-Story Steel Frame Subjected to Earthquake Loading," by R.W. Clough and L.-Y. Li - 1975 (PB 248 841)A05
- EERC 75-36 "Earthquake Simulator Study of a Steel Frame Structure, Volume II - Analytical Results," by D.T. Tang - 1975 (PB 252 926)A10
- EERC 75-37 "ANSR-I General Purpose Computer Program for Analysis of Non-Linear Structural Response," by D.P. Mondkar and G.H. Powell - 1975 (PB 252 386)A08
- EERC 75-38 "Nonlinear Response Spectra for Probabilistic Seismic Design and Damage Assessment of Reinforced Concrete Structures," by M. Murakami and J. Penzien - 1975 (PB 259 530)A05
- EERC 75-39 "Study of a Method of Feasible Directions for Optimal Elastic Design of Frame Structures Subjected to Earthquake Loading," by N.D. Walker and K.S. Pister - 1975 (PB 257 781)A06
- EERC 75-40 "An Alternative Representation of the Elastic-Viscoelastic Analogy," by G. Dasgupta and J.L. Sackman - 1975 (PB 252 173)A03
- EERC 75-41 "Effect of Multi-Directional Shaking on Liquefaction of Sands," by H.B. Seed, R. Pyke and G.R. Martin - 1975 (PB 258 781)A03
- EERC 76-1 "Strength and Ductility Evaluation of Existing Low-Rise Reinforced Concrete Buildings - Screening Method," by T. Okada and B. Bresler - 1976 (PB 257 906)A11
- EERC 76-2 "Experimental and Analytical Studies on the Hysteretic Behavior of Reinforced Concrete Rectangular and T-Beams," by S.-Y.M. Ma, E.P. Popov and V.V. Bertero - 1976 (PB 260 843)A12
- EERC 76-3 "Dynamic Behavior of a Multistory Triangular-Shaped Building," by J. Petrovski, R.M. Stephen, E. Gartenbaum and J.G. Bouwkamp - 1976
- EERC 76-4 "Earthquake Induced Deformations of Earth Dams," by N. Serff and H.B. Seed - 1976

- EERC 76-5 "Analysis and Design of Tube-Type Tall Building Structures," by H. de Clercq and G.H. Powell - 1976 (PB 252 220) A10
- EERC 76-6 "Time and Frequency Domain Analysis of Three-Dimensional Ground Motions, San Fernando Earthquake," by T. Kubo and J. Penzien (PB 260 556)A11
- EERC 76-7 "Expected Performance of Uniform Building Code Design Masonry Structures," by R.L. Mayes, Y. Omote, S.W. Chen and R.W. Clough - 1976
- EERC 76-8 "Cyclic Shear Tests on Concrete Masonry Piers," Part I - Test Results," by R.L. Mayes, Y. Omote and R.W. Clough - 1976 (PB 264 424)A06
- EERC 76-9 "A Substructure Method for Earthquake Analysis of Structure - Soil Interaction," by J.A. Gutierrez and A.K. Chopra - 1976 (PB 257 783)A08
- EERC 76-10 "Stabilization of Potentially Liquefiable Sand Deposits using Gravel Drain Systems," by H.B. Seed and J.R. Booker - 1976 (PB 258 820)A04
- EERC 76-11 "Influence of Design and Analysis Assumptions on Computed Inelastic Response of Moderately Tall Frames," by G.H. Powell and D.G. Row - 1976
- EERC 76-12 "Sensitivity Analysis for Hysteretic Dynamic Systems: Theory and Applications," by D. Ray, K.S. Pister and E. Polak - 1976 (PB 262 859)A04
- EERC 76-13 "Coupled Lateral Torsional Response of Buildings to Ground Shaking," by C.L. Kan and A.K. Chopra - 1976 (PB 257 907)A09
- EERC 76-14 "Seismic Analyses of the Banco de America," by V.V. Bertero, S.A. Mahin and J.A. Hollings - 1976
- EERC 76-15 "Reinforced Concrete Frame 2: Seismic Testing and Analytical Correlation," by R.W. Clough and J. Gidwani - 1976 (PB 261 323)A08
- EERC 76-16 "Cyclic Shear Tests on Masonry Piers, Part II - Analysis of Test Results," by R.L. Mayes, Y. Omote and R.W. Clough - 1976
- EERC 76-17 "Structural Steel Bracing Systems: Behavior Under Cyclic Loading," by E.P. Popov, K. Takanashi and C.W. Roeder - 1976 (PB 260 715)A05
- EERC 76-18 "Experimental Model Studies on Seismic Response of High Curved Overcrossings," by D. Williams and W.G. Godden - 1976
- EERC 76-19 "Effects of Non-Uniform Seismic Disturbances on the Dumbarton Bridge Replacement Structure," by F. Baron and R.E. Hamati - 1976
- EERC 76-20 "Investigation of the Inelastic Characteristics of a Single Story Steel Structure Using System Identification and Shaking Table Experiments," by V.C. Matzan and H.D. McNiven - 1976 (PB 258 453)A07
- EERC 76-21 "Capacity of Columns with Splice Imperfections," by E.P. Popov, R.M. Stephen and R. Philbrick - 1976 (PB 260 378)A04
- EERC 76-22 "Response of the Olive View Hospital Main Building during the San Fernando Earthquake," by S. A. Mahin, R. Collins, A.K. Chopra and V.V. Bertero - 1976
- EERC 76-23 "A Study on the Major Factors Influencing the Strength of Masonry Prisms," by N.M. Mostaghel, R.L. Mayes, R. W. Clough and S.W. Chen - 1976
- EERC 76-24 "GADFLEA - A Computer Program for the Analysis of Pore Pressure Generation and Dissipation during Cyclic or Earthquake Loading," by J.R. Booker, M.S. Rahman and H.B. Seed - 1976 (PB 263 947)A04
- EERC 76-25 "Rehabilitation of an Existing Building: A Case Study," by B. Bresler and J. Axley - 1976
- EERC 76-26 "Correlative Investigations on Theoretical and Experimental Dynamic Behavior of a Model Bridge Structure," by K. Kawashima and J. Penzien - 1976 (PB 263 388)A11
- EERC 76-27 "Earthquake Response of Coupled Shear Wall Buildings," by T. Srichatrapimuk - 1976 (PB 265 157)A07
- EERC 76-28 "Tensile Capacity of Partial Penetration Welds," by E.P. Popov and R.M. Stephen - 1976 (PB 262 899)A03
- EERC 76-29 "Analysis and Design of Numerical Integration Methods in Structural Dynamics," by H.M. Hilber - 1976 (PB 264 410)A06
- EERC 76-30 "Contribution of a Floor System to the dynamic Characteristics of Reinforced Concrete Buildings," by L.J. Edgar and V.V. Bertero - 1976
- EERC 76-31 "The Effects of Seismic Disturbances on the Golden Gate Bridge," by F. Baron, M. Arikan and R.E. Hamati - 1976
- EERC 76-32 "Infilled Frames in Earthquake Resistant Construction," by R.E. Klingner and V.V. Bertero - 1976 (PB 265 892)A13

- UCB/EERC-77/01 "PLUSH - A Computer Program for Probabilistic Finite Element Analysis of Seismic Soil-Structure Interaction," by M.P. Romo Organista, J. Lysmer and H.B. Seed - 1977
- UCB/EERC-77/02 "Soil-Structure Interaction Effects at the Humboldt Bay Power Plant in the Ferndale Earthquake of June 7, 1975," by J.E. Valera, H.B. Seed, C.F. Tsai and J. Lysmer - 1977 (PB 265 795)A04
- UCB/EERC-77/03 "Influence of Sample Disturbance on Sand Response to Cyclic Loading," by K. Mori, H.B. Seed and C.K. Chan - 1977 (PB 267 352)A04
- UCB/EERC-77/04 "Seismological Studies of Strong Motion Records," by J. Shoja-Taheri - 1977 (PB 269 655)A10
- UCB/EERC-77/05 "Testing Facility for Coupled-Shear Walls," by L. Li-Hyung, V.V. Bertero and E.P. Popov - 1977
- UCB/EERC-77/06 "Developing Methodologies for Evaluating the Earthquake Safety of Existing Buildings," by No. 1 - B. Bresler; No. 2 - B. Bresler, T. Okada and D. Zisling; No. 3 - T. Okada and B. Bresler; No. 4 - V.V. Bertero and B. Bresler - 1977 (PB 267 354)A08
- UCB/EERC-77/07 "A Literature Survey - Transverse Strength of Masonry Walls," by Y. Omote, R.L. Mayes, S.W. Chen and R.W. Clough - 1977
- UCB/EERC-77/08 "DRAIN-TABS: A Computer Program for Inelastic Earthquake Response of Three Dimensional Buildings," by R. Guendelman-Israel and G.H. Powell - 1977 (PB 270 693)A07
- UCB/EERC-77/09 "SUBWALL: A Special Purpose Finite Element Computer Program for Practical Elastic Analysis and Design of Structural Walls with Substructure Option," by D.Q. Le, H. Peterson and E.P. Popov - 1977 (PB 270 567)A05
- UCB/EERC-77/10 "Experimental Evaluation of Seismic Design Methods for Broad Cylindrical Tanks," by D.P. Clough
- UCB/EERC-77/11 "Earthquake Engineering Research at Berkeley - 1976," - 1977
- UCB/EERC-77/12 "Automated Design of Earthquake Resistant Multistory Steel Building Frames," by N.D. Walker, Jr. - 1977
- UCB/EERC-77/13 "Concrete Confined by Rectangular Hoops Subjected to Axial Loads," by D. Zalinas, V.V. Bertero and E.P. Popov - 1977
- UCB/EERC-77/14 "Seismic Strain Induced in the Ground During Earthquakes," by Y. Sugimura - 1977
- UCB/EERC-77/15 "Bond Deterioration under Generalized Loading," by V.V. Bertero, E.P. Popov and S. Viwathanatapa - 1977

- UCB/EERC-77/16 "Computer Aided Optimum Design of Ductile Reinforced Concrete Moment Resisting Frames," by S.W. Zagajeski and V.V. Bertero - 1977
- UCB/EERC-77/17 "Earthquake Simulation Testing of a Stepping Frame with Energy-Absorbing Devices," by J.M. Kelly and D.F. Tsztoo 1977
- UCB/EERC-77/18 "Inelastic Behavior of Eccentrically Braced Steel Frames under Cyclic Loadings," by C.W. Roeder and E.P. Popov - 1977
- UCB/EERC-77/19 "A Symplified Procedure for Estimating Earthquake-Induced Deformations in Dams and Embankments," by F.I. Makdisi and H.B. Seed - 1977
- UCB/EERC-77/20 "The Performance of Earth Dams during Earthquakes," by H.B. Seed, F.I. Makdisi and P. de Alba - 1977
- UCB/EERC-77/21 "Dynamic Plastic Analysis Using Stress Resultant Finite Element Formulation," by P. Lukkunapvasit and J.M. Kelly 1977
- UCB/EERC-77/22 "Preliminary Experimental Study of Seismic Uplift of a Steel Frame," by R.W. Clough and A.A. Huckelbridge - 1977
- UCB/EERC-77/23 "Earthquake Simulator Tests of a Nine-Story Steel Frame with Columns Allowed to Uplift," by A.A. Huckelbridge - 1977
- UCB/EERC-77/24 "Nonlinear Soil-Structure Interaction of Skew Highway Bridges," by M.-C. Chen and Joseph Penzien - 1977
- UCB/EERC-77/25 "Seismic Analysis of an Offshore Structure Supported on Pile Foundations," by D.D.-N. Liou - 1977